IJAMS

International Journal of Applied Mathematics and Simulation

VOLUME 1 ISSUE 2 2024

ISSN (PRINT)=2992-1708 EISSN = 2992-1732

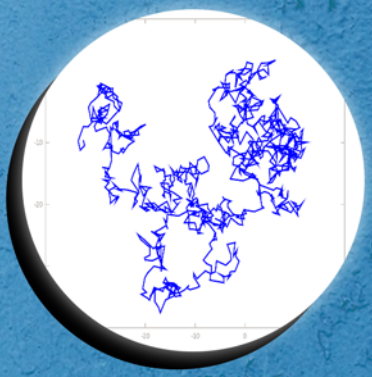

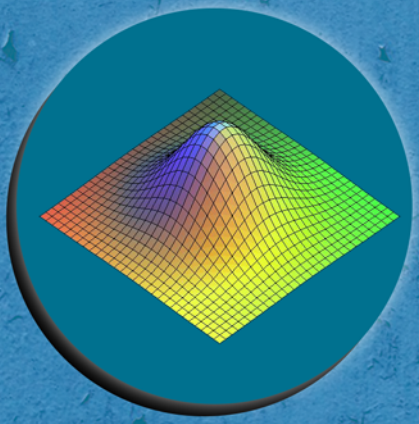

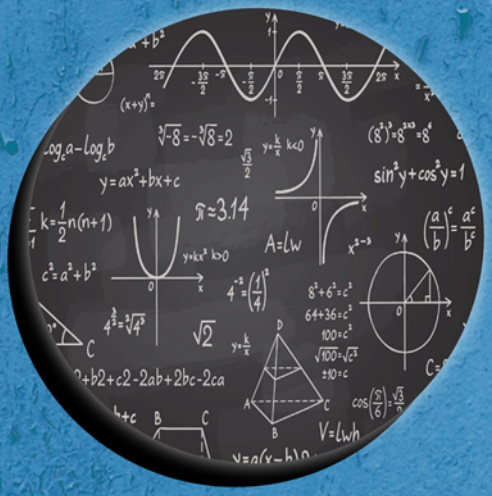

MOHAMED KHIDER UNIVERSITY OF BISKRA

Contents

Studying a Hidden Bifurcation and Finding Hopf Bifurcation with Generated New Saturated Function Series

IJAMS Peer-reviewed journal
International Journal of Applied Mathematics and Simulation

Studying a Hidden Bifurcation and Finding Hopf Bifurcation with Generated New Saturated Function Series

Faiza Zaamoune[1] and Tidjani Menacer[2]

ABSTRACT: In this article, a hidden bifurcation of the multispiral chaotic attractor generated by the new saturated function series has been considered. The general shape of the chaotic attractors is described in terms of the number of spirals (also reffered to as multiscroll attractor) governed by integer parameters p and q. Due to the integer nature of the parameter, it is not possible to observe bifurcations from M spirals when the parameter is increased by two. However, by using the method of hidden bifurcations, an additional real parameter ε was introduced to observe such bifurcations. Additionally, this added parameter allowed us to find the Hopf bifurcation of the multispiral attractor generated by the new saturated function series transitioning from a stable state to a chaotic state. Furthermore, the Routh-Hurwitz criterion was used to study the stability of the original equilibrium point of the system.

Keywords: Saturated function series, hidden bifurcation, Hopf bifurcation, multiscroll.

MSC: 39A21, 39A28, 39A33.

1 INTRODUCTION

In nonlinear dynamics, chaotic systems and their dynamical characteristics are fascinating subjects (physical and engineering systems, climate models and global weather patterns and biological systems...). Such dynamical systems produce significantly differing results for small differences in initial conditions (e.g., rounding errors in numerical computation), making long-term behavior prediction generally difficult. In the last forty years, the scientific, mathematical, and engineering communities have devoted a great deal of attention to the study of chaos, a highly fascinating and complicated nonlinear phenomenon [1], [2], [3], [4].

Dynamical behavior can be effectively explained by the bifurcation theory [5]. When a parameter is changed, the dynamics of bifurcations of arbitrary invariant sets of dynamical systems seem more appealing and complex [5]. Hopf bifurcation, sometimes called Poincare-Andronov-Hopf bifurcation, is the local birth or death of a periodic solution (self-excited oscillation) from an equilibrium as a parameter reaches a critical point [6].
Moreover, while most of these multiscroll generations have been known for a long time, bifurcation theory has only lately been applied to their study [7]. They have also been identified for hidden attractors [8] in the situation of infinitely many equilibria, as well as in the case where equilibrium points exist. The number of scrolls (or spirals) for every multi scroll that is currently known is a fixed integer which is

• [1] *Faiza Zaamoune, Corresponding Author, Department of Methematics, University Mohamed Khider Biskra, Algeria. E-mail: faiza.zaamoune@univ-biskra.dz*

• [2] *Tidjani Menacer, Department of Methematics, University Mohamed Khider Biskra, Algeria. E-mail: menacer.tidjani@univ-biskra.dz*

Communicated Editor: Khaled Zennir
Manuscript received Feb 20, 2024; revised Apr 17, 2024; accepted Mai 01, 2024; published Dec 07, 2024.

depends on one or more discrete characteristics [9].
In 2015, Menacer et al., introduced a hidden bifurcation theory and producing multiscrolls in a family of systems (6) with a continuous bifurcation parameter, modified the paradigm of discrete parameters [10]. This technique was discovered from the hidden attractor theory, first presented by Leonov et al. [12], [13], [14], [15], [16], which constitutes the foundation for this hidden bifurcation theory. We applied this technique to the $1-D$ multiscroll chaotic attractors generated by saturated function series [17]. A saturated function series was proposed for generating multi-scroll chaotic attractors, including 1-D n-scroll, 2-D $n \times m$-grid scroll, and 3-D $n \times m \times l$-grid scroll chaotic attractors [19], [20].
This paper provides two new findings: first, we examined a hidden bifurcation in 1-D multiscroll chaotic attractors created by a new saturated function series. In comparison with previous results [10], [19] we found the difference in behavior and form of spirals; second, we determined the Hopf bifurcation and stability of the origin equilibrium point E_0 concerning ε and we identified a critical point for both. After a lot of calculation, we noticed that Hopf bifurcation was determined in this case only with these values set to me for $\alpha = t_1 = 0.72, \beta = \gamma = 0.8, k = 10, h = 20$.

This paper is organized as follows: In Section 2, the model of multiscroll chaotic attractors generated by the new saturated function series proposed is studied. In Section 3, the localization technique introduced for hidden bifurcation in multiscroll chaotic attractors generated by new saturated function series. In Section 4, Hopf bifurcation and stability of the origin equilibrium point E_0 for ε. Finally, in secion 5, we have a concluding comments. Appendix A presents the technique of Leonov et al., for seeking a hidden attractor.

2 DESIGN MULTISPIRAL CHAOTIC ATTRACTORS FROM SATURATED FUNCTION SERIES.

One of the fundamental PWL circuits is the saturated circuit, which is widely known. Saturated circuit characteristics are effectivly the PWL models for operational amplifiers [7]. This study presents a multi-piecewise non-linear saturated series model [17], which has the following expression:

$$\begin{cases} \dot{x} = y \\ \dot{y} = z \\ \dot{z} = -\alpha x - \beta y - \gamma z + t_1 g(x;k;h;p;q), \end{cases} \tag{1}$$

where

$$g(x;k;h;p;q) = \begin{cases} y_{1,k} \;\; if \; x > qh+1 \\ y_{2,k,i} \;\; if \;\; |x - ih| \leq 1 \\ \qquad\quad -p \leq i \leq q \\ y_{3,k,i} \;\; if \;\; l_{1,i} < x < l_{2,i} \\ \qquad\quad -p < i < q-1 \\ y_{4,k} \;\; if \; x < -ph-1, \end{cases} \tag{2}$$

with

$l_{1,i} = ih + 1$ and $l_{2,i} = (i+1) \times h - 1$,
$y_{1,k} = (2q+1)\,k$, $y_{2,k,i} = k\,(x - ih) + 2ik$,
$y_{3,k,i} = (2i+1)\,k$ and $y_{4,k} = -\,(2p+1)\,k$.
Parameters p, q, h and k are integers, and $\alpha, \beta, \gamma, t_1$ are real numbers. This article aims to examine the attractors' overall form and global geometric characteristics, which are expressed in terms of the number of spirals, a phenomenon referred to as a hidden bifurcation [11]. Hopf bifurcations [5]. This work identifies structurally chaotic attractors with fixed real parameter values of $\alpha = t_1 = 0.72, \beta = \gamma = 0.8, k = 10$ and $h = 20$ (see Fig. 1 and see Fig. 2). The following formula determines the number M of spirals based on two integer inputs, p and q:

$$M = p + q + 2. \tag{3}$$

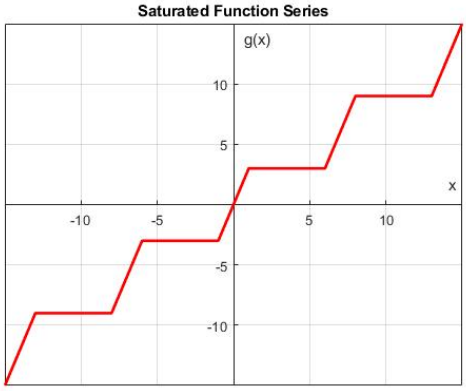

Fig. 1: **Proposed Saturated function series with** $k = 3$, $h = 7$, $p = 2$, $q = 2$

3 Hidden Bifurcations Revealing Technique

A distinctive technique for identifying hidden bifurcations was presented by Menacer et *al.* [5] to overcome this issue. This technique builds on the concept of Leonov and Kuznetsov [8] for examining hidden attractors (i.e., homotopy and numerical continuation, see Appendix A). This method is new when applied to multiscroll chaotic attractors from saturated function series. In this section, we briefly review the process, where the parameters values are fixed at $\alpha = t_1 = 0.72, \beta = \gamma = 0.8, k = 10, h = 20$.
Rewrite system (1)-(2) to the form:

$$\frac{dx}{dt} = Fx + \eta\Psi(\delta^T x), \qquad x \in \mathbb{R}.^3. \tag{4}$$

Where

$$F = \begin{pmatrix} 0 & 1 & 0 \\ 0 & 0 & 1 \\ -\alpha & -\beta & -\gamma \end{pmatrix}, \quad \eta = \begin{pmatrix} 0 \\ 0 \\ t_1 \end{pmatrix}, \quad \delta = \begin{pmatrix} 1 \\ 0 \\ 0 \end{pmatrix}. \tag{5}$$

Presenting the coefficient k^* and small parameter ε, and describe system (4) as

$$\frac{dx}{dt} = F_0 x + \eta\varepsilon\varphi(\delta^T x), \tag{6}$$

where

$$F_0 = F + k^*\eta\delta^T = \begin{pmatrix} 0 & 1 & 0 \\ 0 & 0 & 1 \\ k^*t_1 - \alpha & -\beta & -\gamma \end{pmatrix},$$

$$\rho_{1,2}^{F_0} = \pm i\omega_0, \quad \rho_3^{F_0} = -d.$$

By nonsingular linear transformation $X = SY$ system (6) is became to the form

$$\frac{dy}{dt} = Hy + B\varepsilon\varphi(c^T y), \tag{7}$$

where

$$H = \begin{pmatrix} 0 & -\omega_0 & 0 \\ \omega_0 & 0 & 0 \\ 0 & 0 & -d \end{pmatrix}, \quad B = \begin{pmatrix} b_1 \\ b_2 \\ 1 \end{pmatrix}, \quad c = \begin{pmatrix} 1 \\ 0 \\ -h \end{pmatrix}. \tag{8}$$

The transfer function $W_H(s)$ of system (7) can be presented as

$$W_H(s) = \frac{-b_1 s + b_2\omega_0}{s^2 + \omega_0^2} + \frac{h}{s + d}. \tag{9}$$

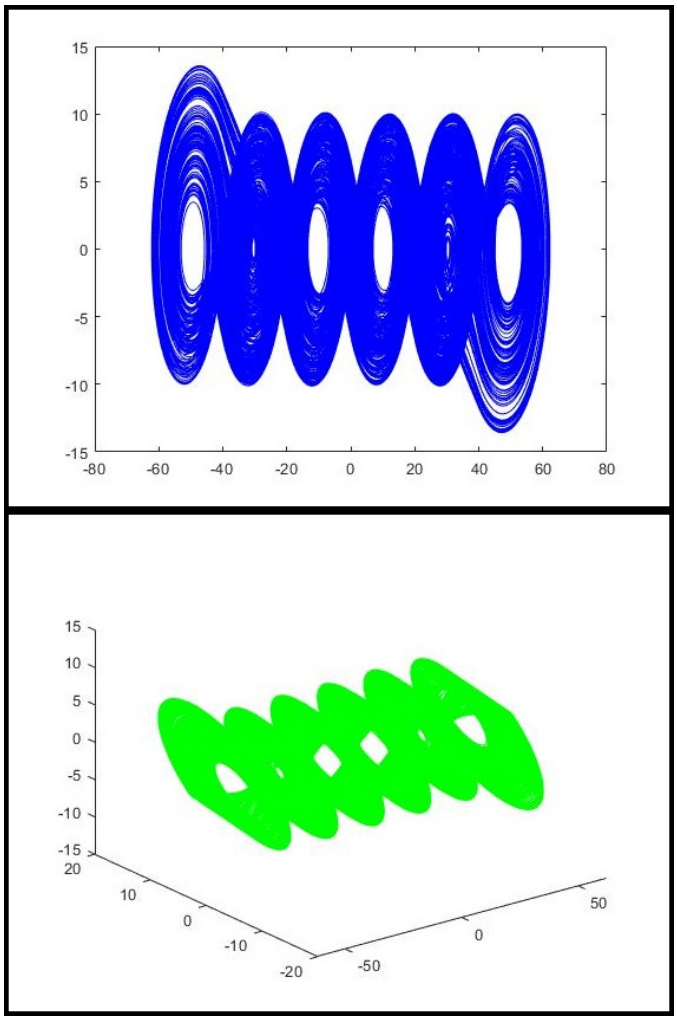

Fig. 2: (a) The 6-spiral attractor generated by equation (1) and (2) for $p = q = 2$ 3-projection into the plane (x, y), (b) The 6-spiral attractor generated by equation (1) and (2) for $p = q = 2$ $3-$ projection into the plane (x, y, z).

Also, utilizing the equality of transfer functions of systems (6) and system (7), we obtain:

$$W_{F_0}(s) = \delta^T (F_0 - sI)^{-1} \eta. \tag{10}$$

This implies the following relations:

$$\begin{aligned} &k^* = \tfrac{\alpha - \omega_0^2 d}{t_1}, \\ &d = c, \\ &h = \tfrac{-t_1}{\omega_0^2 + d^2} = b_1, \\ &b_2 = \tfrac{-\gamma_1}{\omega_0(\omega_0^2 + d^2)}. \end{aligned} \tag{11}$$

Since system (6) can be debilitated to the form (7) by the non-singular linear transformation defined in (A), the following relations can be acquired:

$$H = S^{-1} F_0 S,\ B = S^{-1}\eta,\ c^T = \delta^T S. \tag{12}$$

To solve these matrix equations, we obtain the following transformation matrix :

$$S = \begin{pmatrix} S_{11} & S_{12} & S_{13} \\ S_{21} & S_{22} & S_{23} \\ S_{31} & S_{32} & S_{33} \end{pmatrix},$$

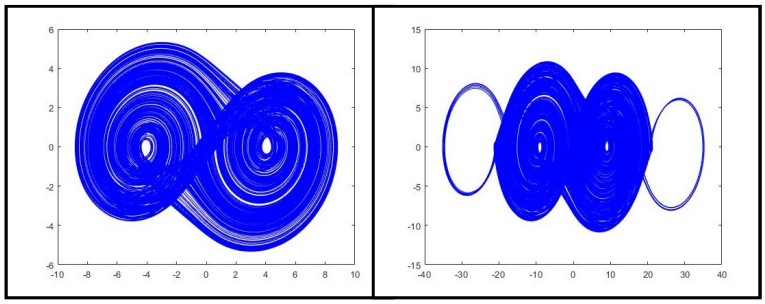

Fig. 3: 2 spiral for ε=0.35 Fig. 4: 4 spirals for ε=0.94

with

$$\begin{array}{lll} S_{11}=1, & S_{12}=0\,, & S_{13}=-h \\ S_{21}=0, & S_{22}=-\omega_0, & S_{23}=dh \\ S_{31}=-\omega_0^3, & S_{32}=0, & S_{33}=d^2h. \end{array} \tag{13}$$

3.1 Numerical Results of the Hidden Bifurcation Technique

Using (A), with a sufficiently small ε we computed initial data for the first step of multistage localization procedure

$$X(0)=SY(0)=S\begin{pmatrix}\varsigma_0\\0\\0\end{pmatrix}=\begin{pmatrix}\varsigma_0 S_{11}\\ \varsigma_0 S_{21}\\ \varsigma_0 S_{31}\end{pmatrix}. \tag{14}$$

For system (4), this gives the initial data

$$X^0(0)=(x^0(0)=\varsigma_0,\ y^0(0)=0,\ z^0(0)=-\varsigma_0\omega_0^3.). \tag{15}$$

The localization process outlined previously is now applied to system 1 with numerous spiral attractors. In order to accomplish this, we calculate a harmonic linearization coefficient and the initial frequency ω_0 as described in the Appendix:

$$\omega_0=0.86,\quad k^*=0.32. \tag{16}$$

Next, we compute the solutions to system (6) with the nonlinearity $\varepsilon\varphi(x)=\varepsilon(\psi(x)-k_1x)$. To do this, we start at the beginning with step 0.35 and increase ε successively from the value $\varepsilon=0.35$ to $\varepsilon=1$. The starting data for the solutions for increasing values of ε, as shown in Table 1, is obtained via (15). So, from the Table 1, we obtain the solutions $X^1(0)$ with one scroll to $X^4(0)$ (See Fig. 3 to Fig 6). In each figure, there is a variant an even number of spirals in the attractor. The number of spirals increases by 2 at each step as shown on Table 2 from 2 to 6 spirals. The values of ε in this table are totally the values of bifurcation points.

Values of ε	$X^i(0)$	x_0	y_0	z_0
0.42	$X^1(0)=X^1(t_{max})$	-0.57	0	0.1252
0.94	$X^2(0)=X^2(t_{max})$	-13.8295	1.7315	5.3924
0.98	$X^3(0)=X^3(t_{max})$	27.1245	3.2587	-8.2567
1	$X^4(0)=X^4(t_{max})$	-1.1235	-2.1587	-7.2025

Table 1: Initial data according to the values of ε

Table 2: Values of the parameter ε at the bifurcation points for $p=q=2$

Values of ε	0.35	0.94	0.98	1
Number of spirals	2 spiral	4 spirals	6 spirals	6 spirals

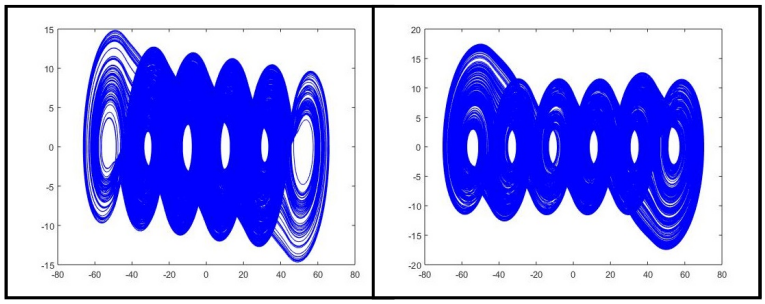

Fig. 5: 6 spirals for ε=0.98 Fig. 6: 1 spirals for ε=1

4 Hopf Bifurcation and Stability of the Origin Equilibrium Point E_0 with Respect to ε

4.1 Stability of the Origin Equilibrium Point E_0 with Respect to ε

In the system (1)-(2) we have $2(p+q)+3$ equilibrium points. They have a positive eigenvalue and a pair of complex eigenvalues with negative real parts. This means that all equilibria of the system are saddle points [17]. Using the conditions established by Routh-Hurwitz [18], we examine the stability of the equilibrium point E_0 in relation to the epsilon of the system (6). In [11], Menacer et al. present the idea of hidden bifurcation in the Chua system by including a new parameter, epsilon, that regulates the spiral number. The number of scrolls reduces as ε increases from 0 to 1. The following polynomial yields the eigenvalues equation corresponding to this equilibrium point:

$$P(s) = s^3 + a_1 s^2 + a_2 s + a_3. \tag{17}$$

Using the result of the Routh-Hurwitz conditions, where the necessary and sufficient condition for the equilibrium point E to be locally asymptotically stable is $a_1 > 0$, $a_3 > 0$ and $a_1 \times a_2 - a_3 > 0$.

In our study, we study the stability and Hopf bifurcation with respect to the parameter ε and the parameters values are $\alpha = t_1 = 0.72, \beta = \gamma = 0.8, p = q = 2, k^* = 0.32$. An equilibrium point of system (1) independent of epsilon is the origin $E_0(0,0,0)$. The evaluation of the Jacobian matrix at the equilibrium point $E_0(0,0,0)$ is:

$$J_{E_0} = \begin{pmatrix} 0 & 1 & 0 \\ 0 & 0 & 1 \\ -\alpha k^* + \alpha\varepsilon(k^*+k) & -\beta & -\gamma \end{pmatrix} = \begin{pmatrix} 0 & 1 & 0 \\ 0 & 0 & 1 \\ 0.2304 + \varepsilon 6.7104 & -0.8 & -0.8 \end{pmatrix}.$$

Its characteristic polynomial is:

$$P(s) = s^3 + 0.8s^2 + 0.8s + (0.2304 + \varepsilon 6.7104).$$

The necessary and sufficient requirement for the equilibrium point is stated in the Routh-Hurwitz criteria. E_0 to be stable is $0.0343 < \varepsilon < 0.1297$.

Proof. we applied the Routh-Hurwitz criteria for origin equilibrium point (0,0,0) we found:

$$\text{First condition} : a_1 = 0.8 > 0 \tag{18}$$

$$\text{Second condition} : a_3 = 0.2304 + \varepsilon 6.7104 > 0 \Longrightarrow \varepsilon > 0.0.0343; \tag{19}$$

$$\text{Third condition} : a_1 \times a_2 - a_3 = 0.64 - 6.7104\varepsilon > 0 \Longrightarrow \varepsilon < 0.1297 \tag{20}$$

so E_0 to be stable when: $0.0343 < \varepsilon < 0.1297$. □

Remark

For the special case $\boldsymbol{\varepsilon = 0}$ **:** the system (1) becomes linear so the attractor as a limit cycle unstable see the figure below :

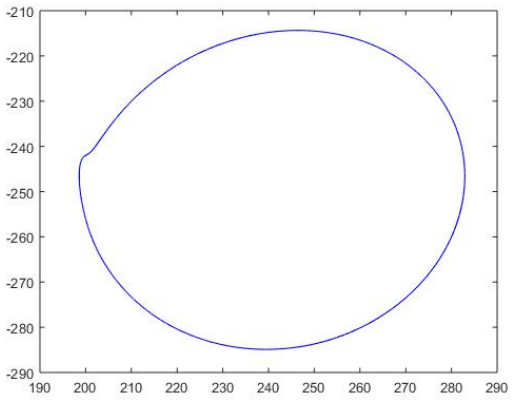

Fig. 7: **The system's attractor (1), in which $\varepsilon = 0$: limit of an unstable cycle.**

4.2 Analysis of Hopf Bifurcation at the Origin Equilibrium Point E_0 Regarding ε

The system (1) attached by the formula (2) has $2(p+q)+3$ equilibrium points which we find by comparing the right sides of the system to zero and which are given in [17]. We studied Hopf bifurcation at the point $(0,0,0)$ with the values $\alpha = t_1 = 0.72, \beta = \gamma = 0.8, p = q = 2$. The conditions of system (1) with $p = q = 2$, to undergo a Hopf bifurcation at the equilibrium point $E(0,0,0)$ when $\varepsilon = \varepsilon^*$
-The Jacobian matrix has two complex-conjugate eigenvalues $s_{1,2} = \Theta(\varepsilon) \pm i\omega(\varepsilon)$ and one real $s_3(\varepsilon)$,
-$\Theta(\varepsilon^*) = 0$, and $s_3(\varepsilon^*) \neq 0$,
-$\omega(\varepsilon^*) \neq 0$,
-$\frac{d\Theta}{d\varepsilon}|_{\varepsilon=\varepsilon^*} \neq 0$.

Proposition 1. *The system (1) undergoes a Hopf bifurcation at $E(0,0,0)$, when the parameter ε crosses the critical values $\varepsilon^* = 0.16039$.*

Proof. For the first condition : $\Theta(0.16039) = 0$, and $s_3(0.16039) = -0.89444 \neq 0$,
For the second condition: $\omega(0.16039) = -0.80002 \neq 0$
For the last condition : $\frac{d\Theta}{d\varepsilon}|_{\varepsilon=0.16039} = 0.46988 \neq 0$. □

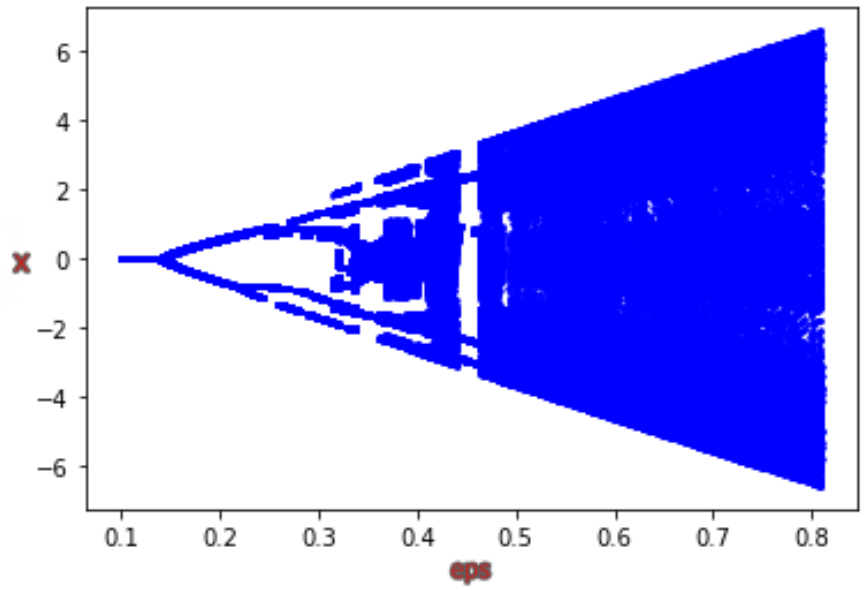

(a)

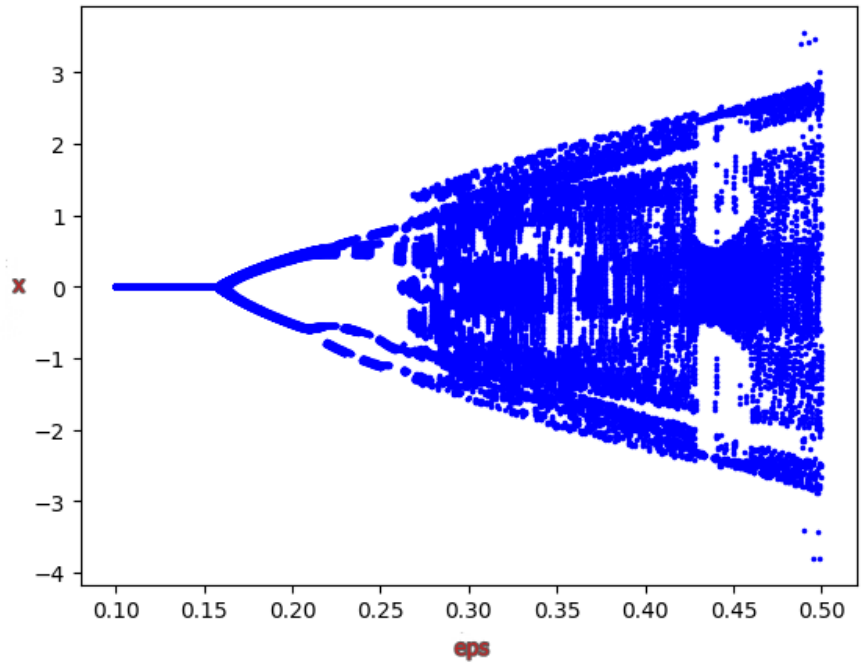

(b)

Fig. 8: **The results of Hopf bifurcation analysis (a): The bifurcation diagram for the critical point** $\varepsilon^* = 0.16039$ **, (b) : Clarify The bifurcation diagram for the critical point** $\varepsilon^* = 0.16039$**.**

5 CONCLUSION

This article examines hidden bifurcations of the multispiral Chaotic attractor produced by the newly discovered saturation function series. The number of spirals, or multiscroll attractor, determined by the integer parameters p, q, has been used to characterize the overall shape of the chaotic attractors. When this parameter is increased by two, bifurcations from M spirals cannot be observed because of its integer character. Nevertheless, an extra real parameter ε was added in order to observe such bifurcations using the hidden bifurcation approach. Additionally, the Hopf bifurcation of the multispiral attractor produced by the new saturated function series from a stable state to a chaotic state may be found thanks to this additional parameter. Furthermore, the stability of the system's initial equilibrium point was examined using the Routh-Hurwitz criteria. In our futur works, we will provide to find a hidden attractors and hidden bifurcations in new systems.

APPENDIX A
TECHNIQUE OF LEONOV ET AL FOR SEEKING A HIDDEN ATTRACTOR

The technique for seeking attractors of multidimensional nonlinear dynamical systems with scalar nonlinearity was proposed by Leonov [12] and Leonov et al. [8], [13], [14], [15], [16]. Their technique is based on numerical continuation: a series of linked systems is built such that, for the first system (the starting system), the initial data for the numerical computation of a potential oscillating solution (the starting oscillation) can be obtained analytically. The proposed technique is extended in [16], [10] to the system of the form

$$\dot{U} = PX + qF(r^T X), \quad X \in \mathbb{R}^n, \tag{21}$$

where q, r are constant n-dimensional vectors, $F(\sigma)$ is a continuous piece- wise differential function reaching the condition $F(0) = 0$, and T implies transpose operation. P is a constant $n \times n$-matrix.

Here, we outline their technique for the simplified case when $n = 3$. Thus, we take into consideration the equation.

$$\dot{X} = PX + qF(r^T X), \quad U \in \mathbb{R}^3, \tag{22}$$

where $F(\sigma)$ is a continuous nonlinear function.

They then define a coefficient of harmonic linearization ϑ (suppose that such ϑ exists) in such a way that the matrix

$$P_0 = P + \vartheta q r^T, \tag{23}$$

of the linear system

$$\dot{X} = PX, \tag{24}$$

has a pair of purely imaginary eigenvalues $\pm i\omega_0, (\omega_0 > 0\ )$ and the other eigenvalue has negative real part. In practice, to determine ϑ and ω_0 they use the transfer function $W(\tau)$ of system(21)

$$W(\tau) = r(P - \tau I)^{-1} q, \tag{25}$$

where τ is a complex variable and I is a unit matrix. The number $\omega_0 > 0$ is determined from the equation $\mathrm{I}\varsigma\, W(i\omega_0) = 0$ and ϑ is calculated by the formula $\vartheta = -\operatorname{Re} W(i\omega_0)^{-1}$.

Therefore, system (21) can rewrite as

$$\dot{X} = P_0 X + qf(r^T X), \quad X \in \mathbb{R}^3, \tag{26}$$

where $f(\sigma) = F(\sigma) - \vartheta\sigma$.

Following that, they introduce a finite sequence of continuous functions $f^0(\varsigma)$, $f^1(\varsigma), ..., f^m(\varsigma)$ in such a way that the graphs of neighboring functions $f^j(\varsigma)$ and $f^{j+1}(\varsigma)$, $(j = 0, ..., m-1)$ in a sense, slightly differ

from each other, the function $f^0(\varsigma)$ is small and $f^m(\varsigma) = f(\varsigma)$. The function $f^0(\varsigma)$, allows the application the method of harmonic linearization (describing function method) to the system

$$\dot{X} = P_0 X + q f^0(r^T X), \quad X \in \mathbb{R}^3, \tag{27}$$

if the stable periodic solution $X^0(t)$ close to harmonic one is determined. Then for the localization of an attractor of the original system (26), one can follow numerically the transformation of this periodic solution (a starting oscillating is an attractor, not including equilibrium, denoted further by A_0) simply increasing j.

By non singular linear transformation S ($X = SZ$) the system (27) can be reduced to the form

$$\begin{cases} \dot{z}_1(t) &= -\omega_0 z_2(t) + b_1 g^0(z_1(t) + c_3^T z_3(t)) \\ \dot{z}_2(t) &= \omega_0 z_1(t) + b_2 g^0(z_1(t) + c_3^T z_3(t)) \\ \dot{z}_3(t) &= a_3 z_3(t) + b_3 g^0(z_1(t) + c_3^T z_3(t)) \end{cases}, \tag{28}$$

where $z_1(t)$, $z_2(t)$, $z_3(t)$ are scalar values, a_3, b_1, b_2, b_3, c_3 are real numbers and $a_3 < 0$.

The describing function H is defined as

$$H(\varsigma) = \int_0^{\frac{2\pi}{\omega_0}} g(\cos(\omega_0 t)\varsigma)\cos(\omega_0 \varsigma) dt. \tag{29}$$

Theorem 2. *[8] If it can be found a positive ς_0 such that*

$$H(\varsigma_0) = 0, \quad b_1 \frac{dH(\varsigma)}{d\varsigma} \mid_{\varsigma=\varsigma_0} < 0,$$

has a stable periodic solution with initial data $X^0(0) = S(z_1(0),\, z_2(0),\, z_3(0))^T$ at the initial step of algorithm one has $z_1(0) = \varsigma_0 + O(\varepsilon)$, $z_2(0) = 0$, $z_3(0) = O_{n-2}(\varepsilon)$, where $O_{n-2}(\varepsilon)$ is an $(n-2)$-dimensional vector such that all it's components are $O(\varepsilon)$.

REFERENCES

[1] lin. H, Wang. Ch, Xu. C, Zhang. X(2022).,*A memristive synapse control method to generate diversified multi-structure chaotic attractors.*, IEEE Transactions on Computer-aided design of integrated circuits and systems, vol. 42.

[2] N Wang, Mengkai. C.U.I, Xihong. Y.U(2023)., *Generating multi-folded hidden Chua's attractors: Two-case study*, Chaos, Solitons and Fractals, vol. 177, p.114242.

[3] Wang. N, Zhang. G., Kuznetsov. N. V., and Li. H(2022)., *Generating grid chaotic sea from system without equilibrium point*, Communications in Nonlinear Science and Numerical Simulation, vol. 107, p.106194.

[4] Wang. N, Dan. X.U, Ze. L.E(2023)., *A general configuration for nonlinear circuit employing current-controlled nonlinearity: Application in Chua's circuit*. Chaos, Solitons and Fractals, vol. 177, p.114233.

[5] Kuznetsov. Y.A(1998), Elements of Applied Bifurcation Theory. *Springer, New York*.

[6] Deng. Q, wang. Ch(2019)., Multi-scroll hidden attractors with two stable equilibrium points. *AIP Publishing Chaos*, vol. 29, pp.093112-093121.

[7] Vandewalle. J and Vandenberghe. L(1995)., Piecewise-linear circuits and piecewise-linear analysis, *in The Circuits and Filters Handbook, W. K. Chen, Ed. Boca Raton, FL: CRC*, pp. 1034-1057.

[8] Leonov. G.A, Vagaitaev. V.I and Kuznetsov. N.V(2010)., Algorithm for localizing Chua attractors based on the harmonic linearization method, *Dokl. Math*,vol. D, pp.663-666.

[9] Lin. H, Wang. Ch, Sun. Y, Wang. T(2023)., *generating n- scroll chaotic attractors from a memristor- based magnetized hopfield neural network*, IEEE Transactions on circuits and system II: Express Briefs, vol. 70, pp.311-315.

[10] Zaamoune. F, Menacer. T, Lozi. R. and Chen. G(2019)., Symmetries in Hidden Bifurcation Routes to Multiscroll Chaotic Attractors Generated by Saturated Function Series, *Journal of Advanced Engineering and Computation*, Vol.3(4), pp.511-522.

[11] Menacer. T, Lozi. R and Chua. L.O(2016)., Hidden bifurcations in the multispiral Chua attractor, *International Journal of Bifurcation and Chaos*, Vol. 16(4), pp.1630039-1630065.

[12] Leonov. G.A(2010)., Effective methods for periodic oscillations search in dynamical systems, Appl. Math Mech, vol. 74, pp.37-73

[13] Leonov. G.A, Kuznetsov. N.V(2016)., and A Prasad, Hidden attractors in dynamical systems, *Physics Reports*, vol. 637, pp.1-50.

[14] Leonov. G.A, Kuznetsov. N.V(2011)., Localization of hidden Chua's attractors, Phys. Lett. A, vol. 375, pp.2230-2233.

[15] Leonov. G.A, Kuznetsov. N.V(2011)., Analytical numerical methods for investigation of hidden oscillations in nonlinear control systems, Proc. 18th IFAC World Congress, Milano, Italy, August, vol. 28, pp.2494-2505.

[16] Leonov. G.A, Kuznetsov. N.V(2013)., Hidden attractors in dynamical systems. From hidden oscillations in Hilbert Kolmogrov, Aizerman, and Kalman problems to hidden chaotic attractor in Chua circuits, International Journal of Bifurcation and Chaos, vol. 23, pp.1330002-1-330002-69.

[17] Lü. J, Chen. G, Yu. X, Leung. H(2004)., Design and analysis of multiscroll chaotic attractors from saturated function series, *IEEE Trans.Circuits Syst*, vol. 51(12), pp.2476-2490.

[18] Ahmed. E, El-Sayed, El-Saka.H.A(2006)., *On some Routh-Hurwitz conditions for fractional order differential equations and their applications in Lorenz, Rossler, Chua and Chen systems*, Physics Letters A, vol. 358, pp.1-4.

[19] Zaamoune.F, Tidjani. M(2022).,*Hidden modalities of spirals of chaotic attractor via saturated function series and numerical results*, Analysis and Mathematical Physics, vol. 108, pp.1-21.

[20] Zaamoune.F, Tidjani. M(2023) *The behavior of hidden bifurcation in 2D scroll via saturated function series controlled by a coefficient harmonic linearization method*, Demonstratio Mathematica, vol. 56(1), pp.20220211.

Bat Algorithm for Solving IVPs of Current Expression in Series RL Circuit Constant Voltage Case

IJAMS Peer-reviewed journal
International Journal of Applied Mathematics and Simulation

Bat Algorithm for Solving IVPs of Current Expression in Series RL Circuit Constant Voltage Case

Fatima Ouaar [1]

ABSTRACT: In this paper, an efficient method for solving Initial Value Problems (IVPs) in Ordinary Differential Equations (ODEs) used in the fields of electronics and electrical engineering is demonstrated. The method is based on the Bat-Inspired Algorithm (BA), which simulates the echolocation navigation system used by bats to detect and pursue their prey. In the case of constant voltage, the IVPs arise from an RL circuit consisting of a resistor and an inductor connected in series. The suggested method's usability and effectiveness are confirmed by the experimental results obtained by numerical example. The findings reveal that the BA algorithm produces a satisfactory and precise approximation of the answers when compared to the exact solution in terms of solution quality.

Keywords: Bat Algorithm (BA), Initial Value Problems (IVP), Series RL circuit

MSC: 65-05, 65L05, 65D99.

1 Introduction

In the field of engineering science, a variety of issues are brought about by the rapid advancement of modern living and require accurate, fast solutions to challenges that are typically complicated and challenging. Therefore, optimization algorithms [19] are the means of solving this problem, with the exception of several heuristic approaches found in conventional optimization techniques, which are still insufficient. Nonetheless, because nature often finds the best solution to an issue, it is seen as a source of inspiration for tackling a variety of challenges [16].

• [1] *Fatima Ouaar, Corresponding Author, Laboratory of Applied Mathematics, Mohamed Khider University, Biskra, Algeria. E-mail: f.ouaar@univ-biskra.dz*

Communicated Editor: Mohamed Berbiche
Manuscript received Mar 28, 2024; revised Nov 20, 2024; accepted Dec 03, 2024; published Dec 07, 2024.

Because of this, several academics from various disciplines are motivated to develop a range of metaheuristic algorithms that take advantage of various operators that are modeled after natural processes [9]. An optimization issue can be solved in the simplest way possible using metaheuristic algorithms [2]. Compared to standard algorithms and iterative approaches, it can typically discover very good solutions with less computing work. It also has a high number of searched variables and a quick convergence time.

By adopting various forms in accordance with the inspired process of the systems [22], such as Particle Swarm Optimization (PSO) [13], Genetic Algorithm (GA) [7], Ant Colony Optimization (ACO) [4], Bee algorithm [12], [5], and the Flower Pollination Algorithm (FPA) [19], [20], etc.

Yang initially presented the Bat Algorithm (BA) as a substitute technique for numerical optimization in 2010 [21], [23]. It produces high echolocation, which is the technique of locating an item by reflected sound, to simulate the behavior of bats in finding prey. By producing loud noises, one may cancel out echoes that reverberate from various environments at varying frequencies [19].

To get beyond its shortcomings and capitalize on their advantages, BA was combined with other nature-inspired metaheuristic algorithms. In this regard, some adjustments have been suggested to enhance BA's performance. In [18], for instance, a BA that uses Lévy Flights and Differential Evolution (DE) operators during optimization is presented. Distribution to boost BA's search skills. A directional BA was reported in 2017 [3], suggesting the use of directed echolocation to enhance BA exploration. A noteworthy enhancement was suggested in [6], whereby the hybridization of BA and DE is employed. In order to improve the search capabilities of BA, the standard BA has also been altered to use chaotic maps rather than normal distribution [17], [14]. Additionally, a version of BA that takes the GA and Invasive Weed Optimization (IWO) [24] into account has been introduced. Numerous fields find use for BA and its expansions, including fuzzy logic, image processing, classifications, clustering and data mining, inverse problems and parameter estimation, combinatorial optimization, scheduling, and fuzzy logic in continuous optimization in engineering design.

A first order RL circuit, also known as an RL filter or RL network [1], in electronics and electrical engineering, is an electric circuit made up of an inductor and a resistor, which may be operated in parallel or series by a current source [10] or a voltage source [11]. This work is significant because it addresses the IVP that result from a series RL circuit when the voltage is constant as an optimization problem. The BA results and the results of the Range Kutta 4^{th} order approach are contrasted with the acquired results since the BA [23] is utilized as a tool to identify optimal numerical solutions to this issue.

The structure of this paper is as follows. Section 2 presents the issue formulation; Section 3 gives an overview of BA and the key procedures for estimating an IVP solution. Essential formulas and a brief explanation of series RL circuit ODEs are provided in Section 4 which exposes also an example of series RL circuit IVPs to show how BA can lead to a satisfactory result for solving IVP. The comments and conclusion are made in section 5.

2 FORMULATION OF THE PROBLEM

Let $f = f(x, y)$ be a real-valued function of two real variables defined for $a \leq x \leq b$, where a and b are

finite, and for all real values of y. The equations

$$\begin{cases} y^{'} = f(x,y) \\ y(a) = y_0 \end{cases}, \tag{1}$$

are called initial-value problem (IVP); they symbolize the following problem: To find a function $y(x)$, continuous and differentiable for $x \in [a,b]$ such that $y' = f(x,y)$ from $y(a) = y_0$ for all $x \in [a,b]$ [8].
This problem possesses unique solution when: f is continuous on $[a,b] \times \mathbb{R}$, and satisfies the Lipschitz condition; it exists a real constant $k > 0$, as $\mid f(x,\theta_1) - f(x,\theta_2) \mid \leq k \mid \theta_1 - \theta_2 \mid$, for all $x \in [a,b]$ and all couple $(\theta_1, \theta_2) \in \mathbb{R} \times \mathbb{R}$.
Finding the optimal solutions numerically of an initial-value problem (IVP) is gotten with approximations: $y(x_0 + h), \ldots, y(x_0 + nh)$ where $a = x_0$ and $h = (b-a)/n$. For more precision of the solution, we must use a very small step size h that includes a larger number of steps, thus more computing time which not available in the useful numerical methods like Euler and Runge-Kutta methods [8], which may approximate solutions of (IVP) and perhaps yield useful information, often sufficing in the absence of exact, analytic solutions.

2.1 Objective function

Utilizing the finite difference formula for the derivative and equation is the algorithm's primary concept (1) we obtain,

$$\frac{y(x_j) - y(x_{j-1})}{h} \approx f(x_{j-1}, y(x_{j-1})),$$

thus,

$$\frac{y_j - y_{j-1}}{h} \approx f\left(x_{j-1}, y_{j-1}\right),$$

consequently, we have to consider the error formula:

$$\left[\frac{y_j - y_{j-1}}{h} - f\left(x_{j-1}, y_{j-1})\right)\right]^2.$$

The objective function, associated to $Y = (y_1, y_2, ..., y_d)$ will be:

$$F(Y) = \sum_{j=1}^{d} \left[\frac{y_j - y_{j-1}}{h} - f\left(x_{j-1}, y_{j-1}\right)\right]^2. \tag{2}$$

2.2 Consistency

We are interested in the calculation of $Y = (y_1, y_2, ..., y_d)$ which minimizes the objective function equation (2). We have from Taylor's formula order 1;

$$y_j = y_{j-1} + hy'_{j-1} + O\left(h^2\right), j = 1, \cdots d.$$

So,

$$\frac{y_j - y_{j-1}}{h} = y'_{j-1} + O(h)$$

If we subtract $f(x_{j-1}, y_{j-1})$ from both sides of last equation, we obtain

$$\frac{y_j - y_{j-1}}{h} - f(x_{j-1}, y_{j-1}) = y'_{j-1} - f(x_{j-1}, y_{j-1}) + O(h), j = 1, \cdots d$$

The last relation shows that the final value $Y = (y_1, y_2, \cdots, y_d)$ is an approximate solution of IVP, for small value of h.

3 BAT ALGORITHM OVERVIEW

Yang introduced the bat method in 2010 [23]. Given that microbats are capable of producing high echolocation, it mimics their echolocation behavior. This advantageuse algorithm may be summarized as [21].

3.1 Idealized rules of BA

1) All bats sense distance via echolocation, and they also somehow magically 'know' the difference between background obstacles and food/prey.
2) Bats look for food by flying randomly at position x_i at velocity v_i, fixed frequency f_{min}, changing wavelength λ, and loudness A_0. Depending on how close their target is, they may automatically modify the wavelength (or frequency) and rate of pulse emission $r \in [0, 1]$.
3) We assume that the loudness changes from a big (positive) A_0 to a minimal constant value A_{min}, even though it might fluctuate in many other ways.

3.2 Mathematical equations

Virtual bats are moved in accordance with the following equations to generate new solutions:

$$f_i = f_{\min} + (f_{\max} - f_{\min})\,\beta$$
$$v_i^t = v_i^{t-1} + \left(x_i^t + x_*\right) f_i$$
$$x_i^t = x_i^{t-1} + v_i^t$$

Where β is a random vector selected from a uniform distribution with $\beta \in [0, 1]$. After comparing every answer among every bat, x_* is the current global best position (solution). the equation's present optimal solution

$$x_{new} = x_{old} + \partial A^t$$

where A^t is the average loudness of all the best at this time step, and $\partial \in [-1, 1]$ is a random value. The volume may be adjusted to any convenient level since, after a bat has discovered its target, it normally becomes quieter while its rate of pulse emission rises.

3.3 Pseudo code of BA

Objective function $f(x)$, $x = (x_1, ..., x_d)^T$

Initialize the bat population $x_i (i = 1, 2, ..., n)$and v_i

Define pulse frequency $f_i$at x_i

Initialize pulse rates $r_i$and the loudness A_i

while ($t < Maxnumberofiterations$)

Generate new solutions by adjusting frequency,

and updating velocities and locations/solutions

if ($rand > r_i$)

Select a solution among the best solutions

Generate a local solution around the selected best solution

end if

Generate a new solution by flying randomly

if ($rand < A_i$& $f(x_i) < f(x_*)$)

Accept the new solutions

Increase ri and reduce A

end if

Rank the bats and find the current best x_*

end while

Postprocess results and visualization

4 NUMERICAL APPLICATION

All calculations for our experimental investigation were carried out using an Intel Duo Core 2.20 GHz PC running MSWindow 2007 Professional and the Matlab environment version R2013a compiler. Graphical and tabular representations of the numerical results are provided. The BA findings are shown in table 2 in comparison to the precise outcomes for the problem under study as well as, the absolute error. Two kinds of parameters are required for the issue treatment: the first is connected to BA , and the second is related to IVP provides. the parameter settings needed to produce the BA is presented via Table 1. Tables 3 and 4 are for computational time results and statistical analysis results respectively.

4.1 Solving Series RL Circuit ODE's as application

In Figure 1, an inductor and a resistor are linked in series to create the RL circuit. When the switch is closed, a constant voltage V is applied [1]. The voltage across the resistor is given by$V_R = Ri$. The voltage across the inductor is given by $V_L = L\frac{di}{dt}$. Kirchhoff's voltage law says that the directed sum of the voltages around a circuit must be zero. This results in the following differential equation [11]:

$$Ri + L\frac{di}{dt} = V.$$

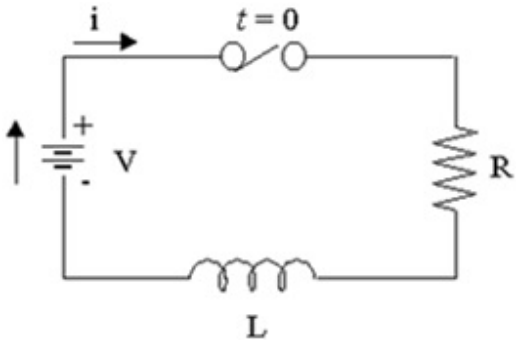

Fig. 1. The RL circuit diagram

Once the switch is closed, the current in the circuit is not constant. Instead, it will build up from zero to some steady state. The solution of this differential equation is

$$i = \frac{V}{R}(1 - e^{(-(\frac{R}{L})t)}). \tag{3}$$

Example study: A series RL circuit with $R = 50\Omega$ and $L = 10H$ has a constant voltage $V = 100V$ applied at $t = 0$ by the closing of a switch. We want to find the current expression in this case, then the formula 3 can be used here only because the voltage is constant and can not work in the alternative case. For application needs eq. 4 is given:

$$i = 2(1 - \exp(-5t)). \tag{4}$$

When plotting eq. 4, the graph shows the transition period during which the current adjusts from its initial value of zero to the final value $\frac{V}{R}$, which is the steady state [10]. The time constant (TC), known as τ of the function is the time at $\frac{R}{L}$ is unity $(= 1)$. Thus for the RL transient, the time constant is $\tau = \frac{L}{R}$ Seconds In this example, the time constant, TC, is 0.2 Seconds.

4.2 Related parameters

BA is a tool for optimization. After that, the discretization form of the fundamental differential equation is converted. When the derivative term in the discretized form is substituted by a difference quotient for approximations, the differential equation may be transformed into discretization form using the backward difference formula.

The following are the parameters linked to IVP:

1) The length of the IVP interval, $h = (b - a)/(n + 1)$, is an evenly partitioned subinterval of length $(n + 1)$.
2) There are nine internal nodes.
3) $h = 0.2$ is the step size.
4) The differential equation is solved between $t > 0$ and the initial condition, $i = 0$ for $t = 0$.

Parameter	Quantity
Dimension of the search variables (d)	10
Number of generations (N)	1000
Population size (n)	20
Loudness (constant or decreasing) (A)	0.5
Pulse rate (constant or decreasing) (r)	0.5

TABLE 1

Parameters adopted by (BA).

i	x_i	$ExactResults$	$NumericalResults$		$AbsoluteError$	
			BA	$RK4$	BA	$RK4$
0	0.00	0.0000	0.0000	0.0010	0.0000	0.001
1	0.14	1.0068	1.0074	1.0079	0.0006	0.0011
2	0.28	1.5068	1.5076	1.5083	0.0008	0.0015
3	0.42	1.7551	1.7560	1.7569	0.0009	0.0018
4	0.56	1.8784	1.8794	1.8805	0.0010	0.0021
5	0.70	1.9396	1.9408	1.9421	0.0012	0.0025
6	0.84	1.9700	1.9715	1.9729	0.0015	0.0029
7	0.98	1.9851	1.9869	1.9884	0.0018	0.0033
8	1.12	1.9926	1.9946	1.9963	0.0020	0.0037
9	1.26	1.9963	1.9986	2.0004	0.0023	0.0041
10	1.40	1.9982	2.0008	2.0028	0.0026	0.0046

TABLE 2

Numerical Results of the Example for d=10

5) The role of the objective

$$\begin{aligned} F(y_1, y_2, ..., y_{10}) &= \sum_{j=1}^{10} \left(\frac{y_j - y_{j-1}}{h} - f(x_{j-1}, y_{j-1}) \right)^2 \\ &= \sum_{j=1}^{10} \left(\frac{y_j - y_{j-1}}{h} - y_{j-1} \right)^2 \end{aligned}$$

The parameters adopted by BA in the treated example are summarized in Table 1:

4.3 Numerical results

The comparison between the performances of BA and $RK4$ face to the exact results are shown in the Table 2 and their graphical representations is in the Figure 2 In both representations of the results confirm that BA is better than $RK4$ because it has a very close curve to the exact curve contrary to $RK4$ method. BA method offers a very negligible absolute error compared to $RK4$ method.

The findings of our simulations show that BA is straightforward, adaptable, and simple to apply. It also saves time by rapidly achieving convergence at an early stage and transitioning from exploration to exploitation. It provides encouraging best practices for resolving IVP.

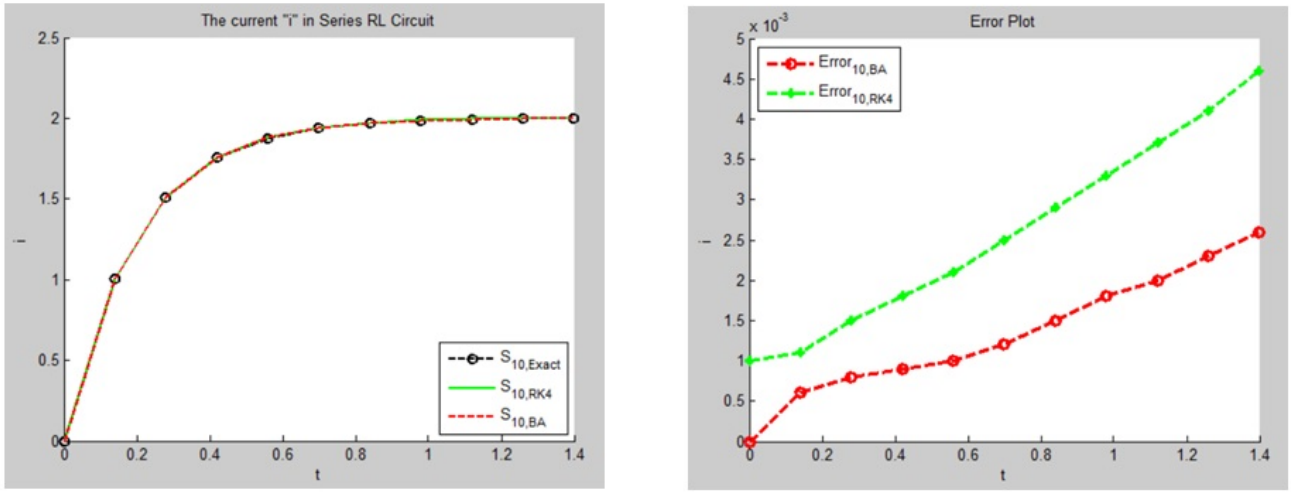

a)- Exact results, BA and RK4 results.

b)- Absolute error.

Fig. 2. Application example results.

Algorithm	Time
BA	4.687
$RK4$	5.039

TABLE 3

Average computational time of up to 50xD iterations by the used algorithms using 50 trials for the example

4.4 Computational time results

The average computing time (in seconds) for each of the 50 distinct trials of the chosen algorithms for the examined case, calculated using the dimensional space $D = 10$, is shown in Table 3. It is evident that the BA algorithm maintained a computing time that was competitive when compared to the Range Kutta 4^{th} $(RK4)$ order approach, which is a significant benefit that stems directly from straightforward population update processes.

4.5 Statistical analysis

This section of the paper deals with the statistical analysis of data acquired by the proposed BA and compared to the $RK4$ technique after demonstrating the advantage of BA with regard to computing times. These studies should give enough information to understand how BA works better than the $RK4$ technique. In the dimension $D = 10$, table 4 presents the mean and standard deviation of the difference between the computed optimum values and the genuine optimum values. The best-performing algorithm, according to the results, was BA.

Algorithm	Mean	STD
BA	0.8334	0.9570
$RK4$	0.8339	0.9573

TABLE 4
Statistical results obtained for the studied example over Dim =10.

5 CONCLUSION

This study discusses the usage of standard BA for solving IVPs when it's applied as a tool to numerically optimize the IVPs that arise in the field of electrical engineering and are ODEs of the series RL circuit in the voltage constant case through a selected example. When the precise answers, algorithmic results, and $RK4$ method results were compared, it was shown that BA outperformed $RK4$ method by providing exact solutions with the least amount of error.

BA excels in handling complex issues and has a remarkable capacity to tackle a wide range of problems, including highly nonlinear situations. Further research on BA will enhance the algorithm through profound studies on parameter tuning, parameter control, accelerating coverage, adding Bat smell observation property, using a wider variety of parameters, conducting more thorough comparison studies with more open-source algorithms, and so on. Additionally, BA ought to be used in a number of engineering and industrial optimization applications.

ACKNOWLEDGEMENT

The author wish to thank the referees and editors for their valuable comments and suggestions which led to improvements in the document.

DECLARATION

The author declares no conflict of interest.

REFERENCES

[1] A .Abdon, N. Juan Jose, Numerical solution for the model of RLC circuit via the fractional derivative without singular kernel. Advances in Mechanical Engineering. 7(10) (2015), 1–7.

[2] A. Askarzadeh, A novel metaheuristic method for solving constrained engineering optimization problems: Crow search algorithm. Computers and Structures, 169(Complete) (2016).

[3] A. Chakri, R. Khelif, M. Benouaret, X.S. Yang, New directional bat algorithm for continuous optimization problems. Expert Systems with Applications. Volume 69, (2017), 159-175.

[4] M. Dorigo, V. Maniezzo, A. Colorni, The ant system: optimization by a colony of cooperating agents. IEEE Trans. Syst. Man Cybern, B 26 (1996), 29-41.

[5] L. Djerou, N. Khelil, S. Aichouche, Artificial Bee Colony Algorithm for Solving Initial Value Problems. Communications in Mathematics and Applications, RGN Publications, 8(2) (2017), 119-125.

[6] I. Fister, D. Fister, X.S. Yang, A hybrid bat algorithm. ELEKTROTEHNIŜKI VESTNIK 80(1-2): 1–7, 2013

[7] D.E. Goldberg, Genetic Algorithms in Search. Optimization and Machine Learning. Addison Wesley. (1989)

[8] P. Henrici, Elements of Numerical Analysis. Mc Graw-Hill. New York, (1964).

[9] J. H. Holland, Adaptation in Natural and Artificial Systems. University of Michigan Press. (1975).

[10] P. Horowitz, W. Hill, The Art of Electronics. 2nd Edition. Cambridge University Press. (1989).

[11] W. N. James, S. A Riedel, Electric Circuits. Prentice Hall Publisher. ISBN: 13:978-0-13-376003-3. (2015).

[12] D. Karaboga, B. Basturk, A powerful and efficient algorithm for numerical function optimization: artificial bee colony (ABC) algorithm. Journal of Global Optimization, 39 (2007), 459-47.

[13] J. Kennedy, R. C. Eberhart, Particle swarm optimization. In: Proceedings of IEEE International Conference on Neural Networks. No. IV. 27 Nov–1 Dec, pp. 1942–1948, Perth Australia, (1995).

[14] X. Meng, X. Gao, Y. Liu, H. Zhang, A novel bat algorithm with habitat selection and doppler effect in echoes for optimization. Expert Systems with Applications, Vol. 42(17-18) 2015, 6350-6364.

[15] G. D., Mateescu . (2005). Optimization by using evolutionary algorithms with genetic acquisitions. Journal for Economic Forecasting, 2(2), 26-30.

[16] S. Nitesh, New inspiration in nature – A survey. International journal of computer applications and information technology, (2012), 21-24.

[17] J. A. Rezaee, Chaotic bat swarm optimisation (cbso). Appl Soft Comput; 26(C):523{30. doi:10.1016/j.asoc.2014.10.010. (2015).

[18] J. A.Xie, Y. A. Zhou, H. Chen, A novel bat algorithm based on differential operator and lévy fights trajectory. Computational Intelligence and Neuroscience; 2013. doi:R10.1155/2013/453812, (2013).

[19] X. S. Yang, Book Nature Inspired Optimization Algorithm. Elsevier. (2014).

[20] X. S. Yang, Flower Pollination Algorithm for Global Optimization, arXiv: 1312.5673v1 [math.OC] 19 Dec, (2013).

[21] X. S. Yang, A. H. Gandomi, Bat algorithm: a novel approach for global engineering optimization. Eng. Comput. 29(5) (2012), 464-483.

[22] X. S. Yang, Nature-Inspired Metaheuristic Algorithms. Luniver Press. (2008)

[23] X. S. Yang, New Metaheuristic Bat-Inspired Algorithm. Berlin, Heidelberg: Springer Berlin Heidelberg. (2008).

[24] S. Yilmaz, E.U. Küçüksille, A new modification approach on bat algorithm for solving optimization problems. Applied Soft Computing, (2015) Volume 28, Pages 259-275.

A Log-Probability-Weighted-Moments type estimator for the extreme value index in a truncation scheme

IJAMS Peer-reviewed journal
International Journal of Applied Mathematics and Simulation

A Log-Probability-Weighted-Moments type estimator for the extreme value index in a truncation scheme.

Souad Benchaira[1], Saida Mancer[2] and Abdelhakim Necir[3]

ABSTRACT: The limit theorems of asymptotic behavior of tail index estimators for right truncation Pareto-like data requires some regularity assumptions either on tail indices ($\gamma_1 < \gamma_2$) or on the dependence structure condition between the truncation variable and the interest one. In this paper, we introduce a new estimator for the tail index based on the Log-Probability-Weighted-Moments method and, getting rid of aforementioned assumptions, we establish its consistency and asymptotic normality. We show, by simulation, that the newly proposed estimator behaves well both in terms of bias and mean squared error.

Keywords: Empirical process, Extreme value index, Product-limit estimator, Truncated data.

MSC: Primary 62G32, 62G30, Secondary 60G70, 60F17.

1 INTRODUCTION

Let (X_i^*, Y_i^*), $i = 1, ..., N \geq 1$ be a sample from a couple (X^*, Y^*) of independent positive random variables (rv's) defined over some probability space $(\Omega, \mathcal{A}, \mathbf{P})$, with continuous distribution functions (df's) F^* and G^* respectively. Suppose that X^* is right-truncated by Y^*, in the sense that X_i^* is only observed when $X_i^* \leq Y_i^*$. Throughout the paper, we will use the notation $\overline{\mathcal{S}}(x) := \mathcal{S}(\infty) - \mathcal{S}(x)$, for any $\mathcal{S}$. We assume that both right-tail functions $\overline{F}^*$ and $\overline{G}^*$ are regularly varying at infinity with respective tail indices $-1/\gamma_1$ and $-1/\gamma_2$, notation: $\overline{F}^* \in \mathcal{RV}_{(-1/\gamma_1)}$ and $\overline{G}^* \in \mathcal{RV}_{(-1/\gamma_2)}$. That is, for any $s > 0$

$$\frac{\overline{F}^*(st)}{\overline{F}^*(t)} \to s^{-1/\gamma_1} \text{ and } \frac{\overline{G}^*(st)}{\overline{G}^*(t)} \to s^{-1/\gamma_2}, \text{ as } t \to \infty. \tag{1.1}$$

Let us now denote (X_i, Y_i), $i = 1, ..., n$, to be the observed data, as copies of a couple of rv's (X, Y) with joint df $\mathcal{T}$, corresponding to the truncated sample (X_i^*, Y_i^*), $i = 1, ..., N$, where $n = n_N$ is a sequence of discrete rv's. By the strong law of the large numbers, we have

$$n_N/N \to \mathbf{P}(X^* \leq Y^*) = \int_0^\infty \overline{G}^*(z)\, dF^*(z) =: p, \tag{1.2}$$

- [1] *Souad Benchaira, Laboratory of Applied Mathematics, Mohamed Khider University, Biskra, Algeria. E-mail: benchaira.s@hotmail.fr*
- [2] *Saida Mancer, Laboratory of Applied Mathematics, Mohamed Khider University, Biskra, Algeria. E-mail: mancer.saida731@gmail.com*
- [3] *Abdelhakim Necir, Corresponding Author, Laboratory of Applied Mathematics, Mohamed Khider University, Biskra, Algeria. E-mail: ah.necir@univ-biskra.dz*

Communicated Editor: Cherfaoui Mouloud
Manuscript received Jan 23, 2024; revised May 13, 2024; accepted May 18, 2024; published Dec 07, 2024.

as $N \to \infty$, almost surely (a.s.), where p stands for the percentage of the observed data. This property allows us to assume, without loss of generality, that for any subsequence a_n of n, we may drop "a.s." in the strong limit $a_n \dot{\to} a \leq \infty$ as $N \to \infty$. For $x, y \geq 0$, we have

$$\mathcal{T}(x,y) := p^{-1} \int_0^y F^*(\min(x,z))\, dG^*(z),$$

having (marginal) right-tails

$$\overline{F}(x) = -p^{-1} \int_x^\infty \overline{G}^*(z)\, d\overline{F}^*(z) \text{ and } \overline{G}(y) = -p^{-1} \int_y^\infty F^*(z)\, d\overline{G}^*(z).$$

Note that $\overline{F} \in \mathcal{RV}_{(-1/\gamma)}$ and $\overline{G} \in \mathcal{RV}_{(-1/\gamma_2)}$, where $\gamma := \gamma_1\gamma_2/(\gamma_1+\gamma_2)$ (see, e.g., [7]). Motivated by an application to real dataset of lifetimes of automobile brake pads ([13], page 69), recently [7] introduced an estimator of γ_1 defined by

$$\widehat{\gamma}_1(k_1,k_2) := \frac{\widehat{\gamma}_2(k_2)\,\widehat{\gamma}(k_1)}{\widehat{\gamma}_2(k_2) - \widehat{\gamma}(k_1)},$$

where $k_1 = k_1(n)$ and $k_2 = k_2(n)$ are two distinct sample fractions used, respectively, in Hill's estimators ([10])

$$\widehat{\gamma}(k_1) := \frac{1}{k_1}\sum_{i=1}^{k_1} \log \frac{X_{n-i+1:n}}{X_{n-k_1:n}} \text{ and } \widehat{\gamma}_2(k_2) := \frac{1}{k_2}\sum_{i=1}^{k_2} \log \frac{Y_{n-i+1:n}}{Y_{n-k_2:n}},$$

of tail indices γ and γ_2, with $X_{1:n} \leq ... \leq X_{n:n}$ and $Y_{1:n} \leq ... \leq Y_{n:n}$ being the order statistics pertaining to the samples $(X_1,...,X_n)$ and $(Y_1,...,Y_n)$ respectively. [2] considered a single sample fraction $k = k_1 = k_2$ satisfying $1 < k < n$, $k \to \infty$ and $k/n \to 0$, as $N \to \infty$, and defined the corresponding estimators of γ, γ_2 and γ_1 by

$$\widehat{\gamma} := \frac{1}{k}\sum_{i=1}^{k} \log \frac{X_{n-i+1:n}}{X_{n-k:n}},\ \widehat{\gamma}_2 := \frac{1}{k}\sum_{i=1}^{k} \log \frac{Y_{n-i+1:n}}{Y_{n-k:n}},$$

and

$$\widehat{\gamma}_1^{(\mathbf{GS})} := \frac{\frac{1}{k}\sum_{i=1}^{k}\sum_{j=1}^{k} \log \frac{X_{n-i+1:n}}{X_{n-k:n}} \log \frac{Y_{n-j+1:n}}{Y_{n-k:n}}}{\sum_{i=1}^{k} \log \frac{Y_{n-i+1:n}X_{n-k:n}}{Y_{n-k:n}X_{n-i+1:n}}}.$$

Assuming regular variation conditions (1.1) and the tail dependence assumption (see, e.g., [16]) , they also provided a Gaussian representation is terms of a two-parameter Wiener process which leads to asymptotic normality of $\widehat{\gamma}_1^{(\mathbf{GS})}$. More recently, [3] proposed a new estimation method based on the product-limit estimator of underlying df F^*, to derive the following estimator

$$\widehat{\gamma}_1^{(\mathbf{BMN})} := \left(\sum_{i=1}^{k} \frac{F_n^*(X_{n-i+1:n})}{C_n(X_{n-i+1:n})}\right)^{-1} \sum_{i=1}^{k} \frac{F_n^*(X_{n-i+1:n})}{C_n(X_{n-i+1:n})} \log \frac{X_{n-i+1:n}}{X_{n-k:n}},$$

where

$$F_n^*(x) := \prod_{i:X_i>x} \exp\left\{-\frac{1}{nC_n(X_i)}\right\},$$

is the so-called product-limit Woodroofe's estimator [18] of df F^* and $C_n(x) := n^{-1}\sum_{i=1}^{n} \mathbb{I}_{\{X_i \leq x \leq Y_i\}}$, where $\mathbb{I}_A$ stands for the indicator function of set A. The authors also established the consistency and asymptotic normality of their estimator but by considering only the case $\gamma_1 < \gamma_2$. More precisely

$$\sqrt{k}\left(\widehat{\gamma}_1^{(\mathbf{BMN})} - \gamma_1\right) \xrightarrow{\mathcal{D}} \mathcal{N}\left(\mu, \sigma_1^2\right), \text{ as } n \to \infty,$$

where

$$\sigma_1^2 := \gamma^2\left(1 + (\gamma_1/\gamma_2)\right)\left(1 + (\gamma_1/\gamma_2)^2\right)/\left(1 - (\gamma_1/\gamma_2)\right).$$

The bias reduction of this estimator was addressed in [4], [3], [11] and more recently in [14]. For their part, [19] proposed a similar estimator to $\widehat{\gamma}_1^{(\mathbf{BMN})}$ (with deterministic threshold) and established its asymptotic normality by assuming condition $\gamma_1 < \gamma_2$ as well. Although this condition seems reasonable, it is better that it is not imposed. In conclusion, as mentioned above, the asymptotic behavior of the already proposed estimators was studied either by making restriction of tail indices or by assuming the tail dependence condition between the truncation and truncated rv's. To get rid of these assumptions, we propose an alternative estimation method that we next give their details.

1.1 New estimator for the tail index γ_1

We have already noticed that both two estimators of the tail index γ_1, given by [3] and [19], are based on the nonparametric product-limit estimators of the underlying df F^*. Although , this approach provides good estimators in terms of bias and the root mean squared error (rmse), their corresponding consistency and asymptotic normality are valid only for Pareto-type models satisfying assumption $\gamma_1 < \gamma_2$. Then our main goal is to define an estimator for γ_1 that works for both $\gamma_1 < \gamma_2$ and $\gamma_1 \geq \gamma_2$. To this end, we introduce a new estimation method inspired by the log probability weighted moments (LPWM) estimation method, for complete data, given recently by [5]. Let us define the following ratio of tail expectations

$$L_t(r,s) := \frac{\mathbf{E}\left[\left(\overline{G}(X)\right)^r (\log(X/t))^s \mid X > t\right]}{\mathbf{E}\left[\left(\overline{G}(X)\right)^r \mid X > t\right]},\ r,s \geq 0,\ t > 0.$$

For suitable values of r and s with large t, the ratio $L_t(r,s)$ serve us to estimate the tail indices $(\gamma, \beta, \gamma_2)$ and also the second-order parameters (ρ_F, ρ_H, ρ_G), given in (2.1) and (2.2), which is out of scope of the paper. Indeed, we showed in Proposition 6.1, that

$$L_t(r,s) \to \left(\frac{\gamma_1\gamma}{(1+r)\gamma_1 - r\gamma}\right)^s \Gamma(s+1),\ \text{as } t \to \infty,$$

where $\Gamma : z \to \int_0^\infty x^{z-1}e^{-x}dx$, $z > 0$, is the usual gamma function. In particular, we have

$$\gamma_t := L_t(0,1) = \frac{\int_t^\infty \log(x/t)\, dF(x)}{\overline{F}(t)} \to \gamma,\ \text{as } t \to \infty$$

and

$$\beta_t := L_t(1,1) = \frac{\int_t^\infty \overline{G}(x)\log(x/t)\, dF(x)}{\int_t^\infty \overline{G}(x)\, dF(x)} \to \beta,\ \text{as } t \to \infty,$$

where

$$\beta := \frac{\gamma_1\gamma}{2\gamma_1 - \gamma} = \frac{\gamma_1\gamma_2}{2\gamma_1 + \gamma_2}.$$

This mean that

$$\overline{H}(x) := \frac{\int_x^\infty \overline{G}(x)\, dF(x)}{\int_0^\infty \overline{G}(x)\, dF(x)}$$

is regularly varying with at infinity with tail index $-1/\beta$. It is clear that the above $\beta-$formula, implies that

$$\gamma_1 = \frac{\beta\gamma}{2\beta - \gamma},$$

which will used to estimate γ_1 by means of Hill's estimators $\widehat{\gamma}$ and $\widehat{\beta}$ that will be defined below. To this end, let us $t = X_{n-k:n}$ and then replace, in β_t above, both F and G by their respective empirical df's

$$F_n(x) := n^{-1}\sum_{i=1}^n \mathbb{I}_{\{X_i \leq x\}} \text{ and } G_n(y) := n^{-1}\sum_{i=1}^n \mathbb{I}_{\{Y_i \leq y\}},$$

to get

$$\frac{\int_{X_{n-k:n}}^\infty \overline{G}_n(x)\log(x/X_{n-k:n})\, dF_n(x)}{\int_{X_{n-k:n}}^\infty \overline{G}_n(x)\, dF_n(x)},$$

which equals

$$\widehat{\beta} := \sum_{i=1}^{k} c_{i,n} \log\left(X_{n-i+1:n}/X_{n-k:n}\right),$$

where

$$c_{i,n} := \frac{\overline{G}_n\left(X_{n-i+1:n}\right)}{\sum_{i=1}^{k} \overline{G}_n\left(X_{n-i+1:n}\right)}.$$

Finally, by using the above formula of γ_1, we end up with a new estimator for γ_1 as follows

$$\widehat{\gamma}_1 := \frac{\widehat{\beta}\widehat{\gamma}}{2\widehat{\beta} - \widehat{\gamma}}. \tag{1.3}$$

To establish the consistency and asymptotic normality of $\widehat{\gamma}_1$, we will make use the tail empirical process technics given in [9], which is used recently by [4] in the truncation case. The tail empirical process corresponding to df F, by

$$D_n^{(1)}(x) := M_n^{(1)}(x) - r_1(x), \text{ for } x \geq 1,$$

where

$$M_n^{(1)}(x) := \frac{\int_{xX_{n-k:n}}^{\infty} dF_n(w)}{\int_{X_{n-k:n}}^{\infty} dF_n(w)} = \frac{n}{k}\overline{F}_n\left(X_{n-k:n}x\right) \text{ and } r_1(x) := x^{-1/\gamma},$$

so that

$$\widehat{\gamma} - \gamma = \int_1^{\infty} x^{-1} D_n^{(1)}(x)\, dx.$$

Likewise, we define the tail empirical process corresponding to df H, by

$$D_n^{(2)}(x) := M_n^{(2)}(x) - r_2(x),\ 2, \text{ for } x \geq 1,$$

where

$$M_n^{(2)}(x) := \frac{\overline{H}_n\left(xX_{n-k:n}\right)}{\overline{H}_n\left(X_{n-k:n}\right)} = \frac{\int_{xX_{n-k:n}}^{\infty} \overline{G}_n(w)\, dF_n(w)}{\int_{X_{n-k:n}}^{\infty} \overline{G}_n(w)\, dF_n(w)} \text{ and } r_2(x) := x^{-1/\beta},$$

so that

$$\widehat{\beta} - \beta = \int_1^{\infty} x^{-1} D_n^{(2)}(x)\, dx.$$

By using formula (1.3), we get

$$\widehat{\gamma}_1 - \gamma_1 = \int_1^{\infty} x^{-1}\left(c_{n1} D_n^{(1)}(x) - c_{n2} D_n^{(2)}(x)\right) dx, \tag{1.4}$$

where

$$c_{n1} := \frac{2\beta^2}{\left(\widehat{\gamma} - 2\beta\right)\left(\gamma - 2\beta\right)} \text{ and } c_{n2} := \frac{\widehat{\gamma}^2}{\left(\widehat{\gamma} - 2\widehat{\beta}\right)\left(\widehat{\gamma} - 2\beta\right)}.$$

By means of previous functional representations and weak approximations corresponding to $D_n^{(1)}(x)$ and $D_n^{(2)}(x)$ below, we establish both consistency and asymptotic normality of $\widehat{\gamma}_1$.The rest of the paper is organized as follows. In Section 2, we state our main results, namely consistency and asymptotic normality of $\widehat{\gamma}_1$. A simulation study is carried out, in Section 3, to illustrate the performance of $\widehat{\gamma}_1$. The proofs are postponed to Appendix 5 whereas some results that are instrumental to our needs are gathered in the Appendix 6.

2 MAIN RESULTS

Next we need to the usual second-order condition that specify the rate of convergence of regular variation functions. More precisely for a given function $\varphi \in \mathcal{RV}_{(-1/\alpha)}$, we assume that

$$\frac{1}{A_\varphi(t)}\left(\frac{\varphi(tx)}{\varphi(t)} - x^{-1/\alpha}\right) \to x^{-1/\alpha}\frac{x^{\tau/\alpha}-1}{\tau\alpha}, \text{ for } x>0,$$

where $|A_\varphi|$ is regularly varying (at infinity) with tail index (second-order parameter) $\tau/\alpha < 0$ [**?**, see, e.g.,]]deHS96. A function φ satisfying this condition is denoted $\varphi \in 2\mathcal{RV}_{(-1/\alpha)}(A_\varphi, \tau)$. For convenience, we set $\mathbb{A}_\varphi := A_\varphi \circ \mathbb{U}_F$, where $\mathbb{U}_L := \left(1/\overline{L}\right)^{\leftarrow}$ with

$$L^{\leftarrow}(u) := \inf\{v : L(v) \geq u\}, \text{ for } 0<u<1,$$

denoting the (left-continuous) the quantile function pertaining to a (right-continuous) df L. Since $\overline{F} \in \mathcal{RV}_{(-1/\gamma)}$ and $\overline{G} \in \mathcal{RV}_{(-1/\gamma_2)}$, then we may assume

$$\overline{F} \in 2\mathcal{RV}_{(-1/\gamma)}(A_F, \rho_F) \text{ and } \overline{G} \in 2\mathcal{RV}_{(-1/\gamma_2)}(A_G, \rho_G). \tag{2.1}$$

Since $\overline{H} \in \mathcal{RV}_{(-1/\beta)}$, thus we may also suppose that

$$\overline{H} \in 2\mathcal{RV}_{(-1/\beta)}(A_H, \rho_H). \tag{2.2}$$

Theorem 2.1. *Assume that condition* (2.1) *holds. Let $k = k_n$ be an integer sequence satisfying $k \to \infty$ and $k/n \to 0$. In addition, if condition* (2.2) *is fulfilled, then, there exists a sequence of Wiener processes $\{W_n(x),\ x \geq 0\}_{n\geq 1}$, such that for every small $0<\nu<1$, we have*

$$\sup_{x\geq 1} x^\nu \left|D_n^{(i)}(x)\right| \xrightarrow{\mathbf{P}} 0,\ i=1,2. \tag{2.3}$$

Moreover

$$\sup_{x\geq 1} x^\nu \left|\sqrt{k}D_n^{(i)}(x) - \mathcal{L}_n^{(i)}(x) - \sqrt{k}\mathcal{B}_n^{(i)}(x)\right| \xrightarrow{\mathbf{P}} 0,\ i=1,2, \tag{2.4}$$

provided that $\sqrt{k}\mathbb{A}_F(n/k)$, $\sqrt{k}\mathbb{A}_G(n/k)$ and $\sqrt{k}\mathbb{A}_H(n/k)$ are asymptotically bounded, where

$$\mathcal{L}_n^{(1)}(x) := W_n\left(x^{-1/\gamma}\right) - x^{-1/\gamma}W_n(1)$$

and

$$\begin{aligned}(\beta/\gamma)\,\mathcal{L}_n^{(2)}(x) := \quad & x^{-1/\beta}\left\{x^{1/\gamma}W_n\left(x^{-1/\gamma}\right) - W_n(1)\right\} \\ & + (1-\gamma/\beta)\int_0^{x^{-1/\gamma}} s^{\gamma/\beta-2}W_n(s)\,ds \\ & - (1-\gamma/\beta)\,x^{-1/\beta}\int_0^1 s^{\gamma/\beta-2}W_n(s)\,ds,\end{aligned}$$

with

$$\mathcal{B}_n^{(1)}(x) := x^{-1/\gamma}\frac{x^{\rho_F/\gamma}-1}{\rho_F\gamma}\mathbb{A}_F(n/k) \text{ and } \mathcal{B}_n^{(2)}(x) := x^{-1/\beta}\frac{x^{\rho_H/\beta}-1}{\rho_H\beta}\mathbb{A}_H(n/k).$$

Thereby, in view of the representation (1.4) and by using respectively the two results of Theorem 2.1 we end up with the consistency and asymptotic normality of $\widehat{\gamma}_1$, given in the following theorem.

Theorem 2.2. *Assume that* (2.1) *holds. Let $k = k_n$ be an integer sequence satisfying $k \to \infty$ and $k/n \to 0$, then*

$$\widehat{\gamma}_1 \xrightarrow{\mathbf{P}} \gamma_1, \text{ as } N \to \infty.$$

In addition, if (2.2) *is fulfilled, then*

$$\sqrt{k}\left(\widehat{\gamma}_1 - \gamma_1\right) = Z_{n1} + Z_{n2} + \mu + o_{\mathbf{P}}(1),$$

where

$$\frac{(\gamma-2\beta)^2}{2\beta^2}Z_{n1} := \gamma\int_0^1 s^{-1}W_n(s)\,ds - \gamma W_n(1)$$

and

$$-\frac{(\gamma-2\beta)^2}{\gamma^2}Z_{n2} := (2\gamma-\beta)\frac{\gamma}{\beta}\int_0^1 s^{\gamma/\beta-2}W_n(s)\,ds - \gamma W_n(1)$$
$$+\left(\frac{\gamma}{\beta}-1\right)\frac{\gamma^2}{\beta}\int_0^1 s^{\gamma/\beta-2}W_n(s)\,(\log s)\,ds,$$

provided that $\sqrt{k}\mathbb{A}_G(n/k) = O(1)$, $\sqrt{k}\mathbb{A}_F(n/k) \to \lambda_F$ *and* $\sqrt{k}\mathbb{A}_H(n/k) \to \lambda_H$, *where*

$$\mu := \frac{2\beta^2(\gamma-2\beta)^{-2}\lambda_F}{1-\rho_F} - \frac{\gamma^2(\gamma-2\beta)^{-2}\lambda_H}{1-\rho_H}. \tag{2.5}$$

This implies that

$$\sqrt{k}(\widehat{\gamma}_1-\gamma_1) \to \mathcal{N}(\mu,\sigma^2), \text{ as } N\to\infty,$$

where

$$\sigma_2^2 := \frac{\gamma^6\beta\left(\beta^2-2\beta\gamma+2\gamma^2\right)}{(2\gamma-\beta)^3(\gamma-2\beta)^4}.$$

Remark 2.3. The complete data case corresponds to the situation when $\beta\equiv\gamma$, in which case we have $\gamma\equiv\gamma_1$. It follows that $\sqrt{k}(\widehat{\gamma}_1-\gamma_1) \xrightarrow{\mathcal{D}} \mathcal{N}\left(\lambda/(1-\rho_F),\gamma_1^2\right)$, as $N\to\infty$, which meets the asymptotic normality of the classical Hill estimator [10], see for instance, Theorem 3.2.5 in [9].

Remark 2.4. In terms of the tail indices γ_1 and γ_2, we have

$$\sigma_2^2 = \gamma_2^3\frac{(\gamma_1/\gamma_2)^2(2(\gamma_1/\gamma_2)+1)^4\left(5(\gamma_1/\gamma_2)^2+4\gamma_1/\gamma_2+1\right)}{(\gamma_1/\gamma_2+1)(3(\gamma_1/\gamma_2)+1)^3}.$$

Remark 2.5. We show that the ratio between the asymptotic variances σ_1^2 and σ_2^2 equals

$$\frac{\sigma_1^2}{\sigma_2^2} = \frac{\left(1-x^3\right)(2x+1)^4\left(5x^2+4x+1\right)}{(1+x^2)(3x+1)^3}, \text{ where } x := \gamma_1/\gamma_2,$$

and

$$\begin{cases} 1<\sigma_1^2/\sigma_2^2<3.2, & \text{for } 0<\gamma_1/\gamma_2<0.94125 \\ 0<\sigma_1^2/\sigma_2^2<1, & \text{for } 0.94125<\gamma_1/\gamma_2<1. \end{cases}$$

The curve of ratio σ_1^2/σ_2^2 in the interval $(0,1)$, given in Figure **??**, illustrates the previous inequalities. We conclude that $\widehat{\gamma}_1$ is asymptotically more efficient than $\widehat{\gamma}_1^{(\mathbf{BMN})}$ for $0<\gamma_1/\gamma_2<0.94125$, otherwise $\widehat{\gamma}_1^{(\mathbf{BMN})}$ is asymptotically more efficient than $\widehat{\gamma}_1$. It is worth mentioning that the comparison is made for $0<\gamma_1/\gamma_2<1$, because the asymptotic normality of $\widehat{\gamma}_1^{(\mathbf{BMN})}$ is established only for $0<\gamma_1<\gamma_2$.

3 SIMULATION STUDY

In this section, we check the finite sample behavior of $\widehat{\gamma}_1$ compared with $\widehat{\gamma}_1^{(\mathbf{BMN})}$ and $\widehat{\gamma}_1^{(\mathbf{GS})}$ in terms of absolute bias and rmse. To this end, let us consider sets of truncated and truncation data drawn from Burr (γ,δ) and Fréchet (γ) models with respective df's

$$\overline{\mathcal{F}}(x) = \left(1+x^{1/\delta}\right)^{-\delta/\gamma},\ x\geq 0,\ \delta>0,\ \gamma>0;$$

and

$$\overline{\mathcal{F}}(x) = 1-\exp\left(-x^{-1/\gamma}\right),\ x\geq 0,\ \gamma>0.$$

Let consider the following scenarios that correspond to df's F^* and G^*:

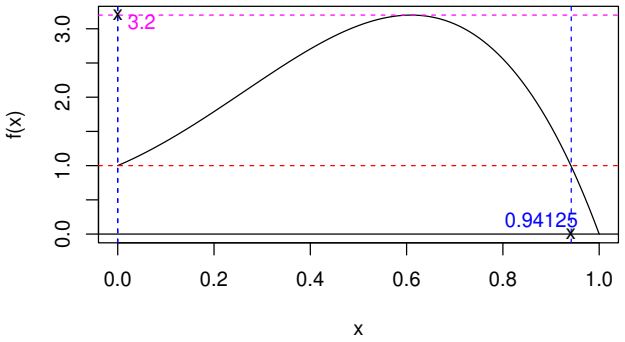

Fig. 2.1. Plotting of the ratio $f(x) := \sigma_1^2/\sigma_2^2$ as function of $x := \gamma_1/\gamma_2$ on the interval $(0, 1)$.

	$\gamma_1 = 0.6, \delta = 1/4$		
	p		
	30% (90%)	40% (60%)	
	γ_2		
[S1]	0.257 (5.4)	0.093 (3.843)	[S2]
[S3]	0.167 (4.701)	0.420 (5.272)	[S4]

TABLE 1. Choices of the tail indices and corresponding percentages of observed sample for each scenario.

- [S1] Burr (γ_1, δ) truncated by Burr(γ_2, δ)
- [S2] Fréchet (γ_1) truncated by Fréchet (γ_2)
- [S3] Fréchet(γ_1) truncated by Burr(γ_2, δ)
- [S4] Burr(γ_1, δ) truncated by Fréchet(γ_2)

First, we fix the values 0.6 for γ_1 and $1/4$ for δ, then choose different values for γ_2 so that the percentage of observed data p given in (1.2), be around of 40% and 60% for both scenarios [S2] and [S4] while we choose 30% and 90% for both scenarios [S1] and [S3]. The choice of parameters provides couples of (γ_1, γ_2) of different order, that is $\gamma_1 < \gamma_2$ and $\gamma_1 > \gamma_2$, which may be obtained by numerically solve, in γ_2, Equation (1.2). The results are recapitulated in the following table:
Thereby, for each scenario, we choose two triplets of parameters (γ_1, γ_2, p) as follows:

- $S1 : (\gamma_1, \gamma_2, p) = (0.6, 0.257, 30\%)\,; (0.6, 4.701.4, 90\%)$
- $S2 : (\gamma_1, \gamma_2, p) = (0.6, 0.093, 40\%)\,; (0.6, 3.843, 60\%)$
- $S3 : (\gamma_1, \gamma_2, p) = (0.6, 0.167, 30\%)\,; (0.6, 4.701, 90\%)$
- $S4 : (\gamma_1, \gamma_2, p) = (0.6, 0.420, 40\%)\,; (0.6, 5.272, 60\%)$

We vary the common size $N = 300, 500, 1000, 1500$ of both samples $(\mathbf{X}_1, ..., \mathbf{X}_N)$ and $(\mathbf{Y}_1, ..., \mathbf{Y}_N)$, then for each size, we generate 1000 independent replicates. For the selection of the optimal numbers of upper order statistics used in the computation of the three aforementioned estimators, we apply the algorithm of [15] page 137. Our illustrations and comparison are made with respect to the absolute biases (abias) and rmse's, which are summarized in the four Tables 2-3-4-5 and the eight Figures 3.2-3.3-3.4-3.5-3.6-3.7-3.8-3.9. In the light of all tables and Figures , the overall conclusion is that $\widehat{\gamma}_1$ behaves well both in terms of bias and rmse and having a finite sample behavior almost close to $\widehat{\gamma}_1^{(\mathbf{BMN})}$. Moreover, both the two estimators perform better than $\widehat{\gamma}_1^{(\mathbf{GS})}$ in particular in small sample case and for small percentage of observed data p, on the other termes the later becomes unstable for small sample sizes. On the other hand, as noted in two Remarks 2.4 and 2.5, that $\widehat{\gamma}_1$ is asymptotically more efficient than $\widehat{\gamma}_1^{(\mathbf{BMN})}$ for "almost" all positive couples (γ_1, γ_2), which also makes our new estimator more advantageous regarding to the two other ones.

		$p = 0.3$					
		$\widehat{\gamma}_1$		$\widehat{\gamma}_1^{(\mathbf{BMN})}$		$\widehat{\gamma}_1^{(\mathbf{GS})}$	
N	n	abias	rmse	abias	rmse	abias	rmse
300	90	0.398	0.448	0.403	0.442	0.445	4.911
500	149	0.236	0.469	0.226	0.320	0.418	3.989
1000	300	0.187	0.459	0.171	0.276	0.460	2.731
1500	450	0.144	0.362	0.144	0.276	0.342	1.830
		$p = 0.9$					
300	270	0.007	0.138	0.004	0.138	0.042	0.346
500	449	0.001	0.110	0.002	0.110	0.016	0.172
1000	899	0.008	0.076	0.005	0.076	0.021	0.117
1500	1350	0.004	0.065	0.002	0.065	0.019	0.098

TABLE 2. Absolute biases and rmse's for the tail index estimators correspond to scenario S1 based on 1000 right-truncated samples.

		$p = 0.4$					
		$\widehat{\gamma}_1$		$\widehat{\gamma}_1^{(\mathbf{BMN})}$		$\widehat{\gamma}_1^{(\mathbf{GS})}$	
N	n	abias	rmse	abias	rmse	abias	rmse
300	125	0.340	0.577	0.319	0.361	0.606	5.983
500	208	0.345	0.565	0.273	0.327	0.607	5.896
1000	416	0.264	0.509	0.243	0.298	0.428	1.326
1500	626	0.212	0.423	0.218	0.279	0.440	1.760
		$p = 0.6$					
300	182	0.008	0.163	0.012	0.164	0.054	7.398
500	304	0.010	0.127	0.014	0.127	0.001	0.208
1000	608	0.008	0.091	0.010	0.091	0.004	0.145
1500	912	0.009	0.076	0.011	0.077	0.004	0.124

TABLE 3. Absolute biases and rmse's for the tail index estimators correspond to scenario S2, based on 1000 right-truncated samples.

4 CONCLUDING NOTES

By using the well-known probability weighted moment estimation method, we derived a new estimator of the tail index for right truncated heavy-tailed data and established its consistency and asymptotic normality without additional assumptions on the underlying df's. Moreover, the proposed method may also serve to estimate the second order parameter ρ_F which is of practical relevance in extreme value

		$p = 0.3$					
		$\widehat{\gamma}_1$		$\widehat{\gamma}_1^{(\mathbf{BMN})}$		$\widehat{\gamma}_1^{(\mathbf{GS})}$	
N	n	abias	rmse	abias	rmse	abias	rmse
300	99	0.371	0.490	0.357	0.411	0.681	4.827
500	165	0.226	0.574	0.233	0.310	0.599	1.803
1000	331	0.181	0.465	0.165	0.278	0.357	2.912
1500	498	0.179	0.401	0.153	0.267	0.422	1.829
		$p = 0.9$					
300	273	0.023	0.147	0.027	0.147	0.513	11.574
500	456	0.011	0.110	0.014	0.110	0.024	0.158
1000	911	0.008	0.078	0.010	0.078	0.011	0.118
1500	1367	0.010	0.067	0.012	0.067	0.005	0.098

TABLE 4. Absolute biases and rmse's for the tail index estimators correspond to scenario S3 , based on 1000 right-truncated samples.

		$p = 0.4$					
		$\widehat{\gamma}_1$		$\widehat{\gamma}_1^{(\mathbf{BMN})}$		$\widehat{\gamma}_1^{(\mathbf{GS})}$	
N	n	abias	rmse	abias	rmse	abias	rmse
300	121	0.177	0.494	0.170	0.317	0.975	11.564
500	201	0.080	0.594	0.112	0.297	0.288	3.733
1000	403	0.059	0.327	0.093	0.247	0.189	1.231
1500	604	0.047	0.256	0.062	0.246	0.164	3.483
		$p = 0.6$					
300	180	0.011	0.158	0.007	0.156	0.057	5.154
500	300	0.008	0.126	0.005	0.125	0.170	4.699
1000	601	0.006	0.091	0.002	0.091	0.011	0.150
1500	902	0.006	0.076	0.003	0.076	0.002	0.116

TABLE 5. Absolute biases and rmse's for the tail index estimators correspond to scenario S4 , based on 1000 right-truncated samples.

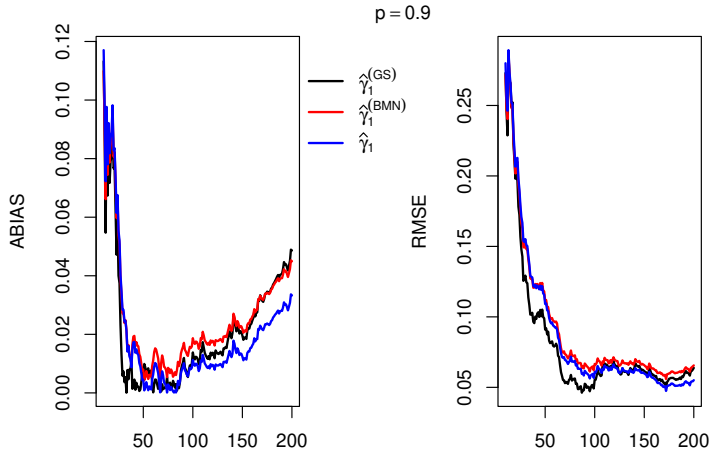

Fig. 3.2. Absolute bias (left panel) and RMSE (right panel) of $\widehat{\gamma}_1$ (blue) and $\widehat{\gamma}_1^{(BMN)}$ (red) and $\widehat{\gamma}_1^{(GS)}$(black), corresponding to scenario $S1$: ($\gamma_1 = 0.6$, $\gamma_2 = 5.4$ and $p = 90\%$) based on 1000 samples of size 500

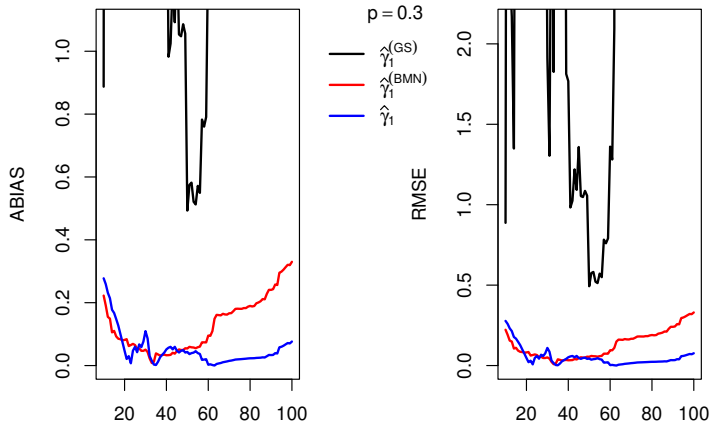

Fig. 3.3. Absolute bias (left panel) and RMSE (right panel) of $\widehat{\gamma}_1$ (blue) and $\widehat{\gamma}_1^{(BMN)}$ (red) and $\widehat{\gamma}_1^{(GS)}$(black), corresponding to scenario $S1$: ($\gamma_1 = 0.6$, $\gamma_2 = 0.257$ and $p = 30\%$) based on 1000 samples of size 500

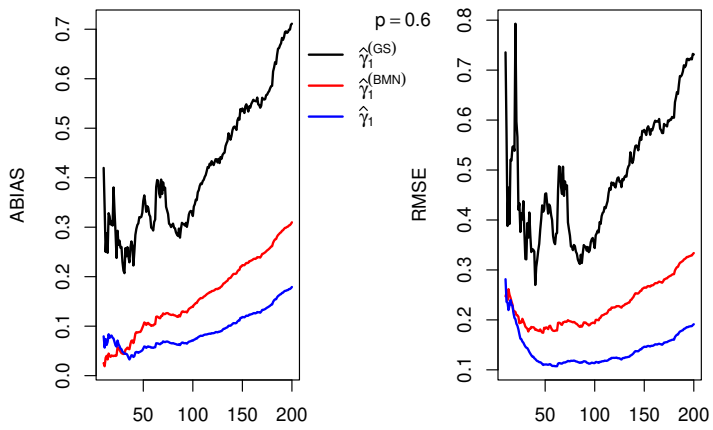

Fig. 3.4. Absolute bias (left panel) and RMSE (right panel) of $\widehat{\gamma}_1$ (blue) and $\widehat{\gamma}_1^{(BMN)}$ (red) and $\widehat{\gamma}_1^{(GS)}$(black), corresponding to scenario $S2$: ($\gamma_1 = 0.6$, $\gamma_2 = 3.843$ and $p = 60\%$) based on 1000 samples of size 500

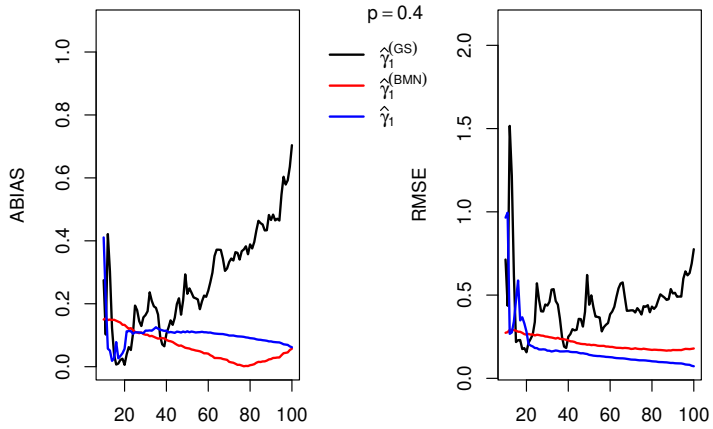

Fig. 3.5. Absolute bias (left panel) and RMSE (right panel) of $\widehat{\gamma}_1$ (blue) and $\widehat{\gamma}_1^{(BMN)}$ (red) and $\widehat{\gamma}_1^{(GS)}$(black), corresponding to scenario $S2$: ($\gamma_1 = 0.6$, $\gamma_2 = 0.093$ and $p = 40\%$) based on 1000 samples of size 500

analysis due its crucial importance in selecting the optimal number of upper order statistics k in tail index estimation (see, e.g., [9]) and to reduce the bias of such estimation. The asymptotic behavior of the obtained reduced bias estimator may be also established by means of the two tail empirical processes $D_n^{(i)}(x)$, $i = 1, 2$. This problem will be addressed in our future work.

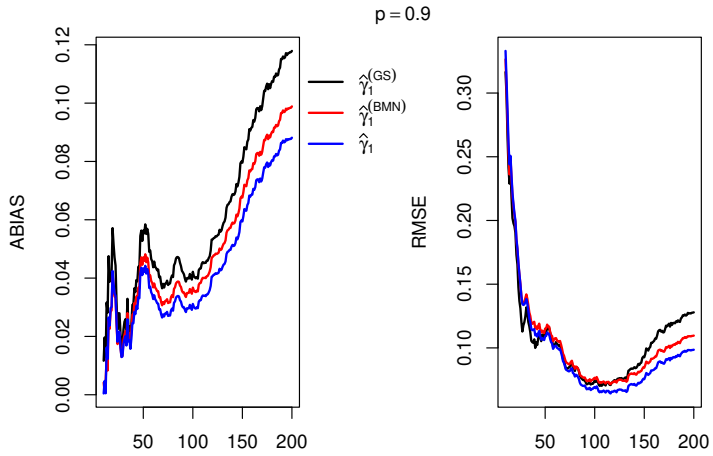

Fig. 3.6. Absolute bias (left panel) and RMSE (right panel) of $\widehat{\gamma}_1$ (blue) and $\widehat{\gamma}_1^{(BMN)}$ (red) and $\widehat{\gamma}_1^{(GS)}$(black), corresponding to scenario $S3$: ($\gamma_1 = 0.6$, $\gamma_2 = 4.701$ and $p = 90\%$) based on 1000 samples of size 500

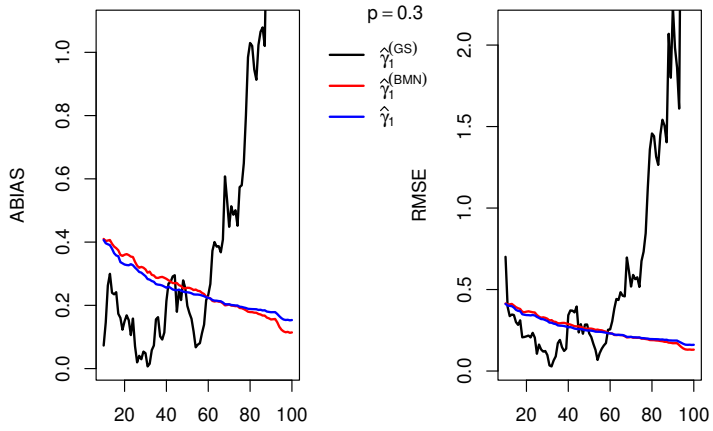

Fig. 3.7. Absolute bias (left panel) and RMSE (right panel) of $\widehat{\gamma}_1$ (blue) and $\widehat{\gamma}_1^{(BMN)}$ (red) and $\widehat{\gamma}_1^{(GS)}$(black), corresponding to scenario $S3$: ($\gamma_1 = 0.6$, $\gamma_2 = 0.167$ and $p = 30\%$) based on 1000 samples of size 500

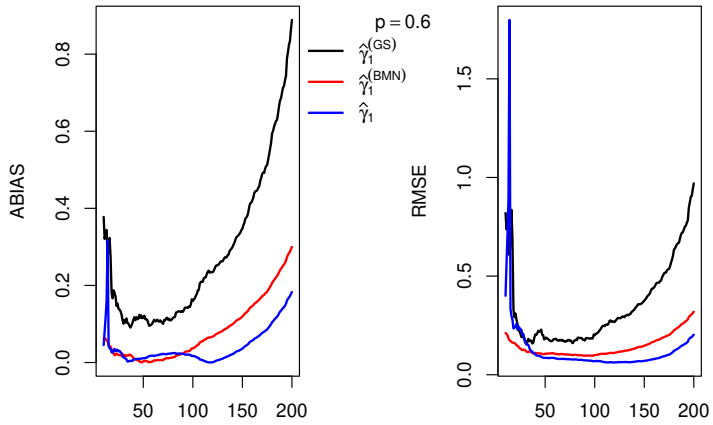

Fig. 3.8. Absolute bias (left panel) and RMSE (right panel) of $\widehat{\gamma}_1$ (blue) and $\widehat{\gamma}_1^{(BMN)}$ (red) and $\widehat{\gamma}_1^{(GS)}$(black), corresponding to scenario $S4$: ($\gamma_1 = 0.6$, $\gamma_2 = 5.272$ and $p = 60\%$) based on 1000 samples of size 500

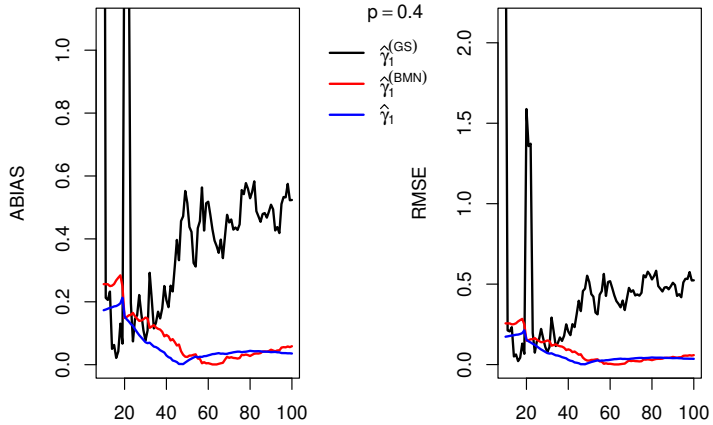

Fig. 3.9. Absolute bias (left panel) and RMSE (right panel) of $\widehat{\gamma}_1$ (blue) and $\widehat{\gamma}_1^{(BMN)}$ (red) and $\widehat{\gamma}_1^{(GS)}$(black), corresponding to scenario $S4$: ($\gamma_1 = 0.6$, $\gamma_2 = 0.420$ and $p = 40\%$) based on 1000 samples of size 500

Acknowledgments

The authors thank the reviewers for their valuable suggestions that led to an improvement of the paper.

REFERENCES

[1] Alexander, K. S., 1986. Sample moduli for set-indexed Gaussian processes. *Ann. Probab.* 14, 598-611.
[2] Benchaira, S., Meraghni, D., Necir, A., 2015. On the asymptotic normality of the extreme value index for right-truncated data. *Statist. Probab. Lett.* **107**, 378-384.
[3] Benchaira, S., Meraghni, D., Necir, A., 2016. Tail product-limit process for truncated data with application to extreme value index estimation. *Extremes* **19**, 219-251.
[4] Benchaira, S., Meraghni, D., Necir, A., 2016. Kernel estimation of the tail index of a right-truncated Pareto-type distribution. *Statist. Probab. Lett.* **119**, 186-193.
[5] Caeiro, F., Prata Gomes, D., 2015. A log probability weighted moment estimator of extreme quantiles. Theory and practice of risk assessment, 293–303, Springer Proc. Math. Stat., 136, Springer, Cham.
[6] Einmahl, J.H.J., 1992. Limit theorems for tail processes with application to intermediate quantile estimation. J. Statist. Plann. Inference **32**, 137-145.
[7] Gardes, L., Stupfler, G., 2015. Estimating extreme quantiles under random truncation. *Test* **24**, 207-227.
[8] de Haan, L., Stadtmüller, U., 1996. Generalized regular variation of second order. J. *Australian Math. Soc. (Series A)* **61**, 381-395.
[9] de Haan, L., Ferreira, A., 2006. Extreme Value Theory: An Introduction. Springer.
[10] Hill, B.M., 1975. A simple general approach to inference about the tail of a distribution. *Ann. Statist*. **3**, 1163-1174.
[11] Haouas, N., Necir, A., Brahimi, B., 2019. Estimating the second-order parameter of regular variation and bias reduction in tail index estimation under random truncation. J. Stat. Theory Pract. **13**, no. 1, Paper No. 7, 33 pp.
[12] Hua, L., Joe, H., 2011. Second order regular variation and conditional tail expectation of
[13] Lawless, J.F., 2002. Statistical Models and Methods for Lifetime Data, Second Edition. Wiley Series in Probability and Statistics. multiple risks. Insurance Math. Econom. **49**, 537-546.
[14] Mancer, S., Necir, A., Benchaira, S., 2023. Bias reduction in kernel tail index estimation for randomly truncated Pareto-type data. Sankhya A **85**, no. 2, 1510–1547.
[15] Reiss, R.D., Thomas, M., 2007. Statistical Analysis of Extreme Values with Applications to Insurance, Finance, Hydrology and Other Fields, 3rd ed. Birkhäuser Verlag, Basel, Boston, Berlin.
[16] Schmidt, R., Stadtmüller, U., 2006. Nonparametric estimation of tail dependence. *Scand. J. Statist.* **33**, 307-335.
[17] Shorack, G. R., Wellner, J. A., 1986. Empirical Processes with Applications to Statistics. *Wiley.*
[18] Woodroofe, M., 1985. Estimating a distribution function with truncated data. *Ann. Statist.* **13**, 163-177.
[19] Worms, J., Worms, R., 2016. A Lynden-Bell integral estimator for extremes of randomly truncated data. Statist. Probab. Lett. 1**09**, 106-117.

5 APPENDIX A

It is worth mentioning that, since $n/N \to p$ a.s. as $N \to \infty$, then for a random sequence $Z_N \xrightarrow{\mathbf{P}} Z$ as $N \to \infty$, we have $Z_n \xrightarrow{\mathbf{P}} Z$ as $N \to \infty$, too. The proof of this matter is similar as that is used in Lemma 3.7 in [3]. In other words, the results regarding to convergence in probability of a sequence of rv's indexed by N can also be used by indexing by n.

5.1 Proof of Theorem 2.1

We will only show the results of the Theorem for $i = 2$, since those of case $i = 1$ become trivial when replacing β by γ. To start, first recall that $D_n^{(2)}(x) = M_n^{(2)}(x) - x^{-1/\beta}$, $x \geq 1$, where

$$M_n^{(2)}(x) = \frac{\overline{H}_n(xX_{n-k:n})}{\overline{H}_n(X_{n-k:n})},$$

and

$$\overline{H}_n(x) = \frac{\int_x^\infty \overline{G}_n(w)\, dF_n(w)}{\int_0^\infty \overline{G}_n(w)\, dF_n(w)}.$$

Observe that $M_n^{(2)}(x) = \Delta_n^{(2)}(x)/\Delta_n^{(2)}(1)$, where

$$\Delta_n^{(2)}(x) := \frac{\frac{n}{k}\int_{xX_{n-k:n}}^\infty \overline{G}_n(w)\, dF_n(w)}{\overline{G}_n(X_{n-k:n})}.$$

Thus, we may write

$$D_n^{(2)}(x) = \frac{\Delta_n^{(2)}(x) - (\beta/\gamma)\, x^{-1/\beta}}{\Delta_n^{(2)}(1)} - x^{-1/\beta}\frac{\Delta_n^{(2)}(1) - \beta/\gamma}{\Delta_n^{(2)}(1)}. \tag{5.1}$$

Let $a_k := \mathbb{U}_F(n/k)$ and decompose $\Delta_n^{(2)}(x) - (\beta/\gamma)\, x^{-1/\beta}$ into the sum of

$$T_{n1}(x) := \frac{n}{k}\left(\frac{1}{\overline{G}_n(X_{n-k:n})} - \frac{1}{\overline{G}(X_{n-k:n})}\right)\int_{xX_{n-k:n}}^{\infty} \overline{G}_n(w)\, dF_n(w),$$

$$T_{n2}(x) := \frac{n/k}{\overline{G}(X_{n-k:n})}\int_{xX_{n-k:n}}^{\infty} \left(\overline{G}_n(w) - \overline{G}(w)\right) dF_n(w),$$

$$T_{n3}(x) := \frac{n}{k}\left(\frac{1}{\overline{G}(X_{n-k:n})} - \frac{1}{\overline{G}(a_k)}\right)\int_{xX_{n-k:n}}^{\infty} \overline{G}(w)\, dF_n(w),$$

$$T_{n4}(x) := \frac{n/k}{\overline{G}(a_k)}\int_{xX_{n-k:n}}^{xa_k} \overline{G}(w)\, dF_n(w),$$

$$T_{n5}(x) := \frac{n/k}{\overline{G}(a_k)}\int_{xa_k}^{\infty} \overline{G}(w)\, d\left(F_n(w) - F(w)\right)$$

and

$$T_{n6}(x) := \frac{n/k}{\overline{G}(a_k)}\int_{xa_k}^{\infty} \overline{G}(w)\, dF(w) - (\beta/\gamma)\, x^{-1/\beta}.$$

Making use of (5.1), we way write

$$\Delta_n^{(2)}(1)\, D_n^{(2)}(x) = \sum_{i=1}^{5}\left(T_{ni}(x) - x^{-1/\beta}T_{ni}(1)\right) + \widetilde{\mathcal{B}}_n^{(2)}(x), \tag{5.2}$$

where

$$\begin{aligned}\widetilde{\mathcal{B}}_n^{(2)}(x) &:= T_{n6}(x) - x^{-1/\beta}T_{n6}(1)\\ &= \frac{n/k}{\overline{G}(a_k)}\int_{xa_k}^{\infty}\overline{G}(w)\, dF(w) - x^{-1/\beta}\frac{n/k}{\overline{G}(a_k)}\int_{a_k}^{\infty}\overline{G}(w)\, dF(w).\end{aligned}$$

Next, we show that for every sufficiently small $0 < \eta, \epsilon < 1/2$, we have

$$\sqrt{k}T_{ni}(x) = o_{\mathbf{P}}\left(\varrho(x)\right), \text{ for } i = 1, 2, \tag{5.3}$$

$$\sqrt{k}\left(T_{n3}(x) + T_{n4}(x) + T_{n5}(x)\right) = \mathcal{L}_n^{(2)}(x) + o_{\mathbf{P}}\left(\varrho(x)\right) \tag{5.4}$$

and

$$\widetilde{\mathcal{B}}_n^{(2)}(x) = x^{-1/\beta}\left(\frac{x^{\rho_H/\beta} - 1}{\rho_H\gamma} + o\left(x^{\epsilon}\right)\right)\mathbb{A}_H(n/k), \tag{5.5}$$

uniformly over $x \geq 1$, where $\varrho(x) = x^{-\eta/\beta+\epsilon}$ and $\mathcal{L}^{(2)}(x)$ is the Gaussian process given in Theorem 2.1.

5.1.1 Preliminaries

Note that F^* and G^* are continuous, then it is easy to verify that both df's F and G are as well, therefore the two rv's $U := \overline{F}(X)$ and $V := \overline{G}(Y)$ are uniformly distributed on $(0,1)$. Let

$$\mathcal{U}_n(s) := n^{-1}\sum_{i=1}^{n}\mathbb{I}_{\{U_i\le s\}} \text{ and } \mathcal{V}_n(s) := n^{-1}\sum_{i=1}^{n}\mathbb{I}_{\{V_i\le s\}},$$

denote the uniform empirical df's pertaining to the samples

$$U_i := \overline{F}(X_i) \text{ and } V_i := \overline{G}(Y_i),\ i=1,...,n,$$

respectively. We have $\overline{F}(x) = \overline{F}(x+)$, then

$$\mathbb{I}\left(U_i \le \overline{F}(x)\right) = \mathbb{I}\left(\overline{F}(X_i) \le \overline{F}(x+)\right)$$

and since $\overline{F}$ is decreasing then this latter equals

$$\mathbb{I}(X_i \ge x+) = 1 - \mathbb{I}(X_i < x+) = 1 - \mathbb{I}(X_i \le x).$$

By using similar arguments, we end up with

$$\mathbb{I}(Y_i \ge y+) = 1 - \mathbb{I}(Y_i < y+) = 1 - \mathbb{I}(Y_i \le y).$$

Hence for $x, y \ge 0$, we may write

$$\overline{F}_n(y) = \mathcal{U}_n\left(\overline{F}(x)\right) \text{ and } \overline{G}_n(y) = \mathcal{V}_n\left(\overline{G}(y)\right). \tag{5.6}$$

Next, we will use a useful weak approximation, due to [6], corresponding to the uniform tail empirical processes, saying that: in the probability space $(\Omega, \mathcal{A}, \mathbf{P})$, there exists a sequence of standard Wiener precesses $\{W_n(x),\ x \ge 0\}$, such that, for every $0 < \eta < 1/2$ and $M > 0$, we have

$$\sup_{0<s\le M} s^{-\eta}\left|\sqrt{k}\left(\frac{n}{k}\mathcal{U}_n\left(\frac{k}{n}s\right) - s\right) - W_n(s)\right| = o_{\mathbf{P}}(1). \tag{5.7}$$

On the other hand, we have $\sup_{0<s\le M} s^{-\eta}|W_n(s)| = O_{\mathbf{P}}(1)$ [**?**, see, e.g., example 1.8 in]]Alex86, which implies that

$$\sup_{0<s\le M} s^{-\eta}\left|\sqrt{k}\left(\frac{n}{k}\mathcal{U}_n\left(\frac{k}{n}s\right) - s\right)\right| = O_{\mathbf{P}}(1). \tag{5.8}$$

The previous result remains valid when replacing $\mathcal{U}_n$ by $\mathcal{V}_n$, that is

$$\sup_{0<s\le M} s^{-\eta}\left|\sqrt{k}\left(\frac{n}{k}\mathcal{V}_n\left(\frac{k}{n}s\right) - s\right)\right| = O_{\mathbf{P}}(1). \tag{5.9}$$

5.1.2 Asymptotic behavior of T_{n1}

Note that $\overline{F}(a_k) = k/n$, and let us write

$$\begin{aligned}\sqrt{k}T_{n1} &= -\frac{\sqrt{k}\left(\overline{G}_n(X_{n-k:n}) - \overline{G}(X_{n-k:n})\right)}{\overline{G}_n(X_{n-k:n})} \\ &\quad\times\int_x^\infty \frac{\overline{G}_n(wX_{n-k:n})}{\overline{G}(X_{n-k:n})}d\frac{F_n(wX_{n-k:n})}{\overline{F}(a_k)}.\end{aligned}$$

Observe that, by letting $s = \frac{n}{k}\overline{G}(X_{n-k:n})$, we have

$$\sqrt{k}\left(\overline{G}_n(X_{n-k:n}) - \overline{G}(X_{n-k:n})\right) = \frac{k}{n}\sqrt{k}\left(\frac{n}{k}\mathcal{V}_n\left(\frac{k}{n}s\right) - s\right),$$

which, by using the result (5.9), equals

$$O_{\mathbf{P}}(1)(k/n)s^{\eta} = O_{\mathbf{P}}(1)(k/n)^{1-\eta}\left(\overline{G}(X_{n-k:n})\right)^{\eta},$$

for some fixed $0 < \eta < 1/2$. It is worth mentioning that, since $X_i < Y_i$, for $i = 1, ..., n$, then $X_{n:n} < Y_{n:n}$, which implies that $V_{1:n} = \overline{G}(Y_{n:n}) < \overline{G}(X_{n-k:n}) < 1$, therefore

$$\frac{\overline{G}(X_{n-k:n})}{\overline{G}_n(X_{n-k:n})} = \frac{\overline{G}(X_{n-k:n})}{\mathcal{V}_n\left(\overline{G}(X_{n-k:n})\right)} < \sup_{V_{1:n}\leq s<1} \frac{s}{\mathcal{V}_n(s)},$$

which, from Proposition 6.2, is equal to $O_{\mathbf{P}}(1)$. On the other hand, $\overline{G}_n(w) = 0$, for $w \geq Y_{n:n}$, it follows that

$$\sqrt{k}T_{n1} = O_{\mathbf{P}}(1)\left(\frac{k/n}{\overline{G}(X_{n-k:n})}\right)^{1-\eta} \int_x^{Y_{n:n}/X_{n-k:n}} \frac{\overline{G}_n(wX_{n-k:n})}{\overline{G}(X_{n-k:n})} d\frac{F_n(wX_{n-k:n})}{\overline{F}(a_k)}.$$

Observe now, that for any $w \geq 1$, we have

$$\frac{\overline{G}_n(wX_{n-k:n})}{\overline{G}(X_{n-k:n})} = \frac{\mathcal{V}_n\left(\overline{G}(wX_{n-k:n})\right)}{\overline{G}(wX_{n-k:n})},$$

and, since $\overline{G}(wX_{n-k:n}) \leq \overline{G}(X_{n-k:n})$, then in view of Proposition 6.2 the latter ratio is less than or equal to $\sup_{V_{1:n}\leq s<1} \mathcal{V}_n(s)/s = O_{\mathbf{P}}(1)$, hence

$$\sqrt{k}T_{n1} = O_{\mathbf{P}}(1)\left(\frac{k/n}{\overline{G}(X_{n-k:n})}\right)^{1-\eta} \int_x^{\infty} \frac{\overline{G}(wX_{n-k:n})}{\overline{G}(X_{n-k:n})} d\frac{F_n(wX_{n-k:n})}{\overline{F}(a_k)}.$$

Next, we require to the following Potter-type inequalities [**?**, see, e.g., Proposition B.1.10, page 369 in]]deHF06 corresponding to regular variation functions.

Proposition 5.1. *Let $g \in \mathcal{RV}_{(\alpha)}$ with $\alpha \in \mathbb{R}$. Then, for any sufficiently small $\epsilon > 0$, there exists $t_0 = t_0(\epsilon) > 0$, such that $|g(ts)/g(t) - s^{-\alpha}| \leq \epsilon s^{-\alpha} \max(s^{-\epsilon}, s^{\epsilon})$, for any $t \geq t_0$ and $s > 0$.*

For the sake of simplicity, we set $x^{\nu\pm\epsilon} := x^{\nu}\max(x^{-\epsilon}, x^{\epsilon})$ and $\pm\epsilon c = \pm\epsilon$ for $\epsilon \downarrow 0$ and any real constants ν and c. Note that $X_{n-k:n}/a_k \xrightarrow{\mathbf{P}} 1$, then by using the previous proposition, we readily show that $\overline{G}(X_{n-k:n})/\overline{G}(a_k) = O_{\mathbf{P}}(1)$ and

$$\frac{\overline{G}(wX_{n-k:n})}{\overline{G}(X_{n-k:n})} = O_{\mathbf{P}}\left(w^{-1/\gamma_2+\epsilon}\right), \text{ as } N \to \infty,$$

uniformly on $w \geq 1$. Thus

$$\sqrt{k}T_{n1} = O_{\mathbf{P}}(1)\left(\frac{k/n}{\overline{G}(a_k)}\right)^{1-\eta} \int_x^{\infty} w^{-1/\gamma_2+\epsilon} d\frac{\overline{F}_n(wX_{n-k:n})}{\overline{F}(a_k)}.$$

Recall that , since $\overline{F}_n(w) = 0$, for $w \geq X_{n:n}$ and $\overline{F}_n(wX_{n-k:n}) = \mathcal{U}_n\left(\overline{F}(wX_{n-k:n})\right)$, then by using an integration by parts to the latter integral and then Proposition 6.2, yields

$$\begin{aligned}\sqrt{k}T_{n1} &= O_{\mathbf{P}}(1)\left(\frac{k/n}{\overline{G}(a_k)}\right)^{1-\eta} \\ &\quad \times \left\{x^{-1/\gamma_2+\epsilon}\frac{\overline{F}(xX_{n-k:n})}{\overline{F}(a_k)} + \int_x^{\infty} \frac{\overline{F}(wX_{n-k:n})}{\overline{F}(a_k)} dw^{-1/\gamma_2+\epsilon}\right\}.\end{aligned}$$

Making use of Proposition 5.1 and after integration, we show that both two quantities between brackets equal $O_{\mathbf{P}}\left(x^{-1/\gamma_1-1/\gamma+\epsilon}\right) = O_{\mathbf{P}}(\varrho(x))$ uniformly on $x \geq 1$. On the hand in view of Proposition 6.4, we have $\overline{G}(a_k) = O(1)(k/n)^{\gamma/\gamma_2}$, then

$$\left(\frac{k/n}{\overline{G}(a_k)}\right)^{1-\eta} = (k/n)^{(1-\eta)(1-\gamma/\gamma_2)}.$$

Recall that $0 < \eta < 1/2$ and $0 < \gamma/\gamma_2 < 1$, then $(k/n)^{(1-\eta)(1-\gamma/\gamma_2)} = o(1)$, it follows that $\sqrt{k}T_{n1} = o_{\mathbf{P}}(\varrho(x))$, uniformly on $x \geq 1$.

5.1.3 Asymptotic behavior of T_{n2}

It is clear that

$$\sqrt{k}T_{n2}=\frac{1}{\overline{G}\left(X_{n-k:n}\right)}\int_{x}^{\infty}\sqrt{k}\left(\overline{G}_{n}\left(wX_{n-k:n}\right)-\overline{G}\left(wX_{n-k:n}\right)\right)d\frac{F_{n}\left(wX_{n-k:n}\right)}{\overline{F}\left(a_{k}\right)}.$$

For convenience, we set $b_k:=\mathbb{U}_G\left(n/k\right)$ so that $\overline{G}\left(b_k\right)=k/n$. It is easy to verify, from (5.6), that

$$\begin{aligned}&\frac{n}{k}\sqrt{k}\left(\overline{G}_{n}\left(wX_{n-k:n}\right)-\overline{G}\left(wX_{n-k:n}\right)\right)\\ =\;&\sqrt{k}\left(\frac{n}{k}\mathcal{V}_{n}\left(\frac{k}{n}\overline{G}\left(wX_{n-k:n}\right)/\overline{G}\left(b_{k}\right)\right)-\overline{G}\left(wX_{n-k:n}\right)/\overline{G}\left(b_{k}\right)\right),\end{aligned}$$

which, by using (5.9), equals $O_{\mathbf{P}}\left(1\right)\left(\overline{G}\left(wX_{n-k:n}\right)/b_k\right)^{\eta}$, uniformly on $w\geq 1$, therefore

$$\sqrt{k}T_{n2}=O_{\mathbf{P}}\left(1\right)\frac{k/n}{\overline{G}\left(X_{n-k:n}\right)}\int_{x}^{\infty}\left(\overline{G}\left(wX_{n-k:n}\right)/\overline{G}\left(b_{k}\right)\right)^{\eta}d\frac{F_{n}\left(wX_{n-k:n}\right)}{\overline{F}\left(a_{k}\right)}.$$

By using the routine manipulations of two Propositions 6.2 and 5.1, we get

$$\sqrt{k}T_{n2}=O_{\mathbf{P}}\left(1\right)\frac{k/n}{\overline{G}\left(X_{n-k:n}\right)}\left(\frac{X_{n-k:n}}{b_{k}}\right)^{-\eta/\gamma_{2}\pm\epsilon}\int_{x}^{\infty}w^{-\eta/\gamma_{2}+\epsilon}dw^{-1/\gamma+\epsilon}.$$

Recall that $X_{n-k:n}=\left(1+o_{\mathbf{P}}\left(1\right)\right)a_k$, then by making use of Proposition 6.4, it is easy to verify that

$$\frac{k/n}{\overline{G}\left(X_{n-k:n}\right)}\left(\frac{X_{n-k:n}}{b_{k}}\right)^{-\eta/\gamma_{2}\pm\epsilon}=O_{\mathbf{P}}\left(1\right)\left(k/n\right)^{(1-\eta)(1-\gamma/\gamma_{2})\pm\epsilon}.$$

Since $\gamma/\gamma_2<1$ and $\int_x^{\infty}w^{-\eta/\gamma_2+\epsilon}dw^{-1/\gamma+\epsilon}=O_{\mathbf{P}}\left(\varrho\left(x\right)\right)$, then $\sqrt{k}T_{n2}=o_{\mathbf{P}}\left(\varrho\left(x\right)\right)$, uniformly on $x\geq 1$.

5.1.4 Asymptotic behavior of T_{n3}

Observe now

$$\sqrt{k}T_{n3}=\sqrt{k}\left(\frac{\overline{G}\left(a_{k}\right)}{\overline{G}\left(X_{n-k:n}\right)}-1\right)\int_{xX_{n-k:n}}^{\infty}\frac{\overline{G}\left(w\right)}{\overline{G}\left(a_{k}\right)}d\frac{F_{n}\left(w\right)}{\overline{F}\left(a_{k}\right)},$$

and

$$\begin{aligned}&\sqrt{k}\left(\frac{\overline{G}\left(a_{k}\right)}{\overline{G}\left(X_{n-k:n}\right)}-1\right)\\ =\;&\sqrt{k}\left(\frac{\overline{G}\left(a_{k}\right)}{\overline{G}\left(X_{n-k:n}\right)}-\left(\frac{a_{k}}{X_{n-k:n}}\right)^{-1/\gamma_{2}}\right)+\sqrt{k}\left(\left(\frac{a_{k}}{X_{n-k:n}}\right)^{-1/\gamma_{2}}-1\right)\\ =:\;&I_{n1}+I_{n2}.\end{aligned}$$

Next we show that $I_{n1}=o_{\mathbf{P}}\left(1\right)$. Indeed, we have $\overline{G}\in 2\mathcal{RV}_{(-1/\gamma_2)}\left(A_G,\rho_G\right)$ which implies that for possibly different functions $\widetilde{A}_G$, with $\widetilde{A}_G\left(t\right)\sim A_G\left(t\right)$, as $t\to\infty$, and for each $0<\epsilon<1$, there exists $t_0=t_0\left(\epsilon\right)$, such that for all $tz\geq t_0$ we have

$$\left|\frac{\overline{G}\left(tz\right)/\overline{G}\left(t\right)-z^{-1/\gamma_{2}}}{\widetilde{A}_{G}\left(t\right)}-z^{-1/\gamma_{2}}\frac{z^{\rho_{G}/\gamma_{2}}-1}{\rho_{G}\gamma_{2}}\right|\leq\epsilon z^{-1/\gamma_{2}\pm\epsilon}. \tag{5.10}$$

[**?**, see, e.g., Proposition 4 and Remark 1 in]]HJ-2011. We will use this inequality with $t=t_n=X_{n-k:n}$ and $z=z_n=a_k/X_{n-k:n}$. Since $z_n=\left(1+o_{\mathbf{P}}\left(1\right)\right)$ then $z_n^{\rho_G/\gamma_2}-1=o_{\mathbf{P}}\left(1\right)$, it follows that

$$\frac{\overline{G}\left(a_{k}\right)}{\overline{G}\left(X_{n-k:n}\right)}-\left(\frac{a_{k}}{X_{n-k:n}}\right)^{-1/\gamma_{2}}=o_{\mathbf{P}}\left(1\right)\left|A_{G}\right|\left(X_{n-k:n}\right).$$

Since $|A_G|$ is regularly varying, then $A_G(X_{n-k:n}) = (1+o_{\mathbf{P}}(1))A_G(a_k)$. Recall that by assumption $\sqrt{k}A_G(a_k) = \sqrt{k}\mathbb{A}_G(n/k) = O(1)$, it follows that $I_{n1} = o_{\mathbf{P}}(1)$. The term I_{n2} may be decomposed into

$$\sqrt{k}\left(\left(\frac{X_{n-k:n}}{a_k}\right)^{1/\gamma_2} - \left(\frac{nU_{k:n}}{k}\right)^{-\gamma/\gamma_2}\right) + \sqrt{k}\left(\left(\frac{nU_{k:n}}{k}\right)^{-\gamma/\gamma_2} - 1\right).$$

By using similar arguments as used for I_{n1}, we also show that the first of the previous quantity equals $o_{\mathbf{P}}(1)$. For the second term, we use assertion (i) in Proposition 6.2, to get

$$\sqrt{k}\left(\left(\frac{nU_{k:n}}{k}\right)^{-\gamma/\gamma_2} - 1\right) = \frac{\gamma}{\gamma_2}W_n(1) + o_{\mathbf{P}}(1).$$

It is now easy to show that

$$\int_{xX_{n-k:n}}^{\infty} \frac{\overline{G}(w)}{\overline{G}(a_k)} d\frac{F_n(w)}{\overline{F}(a_k)} = \frac{x^{-1/\gamma_2-1/\gamma}}{\gamma/\gamma_2+1} + o_{\mathbf{P}}(\varrho(x)),$$

therefore

$$\sqrt{k}T_{n3} = \frac{\gamma}{\gamma+\gamma_2}x^{-1/\gamma_2-1/\gamma}W_n(1) + o_{\mathbf{P}}(\varrho(x)),$$

uniformly on $x \geq 1$, which may be rewritten in terms of tail index $\beta = \gamma_1\gamma/(2\gamma_1-\gamma)$, into

$$\sqrt{k}T_{n3} = (1-\beta/\gamma)x^{-1/\beta}W_n(1) + o_{\mathbf{P}}(\varrho(x)). \tag{5.11}$$

5.1.5 Asymptotic behavior of T_{n4}

Let us write

$$\sqrt{k}T_{n4}(x) = -\sqrt{k}\int_{xX_{n-k:n}/a_k}^{x} \frac{\overline{G}(wa_k)}{\overline{G}(a_k)} d\frac{\overline{F}_n(wa_k)}{\overline{F}(a_k)},$$

which may be decomposed into the sum of

$$\sqrt{k}T_{n4}^{(1)}(x) := -\sqrt{k}\int_{xX_{n-k:n}/a_k}^{x} \left(\frac{\overline{G}(wa_k)}{\overline{G}(a_k)} - w^{-1/\gamma_2}\right) d\frac{\overline{F}_n(wa_k)}{\overline{F}(a_k)},$$

$$\sqrt{k}T_{n4}^{(2)}(x) := -\sqrt{k}\int_{xX_{n-k:n}/a_k}^{x} w^{-1/\gamma_2} d\left(\frac{\overline{F}_n(wa_k) - \overline{F}(wa_k)}{\overline{F}(a_k)}\right),$$

$$\sqrt{k}T_{n4}^{(3)}(x) := -\sqrt{k}\int_{xX_{n-k:n}/a_k}^{x} w^{-1/\gamma_2} d\left(\frac{\overline{F}(wa_k)}{\overline{F}(a_k)} - w^{-1/\gamma}\right)$$

and

$$\sqrt{k}T_{n4}^{(4)}(x) := -\sqrt{k}\int_{xX_{n-k:n}/a_k}^{x} w^{-1/\gamma_2} dw^{-1/\gamma}.$$

We will show that $\sqrt{k}T_{n4}^{(1)}(x) = o_{\mathbf{P}}(\varrho(x))$, the proof of the other terms follow by using similar arguments. For convenience, we set $c_k^- := \min(1, X_{n-k:n}/a_k)$ and $c_k^+ := \min(1, X_{n-k:n}/a_k)$, and apply Proposition 5.1 (to $\overline{G}$), we get

$$\sqrt{k}T_{n4}^{(1)}(x) = o_{\mathbf{P}}(1)\sqrt{k}\int_{xc_k^-}^{xc_k^+} w^{-1/\gamma_2+\epsilon} d\frac{F_n(wa_k)}{\overline{F}(a_k)}.$$

Since $w^{-1/\gamma_2+\epsilon} < \left(xc_k^+\right)^{-1/\gamma_2+\epsilon}$ and $c_k^+ = 1 + o_{\mathbf{P}}(1)$, then

$$\sqrt{k}T_{n4}^{(1)}(x) = o_{\mathbf{P}}\left(x^{-1/\gamma_2+\epsilon}\right)\frac{\sqrt{k}\left|\overline{F}_n(xX_{n-k:n}) - \overline{F}_n(xa_k)\right|}{\overline{F}(a_k)}.$$

Observe that the previous ratio is less than or equal to

$$\sqrt{k}\frac{\left|\overline{F}_n(xX_{n-k:n}) - \overline{F}(xX_{n-k:n})\right|}{\overline{F}(a_k)} + \sqrt{k}\frac{\left|\overline{F}_n(xa_k) - \overline{F}_n(xa_k)\right|}{\overline{F}(a_k)}.$$

By applying (5.8) twice, we show that both terms equal $O_{\mathbf{P}}\left((k/n)^{1/2-\eta}\, x^{-\eta/\gamma+\epsilon}\right)$, it follows that

$$\sqrt{k}T_{n4}^{(1)}(x) = o_{\mathbf{P}}\left(x^{-1/\gamma_2-\eta/\gamma+\epsilon}\right) = o_{\mathbf{P}}\left(\varrho\left(x\right)\right).$$

For the last term we use an elementary integration to write

$$\sqrt{k}T_{n4}^{(4)}(x) = \frac{\gamma_2}{\gamma+\gamma_2}x^{-1/\gamma_2-1/\gamma}\sqrt{k}\left(\left(\frac{X_{n-k:n}}{a_k}\right)^{-1/\gamma_2-1/\gamma} - 1\right),$$

then we make use of assertion (ii) in Proposition 6.4, we obtain

$$\sqrt{k}T_{n4}^{(4)}(x) = -x^{-1/\beta}W_n\left(1\right) + o_{\mathbf{P}}\left(\varrho\left(x\right)\right) = \sqrt{k}T_{n4}(x). \tag{5.12}$$

5.1.6 Asymptotic behavior of T_{n5}

Recall that

$$T_{n5}\left(x\right) := \frac{n/k}{\overline{G}\left(a_k\right)}\int_{xa_k}^{\infty}\overline{G}\left(w\right)d\left(F_n\left(w\right) - F\left(w\right)\right)$$

The change of variables $s = \overline{G}\left(w\right)/\overline{G}\left(a_k\right)$ gives $w = \mathbb{U}_G\left(1/\left(s\overline{G}\left(a_k\right)\right)\right)$ and therefore

$$T_{n5} = \frac{n}{k}\int_0^{\overline{G}(xa_k)/\overline{G}(a_k)} sd\left(\overline{F}_n\left(\mathbb{U}_G\left(\frac{1}{s\overline{G}\left(a_k\right)}\right)\right) - \overline{F}\left(\mathbb{U}_G\left(\frac{1}{s\overline{G}\left(a_k\right)}\right)\right)\right),$$

which by an integration by parts may be rewritten into the sum of

$$T_{n5}^{(1)} := \frac{n}{k}\frac{\overline{G}\left(xa_k\right)}{\overline{G}\left(a_k\right)}\left(\overline{F}_n\left(xa_k\right) - \overline{F}\left(xa_k\right)\right)$$

and

$$T_{n5}^{(2)} := -\frac{n}{k}\int_0^{\overline{G}(xa_k)/\overline{G}(a_k)}\left(\overline{F}_n\left(\mathbb{U}_G\left(\frac{1}{s\overline{G}\left(a_k\right)}\right)\right) - \overline{F}\left(\mathbb{U}_G\left(\frac{1}{s\overline{G}\left(a_k\right)}\right)\right)\right)ds.$$

Observe that

$$\sqrt{k}T_{n5}^{(1)} = \frac{\overline{G}\left(xa_k\right)}{\overline{G}\left(a_k\right)}\sqrt{k}\left\{\frac{n}{k}\mathcal{U}_n\left(\frac{k}{n}\left(\frac{n}{k}\overline{F}\left(xa_k\right)\right)\right) - \frac{n}{k}\overline{F}\left(xa_k\right)\right\},$$

and use weak approximation (5.7) to get

$$\sqrt{k}T_{n5}^{(1)} = \frac{\overline{G}\left(xa_k\right)}{\overline{G}\left(a_k\right)}\left(W_n\left(\frac{n}{k}\overline{F}\left(xa_k\right)\right) + o_{\mathbf{P}}\left(1\right)\left(\frac{n}{k}\overline{F}\left(xa_k\right)\right)^{\eta}\right).$$

By applying Proposition 5.1 twice (for $\overline{G}$ and $\overline{F}$), we get

$$\sqrt{k}T_{n5}^{(1)} = x^{-1/\gamma_2}W_n\left(\frac{n}{k}\overline{F}\left(xa_k\right)\right) + o_{\mathbf{P}}\left(x^{-1/\gamma_2-\eta/\gamma+\epsilon}\right).$$

For convenience, we set $h_n\left(s\right) := \frac{n}{k}\overline{F}\left(\mathbb{U}_G\left(\frac{1}{s\overline{G}(a_k)}\right)\right)$ to write

$$\sqrt{k}T_{n5}^{(2)} = -\int_0^{\overline{G}(xa_k)/\overline{G}(a_k)}\sqrt{k}\left(\frac{n}{k}\mathcal{U}_n\left(\frac{k}{n}h_n\left(s\right)\right) - h_n\left(s\right)\right)ds,$$

which by using weak approximation (5.7) equals

$$-\int_0^{\overline{G}(xa_k)/\overline{G}(a_k)} W_n\left(h_n\left(s\right)\right)ds + o_{\mathbf{P}}\left(1\right)\int_0^{\overline{G}(xa_k)/\overline{G}(a_k)}\left(h_n\left(s\right)\right)^{\eta}ds.$$

Observe that $\overline{F}\left(\mathbb{U}_G\left(1/\overline{G}\left(a_k\right)\right)\right) = k/n$, it follows that

$$h_n\left(s\right) = \overline{F}\left(\mathbb{U}_G\left(\frac{1}{s\overline{G}\left(a_k\right)}\right)\right)/\overline{F}\left(\mathbb{U}_G\left(\frac{1}{\overline{G}\left(a_k\right)}\right)\right).$$

Note that $\overline{F} \circ \mathbb{U}_G(1/\cdot) \in \mathcal{RV}_{(\gamma_2/\gamma)}$ near zero, then by the routine application of Proposition 5.1, we end up with

$$\int_0^{\overline{G}(xa_k)/\overline{G}(a_k)} (h_n(s))^{\eta} ds = O\left(x^{-\eta(1/\gamma_2+1/\gamma)+\epsilon}\right).$$

Hence, we showed that

$$\sqrt{k}T_{n5} = x^{-1/\gamma_2} W_n\left(\frac{n}{k}\overline{F}(xa_k)\right) - \int_0^{\overline{G}(xa_k)/\overline{G}(a_k)} W_n(h_n(s))\, ds + o_{\mathbf{P}}\left(x^{-\eta(1/\gamma_2+1/\gamma)+\epsilon}\right).$$

Observe now that, by using the mean value theorem, we get

$$\int_{x^{-1/\gamma_2}}^{\overline{G}(xa_k)/\overline{G}(a_k)} W_n(h_n(s))\, ds = \left(\frac{\overline{G}(xa_k)}{\overline{G}(a_k)} - x^{-1/\gamma_2}\right) W_n(h_n(g_n(x))),$$

where $g_n(x)$ is between $\overline{G}(xa_k)/\overline{G}(a_k)$ and x^{-1/γ_2}. It is easy to check that

$$h_n(g_n(x)) < (1+\epsilon x^{\epsilon}) x^{-1/\gamma}, \text{ for any } x \geq 1,$$

it follows that

$$\sup_{x\geq 1}\left|(h_n(g_n(x)))^{1/2} W_n(h_n(g_n(x)))\right| \leq \sup_{0\leq u\leq 1+\epsilon} |W_n(u)|,$$

which is stochastically bounded, therefore

$$\int_{x^{-1/\gamma_2}}^{\overline{G}(xa_k)/\overline{G}(a_k)} W_n(h_n(s))\, ds = O_{\mathbf{P}}(1)(h_n(g_n(x)))^{-1/2}\left|\frac{\overline{G}(xa_k)}{\overline{G}(a_k)} - x^{-1/\gamma_2}\right|,$$

uniformly on $x \geq 1$. By using the routine manipulations of Proposition 5.1, we show that

$$\overline{G}(xa_k)/\overline{G}(a_k) - x^{-1/\gamma_2} = o\left(x^{-1/\gamma_2+\epsilon}\right) \text{ and } (h_n(g_n(x)))^{-1/2} = O\left(x^{-1/(2\gamma)+\epsilon}\right),$$

thereby

$$\int_{x^{-1/\gamma_2}}^{\overline{G}(xa_k)/\overline{G}(a_k)} W_n(h_n(s))\, ds = o_{\mathbf{P}}\left(x^{-1/\gamma_2-1/(2\gamma)+\epsilon}\right) = o_{\mathbf{P}}(\varrho(x)),$$

because $0 < \eta < 1/2$. Next we show that

$$W_n\left(\frac{n}{k}\overline{F}(xa_k)\right) = W_n\left(x^{-1/\gamma}\right) + o_{\mathbf{P}}(\varrho(x)),$$

uniformly on $w \geq 1$. Let us fix $d > 0$ and set $\varrho_n(x) := \left|\frac{n}{k}\overline{F}(xa_k) - x^{-1/\gamma}\right|$ to write

$$\begin{aligned} & \mathbf{P}\left(\sup_{w\geq 1} x^{1/(2\gamma)-\epsilon}\left|W_n\left(\frac{n}{k}\overline{F}(xa_k)\right) - W_n\left(x^{-1/\gamma}\right)\right| > d\right) \\ = \; & \mathbf{P}\left(\sup_{w\geq 1} x^{1/(2\gamma)-\epsilon}|W_n(\varrho_n(x))| > d\right) = \mathbf{P}\left(|W_n(1)| \sup_{w\geq 1} x^{1/(2\gamma)-\epsilon}(\varrho_n(x))^{1/2} > d\right), \end{aligned}$$

which, by Markov's inequality, is less than or equal to $d^{-2}\sup_{w\geq 1} x^{1/(2\gamma)-\epsilon}(\varrho_n(x))^{1/2}$. Since $\varrho_n(x) = o\left(x^{-1/\gamma+\epsilon}\right)$, uniformly on $w \geq 1$, then the latter probability equals $o(1)$ as sought. Hence, we showed that

$$\int_0^{x^{-1/\gamma_2}} W_n(h_n(s))\, ds = \int_0^{x^{-1/\gamma_2}} W_n\left(s^{\gamma_2/\gamma}\right) ds + o_{\mathbf{P}}(\varrho(x)),$$

thus

$$\sqrt{k}T_{n5} = x^{-1/\gamma_2} W_n\left(x^{-1/\gamma}\right) - \int_0^{x^{-1/\gamma_2}} W_n\left(s^{\gamma_2/\gamma}\right) ds + o_{\mathbf{P}}(\varrho(x)).$$

By using a change of variables, the latter equation becomes

$$\sqrt{k}T_{n5} = x^{1/\gamma-1/\beta} W_n\left(x^{-1/\gamma}\right) + (1-\gamma/\beta)\int_0^{x^{-1/\gamma}} t^{\gamma/\beta-2} W_n(t)\, dt + o_{\mathbf{P}}(\varrho(x)). \tag{5.13}$$

It follows that, from (5.11), (5.12) and (5.13), that (5.6) is indeed true.

5.1.7 Asymptotic behavior of $\widetilde{\mathcal{B}}_n^{(2)}(x)$

It is easy to verify that

$$\widetilde{\mathcal{B}}_n^{(2)}(x) = \left(\frac{\overline{H}(xa_k)}{\overline{H}(a_k)} - x^{-1/\beta}\right)\left(\int_{a_k}^{\infty} \frac{\overline{G}(w)}{\overline{G}(a_k)} d\frac{F(w)}{\overline{F}(a_k)}\right).$$

By using inequality (5.10) (applied to $\overline{H}$), that for possibly different functions $\widetilde{A}_H$, with $\widetilde{A}_H(t) \sim A_H(t)$, as $t \to \infty$, and for each $0 < \epsilon < 1$, there exists $t_0 = t_0(\epsilon)$, such that for all $t \geq t_0$ and $x \geq 1$, we have

$$\left|\frac{\overline{H}(tx)/\overline{H}(t) - x^{-1/\beta}}{\widetilde{A}_H(t)} - x^{-1/\beta}\frac{x^{\rho_H/\beta} - 1}{\rho_H \beta}\right| \leq \epsilon x^{-1/\beta+\epsilon}.$$

Thus by letting $t = a_k$, we write

$$\frac{\overline{H}(xa_k)}{\overline{H}(a_k)} - x^{-1/\beta} = x^{-1/\beta}\left(\frac{x^{\rho_H/\beta} - 1}{\rho_H \beta} + o(x^{\epsilon})\right)\widetilde{A}_H(a_k).$$

uniformly on $x \geq 1$. Since $\widetilde{A}_H(a_k) \sim \mathbb{A}_H(n/k)$ then

$$\frac{\overline{H}(xa_k)}{\overline{H}(a_k)} - x^{-1/\beta} = x^{-1/\beta}\left(\frac{x^{\rho_H/\beta} - 1}{\rho_H \beta} + o(x^{\epsilon})\right)\sqrt{k}\mathbb{A}_H(n/k).$$

On the other hand, we have

$$\int_{a_k}^{\infty} \frac{\overline{G}(w)}{\overline{G}(a_k)} d\frac{F(w)}{\overline{F}(a_k)} \to \frac{\beta}{\gamma},$$

it follows that $\widetilde{\mathcal{B}}_n^{(2)}(x) = x^{-1/\beta}\left(\frac{x^{\rho_H/\beta} - 1}{\rho_H \gamma} + o(x^{\epsilon})\right)\mathbb{A}_H(n/k)$, uniformly on $x \geq 1$.

5.1.8 Summarize

Up to now we showed that

$$\sqrt{k}\left(\Delta_n^{(2)}(x) - (\beta/\gamma)x^{-1/\beta}\right) = \Theta_n(x) + \sqrt{k}\widetilde{\mathcal{B}}_n^{(2)}(x) + o_{\mathbf{P}}(\varrho(x)),$$

where

$$\Theta_n(x) := x^{1/\gamma - 1/\beta}W_n\left(x^{-1/\gamma}\right) - \frac{\beta}{\gamma}x^{-1/\beta}W_n(1) + \left(1 - \frac{\gamma}{\beta}\right)\int_0^{x^{-1/\gamma}} t^{\gamma/\beta - 2}W_n(t)\,dt,$$

uniformly on $x \geq 1$. Recall that $\varrho(x) = x^{-\eta/\beta}$ and note that $\Theta_n(x) = O_{\mathbf{P}}(\varrho(x))$ and $\widetilde{\mathcal{B}}_n^{(2)}(x) = o_{\mathbf{P}}(\varrho(x))$, because $\mathbb{A}_H(n/k) = o(1)$, it follows that

$$\Delta_n^{(2)}(x) - (\beta/\gamma)x^{-1/\beta} = o_{\mathbf{P}}(\varrho(x)).$$

Let $0 < \nu < \eta < 1/2$ be sufficiently small, then

$$x^{\nu/\beta}\left(\Delta_n^{(2)}(x) - (\beta/\gamma)x^{-1/\beta}\right) = o_{\mathbf{P}}\left(x^{(\nu-\eta)/\beta+\epsilon}\right)$$

uniformly on $x \geq 1$. It follows that

$$\sup_{x \geq 1} x^{\nu/\beta}\left|\Delta_n^{(2)}(x) - (\beta/\gamma)x^{-1/\beta}\right| \xrightarrow{\mathbf{P}} 0$$

and $\Delta_n^{(2)}(1) \xrightarrow{\mathbf{P}} \beta/\gamma$, thus by (5.1) we get $\sup_{x \geq 1} x^{\nu/\beta}\left|D_n^{(2)}(x)\right| \xrightarrow{\mathbf{P}} 0$, as well, which gives (2.3) (for $i = 2$). Observe now that

$$\sqrt{k}\left(\Delta_n^{(2)}(1) - (\beta/\gamma)\right) = \Theta_n(1) + o_{\mathbf{P}}(1),$$

it follows form (5.1), that

$$\sqrt{k}\Delta_n^{(2)}(1)D_n^{(2)}(x) = \Theta_n(x) - x^{-1/\beta}\Theta_n(1) + \sqrt{k}\widetilde{\mathcal{B}}_n^{(2)}(x) + o_{\mathbf{P}}(\varrho(x)).$$

It is ready to check that $\Theta_n(x) - x^{-1/\beta}\Theta_n(1) \equiv \mathcal{L}_n^{(2)}(x)$, thus the weak approximation (2.4) (for $i = 2$) comes. This completes the proof of the theorem.

5.2 Proof of Theorem 2.2

Recall that

$$\widehat{\gamma}-\gamma=\int_1^\infty x^{-1}D_n^{(1)}(x)\,dx \text{ and } \widehat{\beta}-\beta=\int_1^\infty x^{-1}D_n^{(2)}(x)\,dx.$$

By applying respectively the two first results in Theorem 2.1, we easily show that $\widehat{\gamma}\xrightarrow{\mathbf{P}}\gamma$ and $\widehat{\beta}\xrightarrow{\mathbf{P}}\beta$, that we omits further details. To establish the asymptotic normality, let us first write

$$\widehat{\gamma}_1-\gamma_1=\frac{2\beta^2}{(\widehat{\gamma}-2\beta)(\gamma-2\beta)}(\widehat{\gamma}-\gamma)-\frac{\widehat{\gamma}^2}{\left(\widehat{\gamma}-2\widehat{\beta}\right)(\widehat{\gamma}-2\beta)}\left(\widehat{\beta}-\beta\right). \tag{5.14}$$

By making use of, respectively, two Gaussian approximations in Theorem 2.1 yields

$$\sqrt{k}(\widehat{\gamma}-\gamma)=\int_1^\infty x^{-1}\mathcal{L}_n^{(1)}(x)\,dx+\int_1^\infty x^{-1}\sqrt{k}\mathcal{B}_n^{(1)}(x)\,dx+o_{\mathbf{P}}(1)$$

and

$$\sqrt{k}\left(\widehat{\beta}-\beta\right)=\int_1^\infty x^{-1}\mathcal{L}_n^{(2)}(x)\,dx+\int_1^\infty x^{-1}\sqrt{k}\mathcal{B}_n^{(2)}(x)\,dx+o_{\mathbf{P}}(1).$$

By using an integration by parts with a change of variables, we end up with

$$\sqrt{k}(\widehat{\gamma}-\gamma)=\gamma\int_0^1 s^{-1}W_n(s)\,ds-\gamma W_n(1)+\frac{\sqrt{k}\mathbb{A}_F(n/k)}{1-\rho_F}+o_{\mathbf{P}}(1),$$

and

$$\begin{aligned}\sqrt{k}\left(\widehat{\beta}-\beta\right) &= (2\gamma-\beta)\frac{\gamma}{\beta}\int_0^1 s^{\gamma/\beta-2}W_n(s)\,ds-\gamma W_n(1)\\ &\quad+\left(\frac{\gamma}{\beta}-1\right)\frac{\gamma^2}{\beta}\int_0^1 s^{\gamma/\beta-2}W_n(s)(\log s)\,ds+\frac{\sqrt{k}\mathbb{A}_H(n/k)}{1-\rho_H}+o_{\mathbf{P}}(1).\end{aligned}$$

The previous two representations mean that $\sqrt{k}(\widehat{\gamma}-\gamma)$ and $\sqrt{k}\left(\widehat{\beta}-\beta\right)$ are asymptotically Gaussian rv's, which imply that

$$\sqrt{k}(\widehat{\gamma}-\gamma)=O_{\mathbf{P}}(1)=\sqrt{k}\left(\widehat{\beta}-\beta\right).$$

Then in view of (5.14) together with the consistency of $\widehat{\gamma}$ and $\widehat{\beta}$, we get

$$\sqrt{k}(\widehat{\gamma}_1-\gamma_1)=\frac{2\beta^2}{(\gamma-2\beta)^2}\sqrt{k}(\widehat{\gamma}-\gamma)-\frac{\gamma^2}{(\gamma-2\beta)^2}\sqrt{k}\left(\widehat{\beta}-\beta\right)+o_{\mathbf{P}}(1).$$

By assumptions, we have $\sqrt{k}\mathbb{A}_F(n/k)\to\lambda_F$ and $\sqrt{k}\mathbb{A}_H(n/k)\to\lambda_H$, it follows that

$$\sqrt{k}(\widehat{\gamma}_1-\gamma_1)=Z_{n1}+Z_{n2}+\mu+o_{\mathbf{P}}(1),$$

where

$$\frac{(\gamma-2\beta)^2}{2\beta^2}Z_{n1}:=\gamma\int_0^1 s^{-1}W_n(s)\,ds-\gamma W_n(1)$$

and

$$\begin{aligned}-\frac{(\gamma-2\beta)^2}{\gamma^2}Z_{n2} &:= (2\gamma-\beta)\frac{\gamma}{\beta}\int_0^1 s^{\gamma/\beta-2}W_n(s)\,ds-\gamma W_n(1)\\ &\quad+\left(\frac{\gamma}{\beta}-1\right)\frac{\gamma^2}{\beta}\int_0^1 s^{\gamma/\beta-2}W_n(s)(\log s)\,ds,\end{aligned}$$

with μ is as in (2.5). Note that both Z_{n1} and Z_{n2} are centred Gaussian rv's, then it remains to compute the second order moment of $Z_{n1}+Z_{n2}$. To this end, let us define the following quantities

$$\Delta_1(\rho):=\int_0^1 s^{\rho-2}W_n(s)\,ds,\ \Delta_2(\rho):=\int_0^1 s^{\rho-2}W_n(s)(\log s)\,ds,\ \Delta_3:=W_n(1).$$

Thereby, we write

$$\frac{(\gamma-2\beta)^2}{2\beta^2}Z_{n1} := \gamma\Delta_1(1) - \gamma\Delta_3$$

and

$$-\frac{(\gamma-2\beta)^2}{\gamma^2}Z_{n2} := (2\gamma-\beta)\frac{\gamma}{\beta}\Delta_1(\gamma/\beta) - \gamma\Delta_3 + \left(\frac{\gamma}{\beta}-1\right)\frac{\gamma^2}{\beta}\Delta_2(\gamma/\beta).$$

By using elementary computations, we end up with the following expectations:

$$\mathbf{E}\left[\Delta_1^2(\rho)\right] = \frac{2}{\rho(2\rho-1)},\ \mathbf{E}\left[\Delta_2^2(\rho)\right] = \frac{2(4\rho-1)}{\rho^2(2\rho-1)^3},\ \mathbf{E}\left[\Delta_3^2\right] = 1,$$
$$\mathbf{E}\left[\Delta_1(\rho)\Delta_2(\rho)\right] = \frac{1-4\rho}{\rho^2(2\rho-1)^2},\ \mathbf{E}\left[\Delta_1(\rho)\Delta_3\right] = \frac{1}{\rho},\ \mathbf{E}\left[\Delta_2(\rho)\Delta_3\right] = -\frac{1}{\rho^2}.$$

This gives

$$\mathbf{E}\left[Z_{n1}\right]^2 = \frac{4\beta^4\gamma^2}{(\gamma-2\beta)^4},\ \mathbf{E}\left[Z_{n2}\right]^2 = \frac{\beta\gamma^6\left(\beta^2-2\beta\gamma+2\gamma^2\right)}{(2\gamma-\beta)^3(\gamma-2\beta)^4}$$

and

$$\mathbf{E}\left[Z_{n1}Z_{n2}\right] = -\frac{2\beta^4\gamma^2}{(\gamma-2\beta)^4},$$

therefore

$$\begin{aligned}\mathbf{E}\left[\widehat{\gamma}_1-\gamma_1\right]^2 &= \mathbf{E}\left[Z_{n1}\right]^2 + \mathbf{E}\left[Z_{n2}\right]^2 + 2\mathbf{E}\left[Z_{n1}Z_{n2}\right] + o(1)\\ &= \frac{\gamma^6\beta\left(\beta^2-2\beta\gamma+2\gamma^2\right)}{(2\gamma-\beta)^3(\gamma-2\beta)^4} + o(1),\end{aligned}$$

which completes the proof of the lemma.

6 APPENDIX B

Proposition 6.1. *Assume that $\overline{F}\in\mathcal{RV}_{(-1/\gamma_1)}$ and $\overline{G}\in\mathcal{RV}_{(-1/\gamma_2)}$. Then, for every $r,s\geq 0$, we have*

$$\frac{\mathbf{E}\left[\left(\overline{G}(X)\right)^r(\log(X/t))^s \mid X>t\right]}{\mathbf{E}\left[\left(\overline{G}(X)\right)^r \mid X>t\right]} \to \left(\frac{\gamma_1\gamma}{(1+r)\gamma_1-r\gamma}\right)^s\Gamma(s+1),\ \textit{as } t\to\infty.$$

Proof. Observe that

$$\frac{\mathbf{E}\left[\left(\overline{G}(X)\right)^r(\log(X/t))^s \mid X>t\right]}{\mathbf{E}\left[\left(\overline{G}(X)\right)^r \mid X>t\right]} = \frac{\mathcal{I}_t(s)}{\mathcal{I}_t(0)},$$

where

$$\mathcal{I}_t(s) := \int_t^\infty\left(\frac{\overline{G}(x)}{\overline{G}(t)}\right)^r(\log(x/t))^s\frac{dF(x)}{\overline{F}(t)}.$$

Let us decompose $\mathcal{I}_t(s)$ into the sum of

$$\mathcal{I}_{t,1} := -\int_1^\infty\left\{\left(\frac{\overline{G}(tx)}{\overline{G}(t)}\right)^r - x^{-r/\gamma_2}\right\}(\log x)^s\,d\frac{\overline{F}(tx)}{\overline{F}(t)},$$

$$\mathcal{I}_{t,2} := -\int_1^\infty x^{-r/\gamma_2}(\log x)^s\,d\left\{\frac{\overline{F}(tx)}{\overline{F}(t)} - x^{-1/\gamma}\right\}$$

and $\mathcal{I}_{t,3} := -\int_1^\infty x^{-r/\gamma_2}(\log x)^s\,dx^{-1/\gamma}$. Next we show that both $\mathcal{I}_{t,1}$ and $\mathcal{I}_{t,2}$ tend to zero as $t\to\infty$. Indeed, let us write

$$|\mathcal{I}_{t,1}| \leq \int_1^\infty\left|\left(\frac{\overline{G}(tx)}{\overline{G}(t)}\right)^r - x^{-r/\gamma_2}\right|(\log x)^s\,d\frac{F(tx)}{\overline{F}(t)}.$$

Since $\overline{G} \in \mathcal{RV}_{(-1/\gamma_2)}$ then $\overline{G} \in \mathcal{RV}_{(-r/\gamma_2)}$ therefore by applying Proposition 5.1 yields

$$\left(\frac{\overline{G}(tx)}{\overline{G}(t)}\right)^r - x^{-r/\gamma_2} = o\left(x^{-r/\gamma_2+\epsilon}\right) = o(1), \text{ as } t \to \infty,$$

for every small $\epsilon > 0$ and uniformly on $x \geq 1$. It follows that

$$\mathcal{I}_{t,1} = o(1) \int_1^\infty (\log x)^s \, d\frac{F(tx)}{\overline{F}(t)}.$$

By using an integration by parts, we show that

$$\int_1^\infty (\log x)^s \, d\frac{F(tx)}{\overline{F}(t)} = \int_1^\infty \frac{\overline{F}(tx)}{\overline{F}(t)} d(\log x)^s.$$

Once again, from Proposition 5.1, $\overline{F}(tx)/\overline{F}(t) = (1 + o(x^\epsilon)) x^{-1/\gamma}$, then the previous integral becomes

$$\int_1^\infty (1 + o(x^\epsilon)) x^{-1/\gamma} d(\log x)^s.$$

It is clear that

$$\begin{aligned}\int_1^\infty x^{-1/\gamma} d(\log x)^s &= s\int_1^\infty (\log x)^{s-1} x^{-1/\gamma-1} dx \\ &= \gamma^s s \int_0^\infty v^{s-1} e^{-v} dv = \gamma^s s \Gamma(s),\end{aligned}$$

which, from the gamma function properties, is finite for any $s \geq 0$. This implies that

$$\int_1^\infty (1 + o(x^\epsilon)) x^{-1/\gamma} d(\log x)^s < \infty,$$

for any $s \geq 0$ and small $\epsilon > 0$, and therefore $\mathcal{I}_{t,1} = o(1)$. For the term $\mathcal{I}_{t,2}$ we use once gain an integration by parts with similar arguments to get $\mathcal{I}_{t,2} = o(1)$ as well. By using elementary analysis with a change of variables, we show that

$$\mathcal{I}_{t,3} = \frac{\Gamma(s+1)}{\gamma(r/\gamma_2 + 1/\gamma)^{s+1}},$$

thereby

$$\frac{\mathcal{I}_t(s)}{\mathcal{I}_t(0)} = \frac{\Gamma(s+1)}{(r/\gamma_2 + 1/\gamma)^s} + o(1), \text{ as } t \to \infty.$$

Finally, by replacing $1/\gamma_2$ by $1/\gamma - 1/\gamma_1$, we complete the proof of Proposition 6.1. ∎

Proposition 6.2. *Let $\mathcal{R}_n(s) := n^{-1}\sum_{i=1}^n \mathbb{I}(\xi_i \leq s)$, be the uniform empirical df pertaining to a sequence of iid rv's ξ_i, $i = 1, ..., n$ uniformly distributed on $(0,1)$. Then, for $n \geq 1$, we have*

$$\sup_{\xi_{1:n} \leq t \leq 1} \frac{t}{\mathcal{R}_n(t)} = O_{\mathbf{P}}(1) = \sup_{\xi_{1:n} \leq t \leq 1} \frac{\mathcal{R}_n(t)}{t},$$

where $\xi_{1:n} := \min_{1 \leq i \leq n}(\xi_i)$.

Proof. The proofs of the first two assertions may be found in [17] (pages 415 and 416, inequality 2). ∎

Proposition 6.3. *Let $k = k_n$ be an integer sequence satisfying $k \to \infty$ and $k/n \to 0$, then*

$$(i) \ \sqrt{k}\left(1 - \left(\frac{nU_{k:n}}{k}\right)^\alpha\right) = W_n(1) + o_{\mathbf{P}}(1).$$

If the second-order condition (2.1) (for $\overline{F}$) holds, then

$$(ii) \ \sqrt{k}\left(\left(\frac{X_{n-k:n}}{a_k}\right)^\alpha - 1\right) = \alpha\gamma W_n(1) + o_{\mathbf{P}}(1),$$

and

$$(iii)\ \sqrt{k}\left(1-\frac{\overline{F}\left(xX_{n-k:n}\right)}{\overline{F}\left(xa_k\right)}\right)=W_n\left(1\right)+o_{\mathbf{P}}\left(1\right),$$

uniformly on $x\geq 1$, *for every real* α.

Proof. Let us start by to prove assertion (i) for $\alpha=1$. Observe that

$$\sqrt{k}\left(1-nU_{k:n}/k\right)=\sqrt{k}\left(\frac{n}{k}\mathcal{U}_n\left(nU_{k:n}/k\right)-nU_{k:n}/k\right),$$

and from weak approximation (5.7), there exists a sequence of standard Wiener processes $W_n\left(s\right)$, such that

$$\sqrt{k}\left(\frac{n}{k}\mathcal{U}_n\left(nU_{k:n}/k\right)-nU_{k:n}/k\right)=W_n\left(nU_{k:n}/k\right)+o_{\mathbf{P}}\left(1\right).$$

Next we show that $W_n\left(nU_{k:n}/k\right)=W_n\left(1\right)+o_{\mathbf{P}}\left(1\right)$. To this end, let us

$$\epsilon_n:=\left|nU_{k:n}/k-1\right|$$

which tends to zero in probability. It is clear that for any fixed $d>0$, we have

$$\begin{aligned}&\mathbf{P}\left(\left|W_n\left(nU_{k:n}/k\right)-W_n\left(1\right)\right|>d\right)\\ =\ &\mathbf{P}\left(\left|W_n\left(\epsilon_n\right)\right|>d\right)\leq\mathbf{P}\left(\sup_{0\leq s\leq\epsilon_n}\left|W_n\left(s\right)\right|>d\right).\end{aligned}$$

For sufficiently small $\epsilon>0$, the latter probability is less than or equal to

$$\mathbf{P}\left(\left|\sup_{0\leq s\leq\epsilon}\left|W_n\left(s\right)\right|\right|>d\right)+\epsilon\leq\mathbf{P}\left(\left|W_n\left(1\right)\right|>\epsilon^{-1/2}d\right)+\epsilon,$$

which by using Markov's inequality is $\left(d^{-2}+1\right)\epsilon$. This means that $W_n\left(nU_{k:n}/k\right)=W_n\left(1\right)+o_{\mathbf{P}}\left(1\right)$. To show assertion (i) for every real α, it suffices to use the mean value theorem and the fact that $nU_{k:n}/k=1+o_{\mathbf{P}}\left(1\right)$. For assertions (ii) and(iii), let us write

$$\begin{aligned}&\sqrt{k}\left(1-\frac{\overline{F}\left(xX_{n-k:n}\right)}{\overline{F}\left(xa_k\right)}\right)\\ =\ &\sqrt{k}\left(\frac{nU_{k:n}}{k}-\frac{\overline{F}\left(xX_{n-k:n}\right)}{\overline{F}\left(xa_k\right)}\right)+\sqrt{k}\left(1-\frac{nU_{k:n}}{k}\right)\end{aligned}$$

and

$$\begin{aligned}&\sqrt{k}\left(\left(\frac{X_{n-k:n}}{a_k}\right)^{\alpha}-1\right)\\ =\ &\sqrt{k}\left(\left(\frac{X_{n-k:n}}{a_k}\right)^{\alpha}-\left(\frac{nU_{k:n}}{k}\right)^{-\alpha\gamma}\right)+\sqrt{k}\left(\left(\frac{nU_{k:n}}{k}\right)^{-\alpha\gamma}-1\right).\end{aligned}$$

By using similar arguments with the second order condition of $\overline{F}$, we show that both first terms of right-hand of the previous equations tend to zero in probability. To achieve the proof it suffices to apply assertion (i), as sought. ∎

Proposition 6.4. *Assume* $\overline{F}\in 2\mathcal{RV}_{(-1/\gamma)}\left(A_F,\rho_F\right)$ *and* $\overline{G}\in 2\mathcal{RV}_{(-1/\gamma_2)}\left(A_G,\rho_G\right)$. *Then, for all large* x, *there exist constants* $c_1,c_2>0$, *such that*

$$\overline{F}\left(x\right)=\left(1+o\left(1\right)\right)c_1x^{-1/\gamma}\ \textit{and}\ \overline{G}\left(x\right)=\left(1+o\left(1\right)\right)c_2x^{-1/\gamma_2}.$$

Proof. See the proof of Lemma 7.1 in [3]. ∎

Erratum: Moderate Deviations Principle and Central Limit Theorem for Stochastic Cahn-Hilliard Equation in Holder Norm

IJAMS Peer-reviewed journal
International Journal of Applied Mathematics and Simulation

Erratum: Moderate Deviations Principle and Central Limit Theorem for Stochastic Cahn-Hilliard Equation in Hölder Norm.

Ratsarasaina R. M.[1] and Rabeherimanana T.J.[2]

ABSTRACT: We consider a stochastic Cahn-Hilliard partial differential equation driven by a space-time white noise. In this paper, we prove a Central Limit Theorem (CLT) and a Moderate Deviation Principle (MDP) for a perturbed stochastic Cahn-Hilliard equation in Hölder norm. The techniques are based on Freidlin-Wentzell's Large Deviations Principle. The exponential estimates in the space of Hölder continuous functions and the Garsia-Rodemich-Rumsey's lemma plays an important role, an another approach than the Li.R. and Wang.X. Finally, we estabish the CLT and MDP for stochastic Cahn-Hilliard equation with uniformly Lipschitzian coefficients.

Keywords: Large Deviations Principle, Moderate Deviations Principle, Central Limit Theorem, Hölder space, Stochastic Cahn-Hilliard equation, Green's function, Freidlin-Wentzell's method.

MSC: 60H15, 60F05, 35B40, 35Q62

1 INTRODUCTION AND PRELIMINARIES.

The Cahn-Hilliard equation was developed in 1958 to model the phase separation process of a binary mixture (Cahn J.W. and Hilliard J.E. [3,4]). This approach has been extended to many other branches of science as dissimilar as polymer systems, population growth, image processing, spinodal decomposition, among others.

Consider the process $\{X^\varepsilon(t,x)\}_{\varepsilon>0}$ solution of stochastic Cahn-Hilliard with multipicative space time white noise, indexed by $\varepsilon > 0$, given by

$$\begin{cases} \partial_t X^\varepsilon(t,x) = -\Delta(\Delta X^\varepsilon(t,x) - f(X^\varepsilon(t,x))) + \sqrt{\varepsilon}\sigma(X^\varepsilon(t,x))\dot{W}(t,x), \\ \quad \text{in} \quad (t,x) \in [0,T]\times D, \\ X^\varepsilon(0,x) = X_0(x), \\ \frac{\partial X^\varepsilon(t,x)}{\partial \mu} = \frac{\partial \Delta X^\varepsilon(t,x)}{\partial \mu} = 0, \quad \text{on} \quad (t,x) \in [0,T]\times \partial D. \end{cases} \tag{1.1}$$

where $T > 0$, $D = [0,\pi]^3$, $\Delta X^\varepsilon(t,x)$ denotes the Laplacian of $X^\varepsilon(t,x)$ in the x-variable, μ is the outward normal vector, f is a polynomial of degree 3 with positive dominant coefficient such as $f = F'$ where

- [1] *Ratsarasaina R. M., Faculty of Sciences Technology, Departement of Mathematics and Informatics, University of Antananarivo, B.P.906, Ankatso, 101, Antananarivo, Madagascar.*
E-mail: ratsarasainaralphmartial@gmail.com
- [2] *Rabeherimanana T.J., corresponding author, Faculty of Sciences Technology, Departement of Mathematics and Informatics, University of Antananarivo, B.P.906, Ankatso, 101, Antananarivo, Madagascar.*
E-mail: rabeherimanana.toussaint@gmx.fr

Communicated Editor: Chala Adel
Manuscript published Jan 12, 2025.

$F(u) = (1-u^2)^2$, W is a space-time of a Brownian sheet defined on some filtered probability space $(\Omega, \mathcal{F}, (\mathcal{F}_t)_{t\geq 0}, \mathbb{P})$ and $\dot{W} = \frac{\partial^2 W}{\partial t \partial x}$ is the formal derivative of a Brownian sheet W defined on probability space $(\Omega, \mathcal{F}, \mathbb{P})$. The coefficients f, σ are uniform Lipschitz with respect to x, with at most linear growth. More precisely, we suppose that there exists two constants K_f and K_σ such that $\forall x, y \in \mathbb{R}$,

$$\begin{cases} |f(x) - f(y)| \leq K_f |x-y| \\ \\ |\sigma(x) - \sigma(y)| \leq K_\sigma |x-y| \end{cases} \tag{1.2}$$

and that there exists a constant $K > 0$ such that :

$$\sup\{|f(x)| + |\sigma(x)|\} \leq K(1+|x|). \tag{1.3}$$

Let X^0 be the solution of the determinic Cahn-Hilliard equation

$$\partial_t X^0(t,x) = -\Delta(\Delta X^0(t,x) - f(X^0(t,x)))$$

with initial condition $X^0(0,x) = X_0(x)$. We expect that $||X^\varepsilon - X^0||_\alpha \to 0$ in probability as $\varepsilon \to 0^+$ where $||.||_\alpha$ is the Hölder norm (see (2.1)). The LDP, CLT and MDP for stochastic Cahn-Hilliard equation are not new. For example, Boulanba.L. and Mellouk.M. [2] studied the LDP for the mild solution of Stochastic Cahn-Hilliard equation (1.1). Li.R. and Wang.X. [8] studied the CLT and MDP for stochastic perturbed Cahn-Hilliard equation using the weak convergence approach.

However, we study its CLT and MDP for stochastic Cahn-Hilliard equation in the context of Hölder norm using another method. It means, we study the process

$$\eta^\varepsilon(t,x) = \left(\frac{X^\varepsilon - X^0}{\sqrt{\varepsilon}}\right)(t,x) \tag{1.4}$$

and

$$\theta^\varepsilon(t,x) = \left(\frac{X^\varepsilon - X^0}{\sqrt{\varepsilon} h(\varepsilon)}\right)(t,x) \tag{1.5}$$

in order to get a CLT and a MDP respectively.
The techniques are based on the exponential estimates in the space of Hölder continuous functions. The Garsia-Rodemich-Rumsey's lemma plays a very important role.
The paper is organized as follows : in the section one, we prove that $\eta^\varepsilon(t,x)$ defined by (1.4) converges in probability to $\eta^0(t,x)$. More precisely we purpose to prove that $\lim_{\varepsilon\to 0} \mathbb{E}||\eta^\varepsilon - \eta^0||_\alpha^r = 0$. In the section two, we study the LDP for (1.4) as $\varepsilon \to 0$ for $1 < h(\varepsilon) < \frac{1}{\sqrt{\varepsilon}}$, that is to say , the process $\theta^\varepsilon(t,x)$ defined by (1.5) obeys a LDP on $\mathcal{C}^\alpha([0,1]\times D)$ with speed $h^2(\varepsilon)$ and with rate function $\widetilde{I}(.)$ defined later. In section three, we prove the main results. Finally the example for CLT and MDP for stochastic Cahn-Hilliard equation with uniformly Lipschitzian coefficients be given in section four.

2 MAIN RESULTS

Let $\mathbb{H}$ denote the Cameron-Martin space associated with the Brownian sheet $\big\{W(t,x),\ t\in[0,T],\ \ x\in D\big\}$, that is to say,

$$\mathbb{H} = \left\{ h(t) = \int_0^t \int_D |\dot{h}(t,x)|^2 dtdx : \dot{h} \in L^2\big([0,T]\times D\big)\right\}.$$

Let $\mathcal{E}_0$, $\mathcal{E}$ be polish space such that the initial condition $X_0(x)$ takes valued in a compact subspace of $\mathcal{E}_0$ and $\Theta^\varepsilon = \big\{\mathcal{G}^\varepsilon : \mathcal{E}_0 \times \mathcal{C}\big([0,T]\times D, \mathbb{R}\big) \to \mathcal{E},\ \ \varepsilon > 0\big\}$ a family of measurable maps valued in $\mathcal{E}$.
For $X_0 \in \mathcal{E}_0$, define $X^{\varepsilon,X_0} = \mathcal{G}^\varepsilon\big(X_0, \sqrt{\varepsilon}W\big)$ and for $n_0 \in \mathbb{N}$, consider the following $S^{n_0} = \{\Psi \in L^2([0,T]\times D) : \int_0^T \int_D \Psi^2(s,y)dsdy \leq n_0\}$ which is a compact metric space, equipped with the weak topology on $L^2([0,T]\times D)$.
We denote $||.||_\alpha$ the α-hölder norm such that

$$||F||_\alpha = ||F||_\infty + |F|_\alpha \tag{2.1}$$

where

$$\begin{aligned} ||F||_\infty &= \sup\big\{\big|F(s,x)\big| : \ (s,x)\in[0,T]\times D\big\}, \\ |F|_\alpha &= \sup\left\{\frac{|F(s_1,x_1)-F(s_2,x_2)|}{(|s_1-s_2|+|x_1-x_2|^2)^\alpha} : (s_1,x_1),(s_2,x_2)\in[0,T]\times D\right\}. \end{aligned}$$

Let $\mathcal{C}^\alpha([0,T]\times D)$ the space of function $F:[0,T]\times D\longrightarrow\mathbb{R}$ such that $||F||_\alpha<+\infty$.
Schilder's theorem for the Brownian sheet asserts that the family
$\big\{\sqrt{\varepsilon}W(t,x) : \ \varepsilon>0\big\}$ satisfies a LDP on $\mathcal{C}^\alpha([0,T]\times D)$, with the good rate function $I(.)$ defined by

$$I(h)=\begin{cases} \frac{1}{2}\int_0^T\int_D|\dot{h}(t,x)|^2dtdx & \text{for } h\in\mathbb{H} \\ +\infty & \text{otherwise,}\end{cases}$$

For $h\in\mathbb{H}$, let $X^h_{X_0}$ be the solution of the following deterministic partial differential equation

$$\partial_t X^h_{X_0}(t,x)=-\Delta(\Delta X^h_{X_0}(t,x)-f(X^h_{X_0}(t,x)))+\sigma(X^h_{X_0}(t,x))\dot{h}(t,x)$$

with initial condition

$$X^h_{X_0}(0,x)=X_0(x).$$

Theorem 1([2]): *Let σ be continuous on $\mathbb{R}$, f and σ satisfy conditions (1.2) and (1.3). Then, the law of $X^\varepsilon_{X_0}$ satisfies the LDP on $\mathcal{C}^\alpha([0,T]\times D)$ with a good rate fuction $\widetilde{I}_{X_0}(.)$ defined by*

$$\widetilde{I}_{X_0}(\Phi)=\inf_{\left\{\dot{h}\in L^2([0,T]\times D)\ :\ \Phi=\mathcal{G}^0(X_0,I(h))\right\}}\left\{\frac{1}{2}\int_0^T\int_D\dot{h}^2(s,y)dsdy\right\}$$

and $+\infty$ otherwise.
See also for example [1,7].
In addition to (1.2) and (1.3), the coefficient f is differentiable with respect to x and the derivative $f^{'}$ is also uniformly Lipschitz. More precisely, there exists a constante C such that

$$|f^{'}(x)-f^{'}(y)|\leq C|x-y| \tag{2.2}$$

for all $x,y\in\mathbb{R}$.
Combined with the uniform Lipschitz continuity of f, we have

$$|f^{'}(x)|\leq K_f. \tag{2.3}$$

2.1 Central Limit Theorem

In this section, our first main result is the following theorem :

Theorem 2: *Suppose that f, $f^{'}$ and σ satisfy conditions (1.2), (1.3), (2.2) and (2.3). Then for any $\alpha\in[0;\frac{1}{4})$, $r\geq 1$, the process $\eta^\varepsilon(t,x)$ defined by (1.4) converges in L^r to the random process $\eta^0(t,x)$ as $\varepsilon\to 0$ where $\eta^0(t,x)$ verifies the stochastic partial differential equation*

$$\partial_t\eta^0(t,x)=-\Delta(\Delta\eta^0(t,x)-f^{'}(X^0(t,x))\eta^0(t,x))+\sigma(X^0(t,x))\dot{W}(t,x)$$

with initial condition $\eta^0(0,x)=0$.

Let $S(t)=e^{-A^2t}$ be the semi-group generated by the operator $A^2u:=\sum_{i=0}^\infty e^{-\mu_i^2t}u_iw_i$ where $u:=\sum_{i=0}^\infty u_iw_i$. Then the convolution semi-group (see Cardon-Weber.C [5]) is defined by $S(t)U(x)=\sum_{i=0}^\infty e^{-\mu_i^2t}w_i(x)w_i(y)$ for any $U(x)$ in $L^2(D)$, with the associated Green's function G_t such that $G_t(x,y)=\sum_{i=0}^\infty e^{-\mu_i^2t}w_i(x)w_i(y)$. **Lemma 1:** *There exists positive constants C, γ and $\gamma^{'}$ satisfying $\gamma<4-d$, $\gamma\leq 2$ and $\gamma^{'}<1-\frac{d}{4}$ such that for all $y,z\in D$, $0\leq s<t\leq T$ and $0\leq h\leq t$, we have :*

1. $\int_0^t\int_D|G_r(x,y)-G_r(x,z)|^2dxdr\leq C|y-z|^\gamma$,
2. $\int_0^t\int_D|G_{r+h}(x,y)-G_r(x,y)|^2dxdr\leq C|h|^{\gamma^{'}}$,

3. $\int_0^t \int_D |G_r(x,y)|^2 dxdr \leq C|t-s|^{\gamma}$,
4. $\sup_{t\in[0,T]} \int_0^t \int_D |G_{t-u}(x,z) - G_{t-u}(y,z)|^p dudz \leq C|x-y|^{3-p}\ ,\ p \in]\frac{3}{2}, 3[$,
5. $\sup_{x\in D} \int_0^s \int_D |G_{t-u}(x,z) - G_{s-u}(x,z)|^p dudz \leq C|t-s|^{\frac{(3-p)}{2}}\ ,\ p \in]1, 3[$,
6. $\sup_{x\in D} \int_t^s \int_D |G_u(x,z)|^p dudz \leq C|t-s|^{\frac{(3-p)}{2}}\ ,\ p \in]1, 3[$.

2.2 Moderate Deviations Principle

In this paper, our second main result is the MDP for the Stochastic Cahn-Hilliard equation. More precisely, we assume that the process $\{\theta^{\varepsilon}(t,x)\}_{\varepsilon>0}$ defined by (1.5) obeys a LDP on the space $\mathcal{C}^{\alpha}([0,1]\times D)$, with speed $h^2(\varepsilon)$ and rate function $\widetilde{I}_{X_0}(.)$.

Proposition 1: *If f and σ are Lipschitzian, then there exists $C(p,K,K_f,$ $T,X_0)$ depending on p, K, K_f, T, X_0 such that*

$$\mathbb{E}\big(||X^{\varepsilon} - X^0||_{\infty}\big)^p \leq \varepsilon^{\frac{p}{2}} C(p,K,K_f,T,X_0) \longrightarrow 0 \ \text{ as } \ \varepsilon \to 0.$$

Theorem 3: *Let σ be continuous on $\mathbb{R}$ and f, f', σ satisfy the conditions (1.2), (1.3), (2.2) and (2.3).Then, the process $\{\theta^{\varepsilon}(t,x)\}_{\varepsilon>0}$ defined by (1.5) obeys a LDP on the space $\mathcal{C}^{\alpha}([0,1]\times D)$, with speed $h^2(\varepsilon)$ and rate function $\widetilde{I}_{X_0}(.)$ such that:*

$$\widetilde{I}_{X_0}(\phi) = \inf_{\{h\in L^2([0,T]\times D)\ :\ \phi = \mathcal{G}^0(X_0, I(h))\}} \left\{ \frac{1}{2} \int_0^T \int_D \dot{h}^2(s,y) dyds \right\}$$

and $+\infty$ otherwise.

3 PROOF OF MAIN RESULTS

Proof of proposition 1: In Boulanba and Mellouk [2], we know that the stochastic Cahn-Hilliard equation has a solution $\{X^{\varepsilon}(t,x)\}_{\varepsilon>0}$ such that

$$\begin{aligned} X^{\varepsilon}(t,x) &= \int_D G_t(x,y) X_0(y) dy + \int_0^t \int_D \Delta G_{t-s}(x,y) f(X^{\varepsilon}(s,y)) dsdy \\ &+ \sqrt{\varepsilon} \int_0^t \int_D G_{t-s}(x,y) \sigma(X^{\varepsilon}(s,y)) W(ds,dy). \end{aligned}$$

and that $||X^{\varepsilon} - X^0||_{\alpha} \to 0$ in probability as $\varepsilon \to 0^+$ where X^0 is the solution of

$$X^0(t,x) = \int_D G_t(x,y) X_0(y) dy + \int_0^t \int_D \Delta G_{t-s}(x,y) f(X^0(s,y)) dsdy.$$

Then we have

$$\begin{aligned} \big(X^{\varepsilon} - X^0\big)(t,x) &= \int_0^t \int_D \Delta G_{t-s}(x,y) \big[f(X^{\varepsilon}(s,y)) - f(X^0(s,y))\big] dsdy \\ &+ \sqrt{\varepsilon} \int_0^t \int_D G_{t-s}(x,y) \sigma(X^{\varepsilon}(s,y)) W(ds,dy). \end{aligned}$$

Using the inequality $(a+b)^p \leq 2^{p-1}(a^p + b^p)$, we have

$$\begin{aligned} \big(||X^{\varepsilon} - X^0||_{\infty}\big)^p &\leq 2^{p-1} \Bigg(\Bigg[\sup_{\substack{0\leq s\leq T \\ x\in D}} \Bigg| \int_0^t \int_D \Delta G_{t-s}(x,y) [f(X^{\varepsilon}(s,y)) \\ &- f(X^0(s,y))] dsdy \Bigg| \Bigg]^p \\ &+ \varepsilon^{\frac{p}{2}} \Bigg[\sup_{\substack{0\leq s\leq T \\ x\in D}} \Bigg| \int_0^t \int_D G_{t-s}(x,y) \sigma(X^{\varepsilon}(s,y)) W(ds,dy) \Bigg| \Bigg]^p \Bigg). \end{aligned}$$

Denote

$$\begin{aligned}\alpha_1^\varepsilon(t,x) &= \int_0^t\int_D \Delta G_{t-s}(x,y)[f(X^\varepsilon(s,y))-f(X^0(s,y))]dsdy,\\ \alpha_2^\varepsilon(t,x) &= \int_0^t\int_D G_{t-s}(x,y)\sigma(X^\varepsilon(s,y))W(ds,dy).\end{aligned}$$

From (1.2), (1.3) and Hölder inequality, for $p>2$,

$$\mathbb{E}\big(||\alpha_1^\varepsilon||_\infty^T\big)^p \le K_f^p\bigg(\sup_{\substack{0\le s\le T\\ x\in\overline{D}}}\bigg|\int_0^t\int_D \Delta G_t^q(x,y)dsdy\bigg|\bigg)^{\frac{p}{q}}\mathbb{E}\int_0^T |X_{X_0}^\varepsilon - X_{X_0}^0|^p dt$$

where $\frac{1}{p}+\frac{1}{q}=1$.
For any $p>2$ and $q^{'}\in(1,\frac{3}{2})$ such that $\gamma := (3-2q^{'})p/(4q^{'})-2>0$, and for any $x,y\in D$, $t\in[0,T]$, by Burkholder's inequality for stochastic integrals against Brownian sheets (see Walsh.J.B. [9], page 315) and Hölder's inequality, we have

$$\begin{aligned}&\mathbb{E}\big(|\alpha_2^\varepsilon(t,x)-\alpha_2^\varepsilon(t,y)|^p\big)\\ &\le c_p\mathbb{E}\bigg(\int_0^t\int_D |G_{t-u}(x,z)-G_{t-u}(y,z)|^2\sigma^2(X_{X_0}^\varepsilon(u,z))dudz\bigg)^{\frac{p}{2}}\\ &\le c_pK^p\bigg(\int_0^t\int_D |G_{t-u}(x,z)-G_{t-u}(y,z)|^{2q'}dudz\bigg)^{\frac{p}{2q'}}\\ &\quad\times\mathbb{E}\bigg(\int_0^t\int_D (1+|X_{X_0}^\varepsilon(u,z)|)^{2p'}dudz\bigg)^{\frac{p}{2p'}}\\ &\le C(p,K,X_0)|x-y|^{\frac{(3-2q^{'})p}{2q'}},\end{aligned}\tag{3.1}$$

where (1.3) and 4 in Lemma 1 were used, $\frac{1}{p'}+\frac{1}{q'}=1$ and $C(p,K,X_0)$ is independent of ε.
Similary, from 4, 5 and 6 in Lemma 1, for $0\le s\le t\le T$,

$$\begin{aligned}&\mathbb{E}\big(|\alpha_2^\varepsilon(t,y)-\alpha_2^\varepsilon(s,y)|^p\big)\\ &\le c_p\mathbb{E}\bigg(\int_0^s\int_D |G_{t-u}(y,z)-G_{s-u}(y,z)|^2\sigma^2(X_{X_0}^\varepsilon(u,z))dudz\bigg)^{\frac{p}{2}}\\ &\quad+c_p\mathbb{E}\bigg(\int_s^t\int_D |G_{t-u}(y,z)|^2\sigma^2(X_{X_0}^\varepsilon(u,z))dudz\bigg)^{\frac{p}{2}}\\ &\le c_pK^p\bigg(\int_0^s\int_D |G_{t-u}(y,z)-G_{s-u}(y,z)|^{2q'}dudz\bigg)^{\frac{p}{2q'}}\\ &\quad\times\mathbb{E}\bigg(\int_0^s\int_D (1+|X_{X_0}^\varepsilon(u,z)|)^{2p'}dudz\bigg)^{\frac{p}{2p'}}\\ &\quad+c_pK^p\bigg(\int_s^t\int_D |G_{t-u}(y,z)|^{2q'}dudz\bigg)^{\frac{p}{2q'}}\\ &\quad\times\mathbb{E}\bigg(\int_s^t\int_D (1+|X_{X_0}^\varepsilon(u,z)|)^{2p'}dudz\bigg)^{\frac{p}{2p'}}\\ &\le C(p,K,X_0)|t-s|^{\frac{(3-2q^{'})p}{4q'}}\end{aligned}\tag{3.2}$$

Putting together (3.1) and (3.2), by Garsia-Rodemich-Rumsey (see Wang.R. and Zang.T. [10] or Corollary 1.2 in Walsh.J.B. [9]), there exist a random variable $K_{p,\varepsilon}(\omega)$ and a constant c such that

$$\begin{aligned}&\mathbb{E}\big(|\alpha_2^\varepsilon(t,y)-\alpha_2^\varepsilon(s,y)|^p\big)\\ &\leq\ K_{p,\varepsilon}(\omega)^p(|t-s|+|x-y|)^\gamma\left(\log\frac{c}{|t-s|+|x-y|}\right)^2\end{aligned}\tag{3.3}$$

and

$$\sup_\varepsilon \mathbb{E}[K_{p,\varepsilon}^p]<+\infty.$$

choosing $s=0$ in (3.3), we obtain

$$\begin{aligned}\mathbb{E}\Big(\sup_{\substack{0\leq s\leq T\\ x\in D}}\Big|\int_0^t\int_D G_{t-s}(x,y)\sigma(X^\varepsilon(s,y))W(ds,dy)\Big|\Big)^p &\leq C(p,K,X_0)\sup_\varepsilon\mathbb{E}[K_{p,\varepsilon}^p]\\ &< +\infty.\end{aligned}\tag{3.4}$$

Putting (3.1), (3.2) and (3.3) together and using 6 in Lemma 1, there exists a constant $C(p,K,K_f,X_0)$ such that

$$\mathbb{E}(||X_t^\varepsilon-X_t^0||_\infty^T)^p \leq C(p,K,K_f,X_0)\left(\mathbb{E}\int_0^t(||X_s^\varepsilon-X_s^0||_\infty)^p ds+\varepsilon^{\frac{p}{2}}\right)$$

By Gronwall's inequality, we have

$$\mathbb{E}(||X_t^\varepsilon-X_t^0||_\infty)^p \leq \varepsilon^{\frac{p}{2}}C(p,K,K_f,X_0)e^{C(p,K,K_f,X_0)T}.$$

Putting $\varepsilon\to 0$, the proof is complete. □

Proof of Theorem 2 : The following Lemma is a consequence of Garsia-Rodemich-Rumsey's theorem.

Lemma 2: *Let $\widetilde{V}^\varepsilon(t,x)=\{V^\varepsilon(t,x)\ :\ (t,x)\in[0,T]\times D\}$ be a family of real-valued stochastic processes and let $p\in(0,\infty)$. Suppose that $\widetilde{V}^\varepsilon(t,x)$ satisfies the following assumptions :*

A-1°) *For any $(t,x)\in[0,T]\times D$,*

$$\lim_{\varepsilon\to 0}\mathbb{E}|V^\varepsilon(t,x)|^p=0$$

A-2°) *There exists $\gamma>0$ such that for any (t,x), $(s,y)\in[0,T]\times D$*

$$\mathbb{E}|V^\varepsilon(t,x)-V^\varepsilon(s,y)|^p\leq C(|t-s|+|x-y|^2)^{2+\gamma},$$

where C is a constant independent of ε.
In this case, for any $\alpha\in(0,\frac{\gamma}{k})$, $p\in[1,k)$,

$$\lim_{\varepsilon\to 0}\mathbb{E}||V^\varepsilon||_\alpha^p=0.$$

In this section, we prove that

$$\lim_{\varepsilon\to 0}\mathbb{E}||X_t^\varepsilon-X_t^0||_\alpha^r=0.$$

Consider the process $\eta^\varepsilon(t,x)$ defined by (1.4) and

$$\begin{aligned}X^\varepsilon(t,x) &= \int_D G_t(x,y)X_0(y)dy+\int_0^t\int_D\Delta G_{t-s}(x,y)f(X^\varepsilon(s,y))dsdy\\ &+ \sqrt{\varepsilon}\int_0^t\int_D G_{t-s}(x,y)\sigma(X^\varepsilon(s,y))W(ds,dy).\end{aligned}$$

We know that $||X^\varepsilon-X^0||_\alpha\to 0$ in probability as $\varepsilon\to 0^+$ where X^0 is the solution of

$$X^0(t,x) = \int_D G_t(x,y)X_0(y)dy+\int_0^t\int_D\Delta G_{t-s}(x,y)f(X^0(s,y))dsdy.$$

In this case, we have

$$\begin{aligned}\eta^{\varepsilon}(t,x) &= \int_0^t\int_D \Delta G_{t-s}(x,y)\Big(\frac{f(X^{\varepsilon}(s,y))-f(X^0(s,y))}{\sqrt{\varepsilon}}\Big)dsdy\\ &+ \int_0^t\int_D G_{t-s}(x,y)\sigma(X^{\varepsilon}(s,y))W(ds,dy)\end{aligned}$$

then

$$\begin{aligned}\eta^{\varepsilon}(t,x) &= \int_0^t\int_D \Delta G_{t-s}(x,y)f^{'}(X^{\varepsilon}(s,y))\eta^{\varepsilon}(s,y)dsdy\\ &+ \int_0^t\int_D G_{t-s}(x,y)\sigma(X^{\varepsilon}(s,y))W(ds,dy).\end{aligned}$$

For $\varepsilon\to 0$, we have

$$\begin{aligned}\eta^{0}(t,x) &= \int_0^t\int_D \Delta G_{t-s}(x,y)f^{'}(X^{0}(s,y))\eta^{0}(s,y)dsdy\\ &+ \int_0^t\int_D G_{t-s}(x,y)\sigma(X^{0}(s,y))W(ds,dy).\end{aligned}$$

To this end, we verify (A-1), (A-2); for $V^{\varepsilon}=\eta^{\varepsilon}-\eta^0$, write

$$\begin{aligned}V^{\varepsilon}(t,x) &= \int_0^t\int_D \Delta G_{t-s}(x,y)\Big(\frac{f(X^{\varepsilon}(s,y))-f(X^0(s,y))}{\sqrt{\varepsilon}}\\ &- f^{'}(X^0(s,y))\eta^0(s,y)\Big)dsdy\\ &+ \int_0^t\int_D G_{t-s}(x,y)\big(\sigma(X^{\varepsilon}(s,y))-\sigma(X^0(s,y))\big)W(ds,dy).\end{aligned}$$

Let

$$\begin{aligned}k_1^{\varepsilon}(t,x) &= \int_0^t\int_D \Delta G_{t-s}(x,y)\Big(\frac{f(X^{\varepsilon}(s,y))-f(X^0(s,y))}{\sqrt{\varepsilon}}\\ &\quad -f^{'}(X^0(s,y))\eta^{\varepsilon}(s,y)\Big)dsdy,\\ k_2^{\varepsilon}(t,x) &= \int_0^t\int_D \Delta G_{t-s}(x,y)f^{'}(X^0(s,y))\big(\eta^{\varepsilon}(s,y)-\eta^0(s,y)\big)dsdy,\\ k_3^{\varepsilon}(t,x) &= \int_0^t\int_D G_{t-s}(x,y)\big(\sigma(X^{\varepsilon}(s,y))-\sigma(X^0(s,y))\big)W(ds,dy).\end{aligned}$$

Now we shall divide the proof into the following two steps.

Step 1. Following the same calculation as the proof of (3.4) in proposition 1, we deduce that for $p>2$, $0\le t\le 1$

$$\begin{aligned}\mathbb{E}\big(||k_3^{\varepsilon}||_{\infty}^t\big) &\le C(p,K_{\sigma},T)\int_0^t\mathbb{E}\big(||X^{\varepsilon}-X^0||_{\infty}^s\big)^p ds\\ &\le \varepsilon^{\frac{p}{2}}C(p,K,K_{\sigma},T,X_0).\end{aligned}$$

By Taylor's formula, there exists a random field $\beta^{\varepsilon}(t,x)$ taking values in $(0,1)$ such that,

$$\begin{aligned}f(X^{\varepsilon}(s,y))-f(X^0(s,y)) &= f^{'}\big(X^0(s,y)+\beta^{\varepsilon}(t,x)(X^{\varepsilon}(s,y)-X^0(s,y))\big)\\ &\quad\times(X^{\varepsilon}(s,y)-X^0(s,y))\end{aligned}$$

Since $f^{'}$ is also Lipschitz continuous, we have

$$\big|f^{'}\big(X^0(s,y)+\beta^{\varepsilon}(t,x)(X^{\varepsilon}(s,y)-X^0(s,y))\big)-f^{'}\big(X^0(s,y)\big)\big|$$

$$\leq C\beta^{\varepsilon}(t,x)\big|X^{\varepsilon}(t,x)-X^{0}(t,x)\big|.$$

then

$$\begin{aligned}&\big|f^{'}\big(X^{0}(s,y)+\beta^{\varepsilon}(t,x)(X^{\varepsilon}(s,y)-X^{0}(s,y))\big)-f^{'}\big(X^{0}(s,y)\big)\big|\\&\leq C\big|X^{\varepsilon}(t,x)-X^{0}(t,x)\big|.\end{aligned}$$

Hence

$$\begin{aligned}\big|k_1^{\varepsilon}(t,x)\big| &\leq C\int_0^t\int_D \Delta G_{t-s}(x,y)\big|\big(X^{\varepsilon}(t,x)-X^{0}(t,x)\big)\eta^{\varepsilon}(s,y)\big|dsdy\\&= \sqrt{\varepsilon}C\int_0^t\int_D \Delta G_{t-s}(x,y)\big(\eta^{\varepsilon}(s,y)\big)^2dsdy. \qquad (3.5)\end{aligned}$$

By Hölder's inequality, for $p>2$

$$\begin{aligned}&\mathbb{E}\big(\big|k_1^{\varepsilon}\big|_{\infty}^{t}\big)^p\\&\leq \varepsilon^{\frac{p}{2}}C^p\bigg(\sup_{0\leq s\leq T\ ,x\in D}\ \bigg|\int_0^t\int_D \Delta G_s^q(x,y)dsdy\bigg|\bigg)^{\frac{p}{q}}\times\int_0^t\mathbb{E}\big(||\eta^{\varepsilon}||_{\infty}^{s}\big)^{2p}ds\end{aligned}$$

where $\frac{1}{p}+\frac{1}{q}=1$.

Using (2.2) and applying proposition 1, there exists a constant $C(p,K,K_f,C,K_\sigma,T,X_0)$ depending on p, K, K_f, C, K_σ, T, X_0 such that

$$\mathbb{E}\big(\big|k_1^{\varepsilon}(t,x)\big|\big)^p \leq \varepsilon^{\frac{1}{2}}C(p,K,K_f,C,K_\sigma,T,X_0) \qquad (3.6)$$

Noticing that $|f^{'}|\leq K_f$, by Hölder inequality, we deduce that for $p>2$

$$\begin{aligned}&\mathbb{E}\big(\big|k_2^{\varepsilon}(t,x)\big|\big)^p\\&\leq K_f^p\big(\sup_{\substack{0\leq s\leq T\\ x\in D}}\ \big|\int_0^t\int_D \Delta G_s^q(x,y)dsdy\big|\big)^{\frac{p}{q}}\int_0^t\mathbb{E}\big(||\eta^{\varepsilon}-\eta^{0}||_{\infty}^{s}\big)^p ds \qquad (3.7)\end{aligned}$$

where $\frac{1}{p}+\frac{1}{q}=1$.

Putting (3.5), (3.6) and (3.7) together, we have

$$\mathbb{E}\big(||\eta^{\varepsilon}-\eta^{0}||_{\infty}^{s}\big)^p\leq C(p,K,K_f,C,K_\sigma,T,X_0)\bigg(\varepsilon^{\frac{1}{2}}+\int_0^t\mathbb{E}\big(||\eta^{\varepsilon}-\eta^{0}||_{\infty}^{s}\big)^p ds\bigg)$$

By Gronwall's inequality, we obtain

$$\mathbb{E}\big(||\eta^{\varepsilon}-\eta^{0}||_{\infty}^{s}\big)^p\leq\varepsilon^{\frac{1}{2}}C(p,K,K_b,C,K_\sigma,T,X_0)\longrightarrow 0\ \text{ for }\ \varepsilon\to 0.$$

Step 2. We show that all the terms k_i^ε, $i = 1, 2, 3$ satisfy the condition (A-2) in Lemma 2. For any $p > 2$ and $q^{'} \in (1, \frac{3}{2})$ such that $\gamma := (3 - 2q^{'})p/(4q^{'}) - 2 > 0$, for all $x, y \in D$, $0 \le t \le T$, by Burkholder's inequality and Hölder's inequality, we have

$$\begin{aligned}
\mathbb{E}\big|k_3^\varepsilon(t,x) - k_3^\varepsilon(t,y)\big|^p &\le C_p\mathbb{E}\bigg(\int_0^t\int_D |G_{t-u}(x,z) - G_{t-u}(y,z)|^2 \\
&\quad \times(\sigma(X^\varepsilon(u,z)) - \sigma(X^0(u,z)))^2 dudz\bigg)^{\frac{p}{2}} \\
&\le C_p\bigg(\int_0^t\int_D (|G_{t-u}(x,z) - G_{t-u}(y,z)|)^{2q^{'}} dudz\bigg)^{\frac{p}{2q^{'}}} \\
&\quad \times K_\sigma^p\mathbb{E}\bigg(\int_0^t\int_D |X^\varepsilon(u,z) - X^0(u,z)|^{2p^{'}} dudz\bigg)^{\frac{p}{2p^{'}}} \\
&\le C(p, q^{'}, K_\sigma, K, T)|x-y|^{\frac{(3-2q^{'})p}{2q^{'}}} \qquad (3.8)
\end{aligned}$$

where (1.3), 4 in Lemma 1 and Proposition 1 were used, $\frac{1}{p^{'}} + \frac{1}{q^{'}} = 1$.
Similarly, in view of 5 , 6 in Lemma 1; it follows that for $0 \le s \le t \le T$, we have

$$\begin{aligned}
&\mathbb{E}\big|k_3^\varepsilon(t,y) - k_3^\varepsilon(s,y)\big|^p \\
&\le C_p\mathbb{E}\big(\int_0^s\int_D |G_{t-u}(y,z) - G_{s-u}(y,z)|^2\big(\sigma(X^\varepsilon(u,z)) - \sigma(X^0(u,z))\big)^2 dudz\big)^{\frac{p}{2}} \\
&+ C_p\mathbb{E}\big(\int_s^t\int_D |G_{t-u}(y,z)|^2\big(\sigma(X^\varepsilon(u,z)) - \sigma(X^0(u,z))\big)^2 dudz\big)^{\frac{p}{2}} \\
&\le C_p\bigg(\int_0^t\int_D |G_{t-u}(y,z) - G_{s-u}(y,z)|^{2q^{'}} dudz\bigg)^{\frac{p}{2q^{'}}} \\
&\quad \times K_\sigma^p\mathbb{E}\bigg(\int_0^t\int_D |X^\varepsilon(u,z) - X^0(u,z)|^{2p^{'}} dudz\bigg)^{\frac{p}{2p^{'}}} \\
&+ C_p\big(\int_s^t\int_D |G_{t-u}(y,z)|^{2q^{'}} dudz\big)^{\frac{p}{2q^{'}}} \\
&\quad \times K_\sigma^p\mathbb{E}\bigg(\int_0^t\int_D |X^\varepsilon(u,z) - X^0(u,z)|^{2p^{'}} dudz\bigg)^{\frac{p}{2p^{'}}} \\
&\le C(p, q^{'}, K_\sigma, K, T)|t-s|^{\frac{(3-2q^{'})p}{4q^{'}}} \qquad (3.9)
\end{aligned}$$

where Proposition 1 were used, $\frac{1}{p^{'}} + \frac{1}{q^{'}} = 1$, $C(p, q^{'}, K_\sigma, K, T)$ is independent of ε.
Putting together (3.8) and (3.9), we have

$$\mathbb{E}\big|k_3^\varepsilon(t,x) - k_3^\varepsilon(s,y)\big|^p \le C(p, q^{'}, K_\sigma, K, T)\big(|t-s| + |x-y|^2\big)^\gamma \qquad (3.10)$$

Consequently, from 4, 6 in Lemma 1, proposition 1 and the result of step 1, we also have :

$$\mathbb{E}\big|k_i^\varepsilon(t,x) - k_i^\varepsilon(s,y)\big|^p \le C\big(|t-s| + |x-y|^2\big)^\gamma \ , \ \ i = 2, 3. \qquad (3.11)$$

Putting together (3.10) and (3.11), we obtain that there exists a constant C independent of ε satisfying that

$$\mathbb{E}\big|(\eta^\varepsilon(t,x) - \eta^0(t,x)) - (\eta^\varepsilon(s,y) - \eta^0(s,y))\big|^p \le C\big(|t-s| + |x-y|^2\big)^\gamma$$

For any $\alpha \in (0, \frac{1}{4})$, $r \ge 1$, choosing $p > 2$, and $q^{'} \in (1, \frac{1}{4})$ such that $\alpha \in (0, \frac{\gamma}{p})$ and $r \in [1, p)$, Lemma 2 we have

$$\lim_{\varepsilon\to 0}\mathbb{E}||\eta^\varepsilon - \eta||_\alpha^r = 0.$$

The proof is complete . □

Proof of Theorem 3 : Recall the following lemma from Chenal.F and Millet.A [6].

Lemma 3: *Let* $F : ([0,T] \times D)^2 \longrightarrow \mathbb{R}$, $\alpha_0 > 0$ *and* $C_F > 0$ *be such that for any* $(t,x),(s,y) \in [0,T] \times D$, *set*

$$\int_0^T \int_D |F(t,x,u,z) - F(s,y,u,z)|^2 dudz \leq C(|t-s| + |x-y|^2)^{\alpha_0}. \tag{3.12}$$

Let $N : [0,T] \times D \longrightarrow \mathbb{R}$ *be an almost surely continuous,* $\mathcal{F}_t-$*adapted such that* $\sup\{|N(t,x)| : (t,x) \in [0,T] \times D\} \leq \rho$,*a.s., and for* $(t,x) \in [0,T] \times D$, *set*

$$\mathfrak{F}(t,x) = \int_0^T \int_D F(t,x,u,z) N(u,z) W(dudz)$$

Then for all $\alpha \in]0, \frac{\alpha_0}{2}[$, *there exists a constant* $C(\alpha,\alpha_0)$ *such that for all* $M \geq \rho C_F C(\alpha,\alpha_0)$

$$\mathbb{P}(||\mathfrak{F}||_\alpha \geq M) \leq (\sqrt{2}T^2 + 1) \exp\left(- \frac{M^2}{\rho^2 C_F C^2(\alpha,\alpha_0)} \right)$$

Proof of Theorem 3 : Now, we prove the MDP, that is to say, the process θ^ε defined by (1.5) obeys a LDP on $\mathcal{C}^\alpha([0,T] \times D)$, with the speed function $h^2(\varepsilon)$ and the rate function $\widetilde{I}(.)$. More precisely, to prove the LDP of $\frac{\eta^\varepsilon}{h(\varepsilon)}$, it is enough to show that $\frac{\eta^\varepsilon}{h(\varepsilon)}$ is $h^2(\varepsilon)$-exponentially equivalent to $\frac{\eta^0}{h(\varepsilon)}$,that is to say, for any $\delta > 0$, we have

$$\limsup_{\varepsilon \to 0} h^{-2}(\varepsilon) \ \log \ \mathbb{P}\left(\frac{||\eta^\varepsilon - \eta^0||_\alpha}{h(\varepsilon)} > \delta \right) = -\infty. \tag{3.13}$$

Since

$$||\eta^\varepsilon - \eta^0||_\alpha \leq (1 + (1+T)^\alpha) |\eta^\varepsilon - \eta^0|_\alpha^T$$

to prove (3.13), it is enough to prove that

$$\limsup_{\varepsilon \to 0} h^{-2}(\varepsilon) \ \log \ \mathbb{P}\left(\frac{|\eta^\varepsilon - \eta^0|_\alpha^T}{h(\varepsilon)} > \delta \right) = -\infty \quad , \qquad \forall \delta > 0.$$

Recall the decomposition in Proof of Theorem 2,

$$\eta^\varepsilon(t,x) - \eta^0(t,x) = k_1^\varepsilon(t,x) + k_2^\varepsilon(t,x) + k_3^\varepsilon(t,x).$$

For any q in $(\frac{3}{2},3)$, $\frac{1}{p} + \frac{1}{q} = 1$, and $x,y \in D$, $0 \leq s \leq t \leq T$, by Hölder's inequality, 4 in Lemma 1 and (2.3), we have

$$\begin{aligned} \left|k_2^\varepsilon(t,x) - k_2^\varepsilon(t,y)\right|^p &\leq K_f \left(\int_0^t \int_D |\Delta G_{t-u}(x,z) - \Delta G_{t-u}(y,z)|^q dudz \right)^{\frac{1}{q}} \\ &\quad \times \left(\int_0^t \int_D |\eta^\varepsilon(u,z) - \eta^0(u,z)|^p dudz \right)^{\frac{1}{p}} \\ &\leq K_f |x-y|^{\frac{3-q}{q}} \times \left(\int_0^t (||\eta^\varepsilon - \eta^0||_\infty^u)^p du \right)^{\frac{1}{p}} \end{aligned} \tag{3.14}$$

Similarly, in view of 5 and 6 in Lemma 1, it follows that for $0 \le s \le t \le T$,

$$\begin{aligned}\left|k_2^\varepsilon(t,y)-k_2^\varepsilon(s,y)\right|^p &\le K_f\bigg(\int_0^s\int_D |\Delta G_{t-u}(y,z)-\Delta G_{s-u}(y,z)|^q dudz\bigg)^{\frac{1}{q}}\\ &\quad\times\bigg(\int_0^s\int_D |\eta^\varepsilon(u,z)-\eta^0(u,z)|^p\bigg)^{\frac{1}{p}}\\ &\quad+\bigg(\int_s^t\int_D |\Delta G_{t-u}(y,z)|^q dudz\bigg)^{\frac{1}{q}}\\ &\quad\times\bigg(\int_0^t\int_D |\eta^\varepsilon(u,z)-\eta^0(u,z)|^p\bigg)^{\frac{1}{p}}\\ &\le 2K_f|t-s|^{\frac{3-q}{2q}}\times\bigg(\int_0^t(||\eta^\varepsilon-\eta^0||_\infty^u)^p du\bigg)^{\frac{1}{p}} \qquad (3.15)\end{aligned}$$

Putting together (3.14), (3.15), we have

$$\left|k_2^\varepsilon(t,y)-k_2^\varepsilon(s,y)\right|^p \le C(K_f)(|t-s|+|x-y|^2)^{\frac{3-q}{2q}}\times\bigg(\int_0^t(||\eta^\varepsilon-\eta^0||_\infty^u)^p du\bigg)^{\frac{1}{p}}.$$

Choosing $q\in(\frac{3}{2},3)$, such that $\alpha=(3-q)/2q$ and noticing that $||\eta^\varepsilon-\eta^0||_\infty^u \le (1+u)^\alpha|\eta^\varepsilon-\eta|_\alpha^u$, we obtain that

$$|k_2^\varepsilon|_\alpha^t \le C(K_f)\bigg(\int_0^t((1+u)^\alpha|\eta^\varepsilon-\eta^0|_\alpha^u)^p du\bigg)^{\frac{1}{p}}$$

Thus, for $t\in[0,1]$, we have

$$(|\eta_t^\varepsilon-\eta_t^0|_\alpha^t)^p \le C(p,T,K_f)\bigg[\big(|k_1^\varepsilon(t)|_\alpha^t+|k_3^\varepsilon(t)|_\alpha^t\big)^p+\int_0^t(|\eta^\varepsilon-\eta^0|_\alpha^s)^p ds\bigg]$$

Applying Gronwall's Lemma, we have

$$(|\eta_t^\varepsilon-\eta_t^0|_\alpha^t)^p \le C(p,T,K_f)\bigg[\big(|k_1^\varepsilon(t)|_\alpha^t+|k_3^\varepsilon(t)|_\alpha^t\big)^p\bigg]e^{C(p,T,K_f)T} \qquad (3.16)$$

By (3.15) and (3.16), its sufficient to prove that for any $\delta>0$

$$\limsup_{\varepsilon\to0}h^{-2}(\varepsilon)\log\mathbb{P}\bigg(\frac{|k_i^\varepsilon(t)|_\alpha^T}{h(\varepsilon)}>\delta\bigg)=-\infty \qquad i=1,3.$$

Step 1. For any $\varepsilon>0$, $\eta>0$ we have

$$\begin{aligned}\mathbb{P}\big(|k_3^\varepsilon|_\alpha^T>h(\varepsilon)\delta\big) &\le \mathbb{P}\big(|k_3^\varepsilon|_\alpha^T>h(\varepsilon)\delta,|X^\varepsilon-X^0|_\infty^T<\eta\big)\\ &+ \mathbb{P}(|X^\varepsilon-X^0|_\infty^T\ge\eta) \qquad (3.17)\end{aligned}$$

By 4 and 6 in Lemma 1, $G_{t-u}(x,z)1_{[u\le t]}$ satisfies (3.12)(see Lemma 3) for $\alpha_0=\frac{1}{2}$. Applying Lemma 3, we have

$$F(t,x,u,z)=G_{t-u}(x,z)1_{[u\le t]},\alpha_0=\frac{1}{2},C_F=C,M=h(\varepsilon)\delta,\rho=\eta K_\sigma,$$

$$\widetilde{Y}(t,x)=\big(\sigma(X_{X_0}^\varepsilon(t,x))-\sigma(X_{X_0}^0(t,x))\big)1_{||X^\varepsilon-X^0||_\infty^T>\eta}$$

, we obtain that for all ε sufficiently small such that $h(\varepsilon)\delta\ge\rho CC(\alpha,\frac{1}{2})$,

$$\begin{aligned}&\mathbb{P}\big(|k_3^\varepsilon(t)|_\alpha^T>h(\varepsilon)\delta,||X^\varepsilon-X^0||_\infty^T<\eta\big)\\ &\le(\sqrt{2}T^2+1)\exp\bigg(-\frac{h^2(\varepsilon)\delta^2}{\eta^2K_\sigma^2CC^2(\alpha,\frac{1}{2})}\bigg). \qquad (3.18)\end{aligned}$$

Since $X^{\varepsilon}_{X_0}$ satisfies the LDP on $\mathcal{C}^{\alpha}([0,T]\times D)$, see Theorem 1

$$\begin{aligned}\limsup_{\varepsilon\to 0}\varepsilon\log\mathbb{P}(||X^{\varepsilon}-X^0||^T_{\infty}\geq\eta) &\leq \limsup_{\varepsilon\to 0}\varepsilon\log\mathbb{P}(||X^{\varepsilon}-X^0||_{\alpha}\geq\eta)\\ &\leq -\inf\{I_{X_0}(f):\ ||f-X^0||_{\alpha}\geq\eta\}\end{aligned}$$

In this case, the good rate function $\mathcal{I}=\{I_{X_0}(f):\ ||f-X^0||_{\alpha}\geq\eta\}$ has compact level sets, the "$\inf\{I_{X_0}(f)\ :\ ||f-X^0||_{\alpha}\geq\eta\}$" is obtained at some function f_0. Because $I_{X_0}(f)=0$ if and only if $f=X^0_{X_0}$, we conclude that

$$-\inf\{I_{X_0}(f)\ :\ ||f-X^0||_{\alpha}\geq\eta\}<0.$$

For $h(\varepsilon)\to\infty$, $\sqrt{\varepsilon}h(\varepsilon)\to 0$, we have

$$\limsup_{\varepsilon\to 0}h^{-2}(\varepsilon)\log\mathbb{P}\big(||X^{\varepsilon}-X^0||^T_{\infty}\geq\eta\big)=-\infty. \tag{3.19}$$

Since $\eta>0$ is arbitrary, putting together (3.17), (3.18) and (3.19), we obtain

$$\limsup_{\varepsilon\to 0}h^{-2}(\varepsilon)\log\mathbb{P}\left(\frac{||k^{\varepsilon}_3||_{\alpha}}{h(\varepsilon)}\geq\delta\right)=-\infty. \tag{3.20}$$

Step 2. For the first term $k^{\varepsilon}_1(t)$, let

$$k^{\varepsilon}_1(t,x)=\int_0^t\int_D\Delta G_{t-s}(x,y)\mathfrak{B}^{\varepsilon}(s,y)dsdy,$$

where

$$\mathfrak{B}^{\varepsilon}(s,y)=\left(\frac{f(X^{\varepsilon}(s,y))-f(X^0(s,y))}{\sqrt{\varepsilon}}-f^{'}(X^0(s,y))\eta^{\varepsilon}(s,y)\right),$$

as stated in the proof of Theorem 2, we have

$$||\mathfrak{B}^{\varepsilon}||^T_{\infty}\leq C\frac{(||X^{\varepsilon}_{X_0}-X^0_{X_0}||^T_{\infty})^2}{\sqrt{\varepsilon}}.$$

However, by Hölder's continuity of Green function G, it is easy to prove that, for any $\alpha\in(0,\frac{1}{4})$

$$|k^{\varepsilon}_2|^T_{\alpha}\leq C(\alpha,T)||\mathfrak{B}^{\varepsilon}||^T_{\infty}.$$

From the proof of proposition 1, we obtain that

$$||X^{\varepsilon}_{X_0}-X^0_{X_0}||^T_{\infty}\leq C(K_b,T)||\widetilde{k}^{\varepsilon}_2||^T_{\infty}$$

where

$$\widetilde{k}^{\varepsilon}_2(t,x)=\left(\varepsilon\int_0^t\int_D\Delta G_{t-s}(x,y)\sigma(X^{\varepsilon}_{X_0}(s,y))W(dsdy)\right)^{\frac{1}{2}}.$$

Applying lemma 3, we have

$$F(t,x,u,z)=G_{t-u}(x,z)1_{[u\leq t]},\alpha_0=\frac{1}{2},C_F=C,\rho=\sqrt{\varepsilon}K(1+||X^T_{X_0}||^T_{\infty}+\eta)$$

$$\widetilde{Z}(t,x)=\sqrt{\varepsilon}\sigma(X^{\varepsilon}_{X_0}(t,x))1_{[||X^{\varepsilon}_{X_0}||^T_{\infty}<||X^0_{X_0}||^T_{\infty}+\eta]},$$

for any $\eta>0$, we obtain that for all ε is sufficiently small such that
$M\geq\sqrt{\varepsilon}K(1+||X^T_{X_0}||^T_{\infty}+\eta)CC(\alpha,\frac{1}{2})$,

$$\begin{aligned}&\mathbb{P}(||\widetilde{k}^{\varepsilon}_2||^T_{\infty}\geq M,||X^{\varepsilon}_{X_0}||^T_{\infty}<||X^0_{X_0}||^T_{\infty}+\eta)\\ &\leq(\sqrt{2}T^2+1)\exp\left(-\frac{M^2}{\varepsilon K^2CC^2(\alpha,\frac{1}{2})(1+||X^0_{X_0}||^T_{\infty}+\eta)^2}\right).\end{aligned}$$

For the same reason as (3.20), we obtain

$$\begin{aligned}\limsup_{\varepsilon\to 0} h^{-2}(\varepsilon)\log\mathbb{P}(||X^{\varepsilon}_{X_0}||^T_\infty \geq ||X^0_{X_0}||^T_\infty+\eta) &\\ \leq \limsup_{\varepsilon\to 0} h^{-2}(\varepsilon)\log\mathbb{P}(||X^{\varepsilon}_{X_0}-X^0_{X_0}||^T_\infty\geq\eta)&\\ = -\infty.&\end{aligned}$$

For any $\eta>0$, by Bernstein's inequality and the continuity of σ, we have

$$\limsup_{\varepsilon\to 0} h^{-2}(\varepsilon)\log\mathbb{P}\left(\frac{|k^{\varepsilon}_1(t)|^T_\alpha}{h(\varepsilon)}\geq\delta\right)$$

$$\begin{aligned}&\leq \limsup_{\varepsilon\to 0} h^{-2}(\varepsilon)\log\mathbb{P}\left(\left(||\widetilde{k}^{\varepsilon}_2||^T_\infty\right)^2\geq\frac{\sqrt{\varepsilon}h(\varepsilon)\delta}{C(\alpha,T,K_f,C)}\right)\\ &\leq \limsup_{\varepsilon\to 0} h^{-2}(\varepsilon)\log\Bigg[\mathbb{P}\Bigg(\left(||\widetilde{k}^{\varepsilon}_2(t)||^T_\infty\right)^2\geq\frac{\sqrt{\varepsilon}h(\varepsilon)\delta}{C(\alpha,T,K_f,C)},\\ &\quad ||X^{\varepsilon}_{X_0}||<||X^0_{X_0}||^T_\infty+\eta\Bigg)+\mathbb{P}(||X^{\varepsilon}_{X_0}||\geq||X^0_{X_0}||^T_\infty+\eta)\Bigg]\\ &\leq \left(\limsup_{\varepsilon\to 0}\frac{-\delta}{\sqrt{\varepsilon}h(\varepsilon)C(\alpha,T,K_f,C)K^2CC^2(\alpha,\frac{1}{2})(1+||X_{X_0}||^T_\infty+\eta)^2}\right)\\ &\vee\left(\limsup_{\varepsilon\to 0} h^{-2}(\varepsilon)\log\mathbb{P}(||X^{\varepsilon}_{X_0}||\geq||X^0_{X_0}||^T_\infty+\eta)\right)=-\infty.\end{aligned}$$

□

4 A FEW EXAMPLES

4.1 Example one. Central limit theorem for stochastic Cahn-Hilliard equation with uniformly Lipschitzian coefficients

Let $\mathcal{O}$ be an open connected set in $\mathbb{R}^3$ such that $\mathcal{O}=[0,\pi]^3$ and $\mathcal{C}^\alpha([0,1]\times\mathcal{O})$ denotes the set of α-Hölder continuous fonctions. Let $\{u^\varepsilon(t,x)\}_{\varepsilon>0}$ be the solution of stochastic Cahn-Hilliard equation indexed by $\varepsilon>0$, given by

$$\begin{cases}\partial_t u^\varepsilon(t,x)=-\Delta\big(\Delta u^\varepsilon(t,x)-4(u^\varepsilon(t,x))^3+4u^\varepsilon(t,x)\big)+\sqrt{\varepsilon}(1-u^\varepsilon(t,x))\dot{W},\\ \frac{\partial u^\varepsilon(t,x)}{\partial\nu}=\frac{\partial\Delta u^\varepsilon(t,x)}{\partial\nu}=0,\ \text{on}\quad (t,x)\in[0,T]\times\partial\mathcal{O}\\ u^\varepsilon(0,x)=u_0(x)\end{cases}\tag{4.1}$$

where the coefficients f and σ are bounded, uniformly Lipschitz and verify the condition (1.2) and (1.3) such that $K_f=16$ and $K_\sigma=1$. Consider the process $\beta^\varepsilon(t,x)$ such that

$$\beta^\varepsilon(t,x)=\left(\frac{u^\varepsilon-u^0}{\sqrt{\varepsilon}}\right)(t,x).\tag{4.2}$$

In this section, we establish the CLT for the stochastic Cahn-Hilliard equation with uniformly Lipschitzian coefficients in Hölder norm $||.||_\alpha$ such that for all $u:[0,1]\times\mathcal{O}\longrightarrow\mathbb{R}$,

$$||u||_\alpha=\sup_{(s,x)\in[0,T]\times\mathcal{O}}|u(s,x)|+\sup_{\substack{(s_1,x_1)\in[0,T]\times\mathcal{O}\\(s_2,x_2)\in[0,T]\times\mathcal{O}}}\frac{|u(s_1,x_1)-u(s_2,x_2)|}{(|s_1-s_2|+|x_1-x_2|^2)^\alpha}.$$

Now, we obtain the main results similary to Theorem 2.

Theorem 5: *For any $\alpha\in[0,\frac{1}{4})$, $r\geq 1$, the process $\beta^\varepsilon(t,x)$ defined by (4.2) converges in L^r to the random process $\beta^0(t,x)$ as $\varepsilon\to 0$ where $\beta^0(t,x)$ verifies the stochastic partial differential equation*

$$\partial_t\beta^0(t,x)=-\Delta(\Delta\beta^0(t,x)-4\big(3(u^0(t,x))^2-1\big)\beta^0(t,x)\big)+(1-u^0(t,x))\dot{W}(t,x)$$

with initial condition $\eta^0(0,x)=0$.

Proof of Theorem 5 : Consider the process $\beta^\varepsilon(t,x)$ defined by (4.2) depending on $u^\varepsilon(t,x)$ and $u^0(t,x)$ such that

$$\begin{aligned}&\beta^\varepsilon(t,x)\\ &= 4\int_0^t\int_{\mathcal{O}}\Delta_{t-s}G(x,y)\Big(\frac{(u^\varepsilon(s,y))^3-u^\varepsilon(s,y)-((u^0(s,y))^3-u^0(s,y))}{\sqrt{\varepsilon}}\Big)dsdy\\ &+ \int_0^t\int_{\mathcal{O}}\Big(\sum_{i=0}^{\infty}e^{-\mu_i^2(t-s)}w_i(x)w_i(y)\Big)(1-u^\varepsilon(s,y))W(ds,dy).\end{aligned}$$

Using the equality $\forall a,b\neq 0, \frac{a^3-b^3}{a-b}=a^2+ab+b^2$, we obtain

$$\begin{aligned}\beta^\varepsilon(t,x) &= 4\int_0^t\int_{\mathcal{O}}\Delta_{t-s}G(x,y)\big[(u^\varepsilon(s,y))^2+u^\varepsilon(s,y).u^0(s,y)\\ &+ (u^0(s,y))^2-1\big]\beta^\varepsilon(s,y)dsdy\\ &+ \int_0^t\int_{\mathcal{O}}\Big(\sum_{i=0}^{\infty}e^{-\mu_i^2(t-s)}w_i(x)w_i(y)\Big)(1-u^\varepsilon(s,y))W(ds,dy)\end{aligned}$$

For $\varepsilon\to 0$, we obtain

$$\begin{aligned}\beta^0(t,x) &= 4\int_0^t\int_{\mathcal{O}}\Delta_{t-s}G(x,y)\big(3(u^0(s,y))^2-1\big)\beta^0(s,y)dsdy\\ &+ \int_0^t\int_{\mathcal{O}}\Big(\sum_{i=0}^{\infty}e^{-\mu_i^2(t-s)}w_i(x)w_i(y)\Big)(1-u^0(s,y))W(ds,dy).\end{aligned}$$

Denote the process $\mathcal{R}^\varepsilon=\beta^\varepsilon-\beta^0$ such that

$$\mathcal{R}^\varepsilon = m_1^\varepsilon(t,x)+m_2^\varepsilon(t,x)+m_3^\varepsilon(t,x)$$

where

$$\begin{aligned}m_1^\varepsilon(t,x) &= 4\int_0^t\int_{\mathcal{O}}\Delta G_{t-s}(x,y)\Big[\Big(\frac{(u^\varepsilon(s,y))^3-(u^0(s,y))^3}{\sqrt{\varepsilon}}\Big)\\ &-\Big(\frac{u^\varepsilon(s,y)-u^0(s,y)}{\sqrt{\varepsilon}}\Big)-\big(3(u^0(s,y))^2-1\big)\beta^\varepsilon(s,y)\Big]dsdy,\\ m_2^\varepsilon(t,x) &= 4\int_0^t\int_{\mathcal{O}}\Delta G_{t-s}(x,y)\big(3(u^0(s,y))^2-1\big)\big(\beta^\varepsilon(s,y)-\beta^0(s,y)\big)dsdy,\\ m_3^\varepsilon(t,x) &= \int_0^t\int_{\mathcal{O}}\Big(\sum_{i=0}^{\infty}e^{-\mu_i^2(t-s)}w_i(x)w_i(y)\Big)(u^0(s,y)-u^\varepsilon(s,y))W(ds,dy).\end{aligned}$$

Step 1. For $p>2$ and $t\in[0,1]$, we obtain

$$\begin{aligned}\mathbb{E}\big(||m_3^\varepsilon(t,x)||_\infty^t\big) &\leq C(p,T)\int_0^t\mathbb{E}\big(||u^\varepsilon-u^0||_\infty^s\big)^p ds\\ &\leq \sqrt{\varepsilon}C(p,T,u_0).\end{aligned}$$

By Taylor's formula, there exists a random field $\gamma^\varepsilon(t,x)$ taking values in $[0,1]$ such that

$$\begin{aligned}&f(u^\varepsilon(s,y))-f(u^0(s,y))\\ &= f'\big(u^0(s,y)+\beta^\varepsilon(t,x)(u^\varepsilon(s,y)-u^0(s,y))\big)(u^\varepsilon(s,y)-u^0(s,y))\end{aligned}$$

For the first term $m_1^\varepsilon(t,x)$, we have

$$\big|m_1^\varepsilon(t,x)\big| \;\leq\; 4\sqrt{\varepsilon}C\int_0^t\int_{\mathcal{O}}\Delta G_{t-s}(x,y)\big(\beta^\varepsilon(s,y)\big)^2 dsdy. \tag{4.3}$$

By Hölder's inequality, for $p>2$

$$\mathbb{E}\big(\big|m_1^\varepsilon(t,x)\big|_\infty^t\big)^p \leq (\sqrt{\varepsilon})^p C^p\bigg(\sup_{0\leq s\leq T\ ,\ x\in\mathcal{O}}\bigg|\int_0^t\int_{\mathcal{O}}\Delta G_s^q(x,y)dsdy\bigg|\bigg)^{\frac{p}{q}}\times\int_0^t\mathbb{E}\big(||\beta^\varepsilon||_\infty^s\big)^{2p}ds$$

where $\frac{1}{p}+\frac{1}{q}=1$. Using (1.5) and applying proposition 1, there exists a constant $\aleph_{p,K,C}$ depending on p, K, C such that

$$\mathbb{E}|m_1^\varepsilon(t,x)\big|^p \;\leq\; \sqrt{\varepsilon}.\aleph_{p,K,C}. \tag{4.4}$$

Since $|f^{'}|\leq 16$,by Hölder inequality , we deduce that for $p>2$

$$\mathbb{E}|m_2^\varepsilon(t,x)|^p \;\leq\; 2^{4p}\bigg(\sup_{0\leq s\leq T\ ,x\in}\bigg|\int_0^t\int_{\mathcal{O}}\Delta G_s^q(x,y)dsdy\bigg|\bigg)^{\frac{p}{q}} \times\int_0^t\mathbb{E}\big(||\beta^\varepsilon-\beta^0||_\infty^s\big)^p ds \tag{4.5}$$

where $\frac{1}{p}+\frac{1}{q}=1$.

Putting (4.3),(4.4) and (4.5) together, we have

$$\mathbb{E}\big(||\beta^\varepsilon-\beta^0||_\infty^s\big)^p \;\leq\; \aleph_{p,K,C}\big(\sqrt{\varepsilon}+\int_0^t\mathbb{E}\big(||\beta^\varepsilon-\beta^0||_\infty^s\big)^p ds\big).$$

By Gronwall's inequality, we obtain

$$\mathbb{E}\big(||\beta^\varepsilon-\beta^0||_\infty^s\big)^p \;\leq\; \sqrt{\varepsilon}\aleph_{p,K,C}\to 0 \ \text{ for } \ \varepsilon\to 0.$$

Step 2. We prove that the terms $k_i^\varepsilon\ ,\ \ i=1,2,3$ satisfy the condition (A-2) in Lemma 2.
For any $p>2$ and $q^{'}\in(1,\frac{3}{2})$such that $\gamma:=(3-2q^{'})p/(4q^{'})-2>0$, for all $x,y\in\mathcal{O}$, $0\leq t\leq T$,by Burkholder's inequality and Hölder's inequality, we have

$$\mathbb{E}\big|m_3^\varepsilon(t,x)-m_3^\varepsilon(t,y)\big|^p \;\leq\; C(p,q^{'},K,T)|x-y|^{\frac{(3-2q^{'})p}{2q^{'}}} \tag{4.6}$$

where (1.3), 4 in Lemma 1 and Proposition 1 were used, $\frac{1}{p^{'}}+\frac{1}{q^{'}}=1$.
Similarly, in view of 5, 6 in Lemma 1; its follows that for $0\leq s\leq t\leq T$, we have

$$\mathbb{E}\big|m_3^\varepsilon(t,y)-m_3^\varepsilon(s,y)\big|^p \;\leq\; C(p,q^{'},K,T)|t-s|^{\frac{(3-2q^{'})p}{4q^{'}}} \tag{4.7}$$

where Proposition 1 were used, $\frac{1}{p^{'}}+\frac{1}{q^{'}}=1$, $C(p,q^{'},K,T)$ is independent of ε .
Putting together (4.6) and (4.7), we have

$$\mathbb{E}\big|m_3^\varepsilon(t,x)-m_3^\varepsilon(s,y)\big|^p\leq C(p,q^{'},K_\sigma,K,T)\big(|t-s|+|x-y|^2\big)^\gamma. \tag{4.8}$$

Consequently, from 4, 6 in Lemma 1, proposition 1 and the result of step 1, we also have :

$$\mathbb{E}\big|m_i^\varepsilon(t,x)-m_i^\varepsilon(s,y)\big|^p\leq C\big(|t-s|+|x-y|^2\big)^\gamma\ \ ,\ \ i=2,3. \tag{4.9}$$

Putting together (4.8) and (4.9), we obtain that there exists a constant C independent of ε satisfying that

$$\mathbb{E}\big|(\beta^\varepsilon(t,x)-\beta^0(t,x))-(\beta^\varepsilon(s,y)-\beta^0(s,y))|^p\leq C\big(|t-s|+|x-y|^2\big)^\gamma.$$

For any $\alpha\in(0,\frac{1}{4})$, $r\geq 1$, choosing $p>2$, and $q^{'}\in(1,\frac{3}{2})$ such that $\alpha\in(0,\frac{\gamma}{p})$ and $r\in[1,p)$, Lemma 2 we have

$$\lim_{\varepsilon\to 0}\mathbb{E}||\beta^\varepsilon-\beta||_\alpha^r=0.$$

4.2 Example two. Moderate Deviations Principle for stochastic Cahn-Hilliard equation with uniformly Lipschitzian coefficient

In this section we establish the MDP for the stochastic Cahn-Hilliard equation (4.1). Consider the process $\Theta^\varepsilon(t,x)$ such that

$$\Theta^\varepsilon(t,x) := \left(\frac{u^\varepsilon - u^0}{\sqrt{\varepsilon}a(\varepsilon)}\right)(t,x). \tag{4.10}$$

In this section, we study the LDP for $\Theta^\varepsilon(t,x)$ defined by (4.10) as $\varepsilon \to 0$ with $1 < a(\varepsilon) < \frac{1}{\sqrt{\varepsilon}}$.

Theorem 6: *The process $\{\Theta^\varepsilon(t,x)\}_{\varepsilon>0}$ defined by (4.10) obeys a LDP on the space $\mathcal{C}^\alpha([0,1]\times\mathcal{O})$, with speed $a^2(\varepsilon)$ and rate function $\mathcal{J}_{M.D.P}(.)$ such that :*

$$\mathcal{J}_{M.D.P}(g) = \inf_{g=\mathcal{G}^0(u_0,\mathcal{I}(h))}\left\{\frac{1}{2}\int_0^T\int_0^\pi\int_0^\pi\int_0^\pi \dot{h}^2(t,x)dtdx_1dx_2dx_3\right\}$$

and $+\infty$ otherwise.

Proof of Theorem 6: It is sufficient to prove that

$$\limsup_{\varepsilon\to 0} a^{-2}(\varepsilon) \quad \log \quad \mathbb{P}\left(\frac{|\beta^\varepsilon - \beta^0|_\alpha}{a(\varepsilon)} > \delta\right) = -\infty \quad , \quad \forall\delta > 0.$$

Recall the decomposition in the proof of Theorem 5

$$\beta^\varepsilon(t,x) - \beta^0(t,x) = m_1^\varepsilon(t,x) + m_2^\varepsilon(t,x) + m_2^\varepsilon(t,x).$$

For any q in $(\frac{3}{2},3)$, $\frac{1}{p}+\frac{1}{q}=1$, and $x,y\in\mathcal{O}$, $0\le s\le t\le T$, by Hölder's inequality, 4 in Lemma 1 and (2.3), we have

$$\left|m_2^\varepsilon(t,x) - m_2^\varepsilon(t,y)\right|^p \quad \le \quad 16|x-y|^{\frac{3-q}{q}} \times \left(\int_0^t (||\beta^\varepsilon - \beta^0||_\infty^u)^p du\right)^{\frac{1}{p}}. \tag{4.11}$$

Similarly, in view of 5 and 6, it follows that for $0\le s\le t\le T$,

$$\left|m_2^\varepsilon(t,y) - m_2^\varepsilon(s,y)\right|^p \quad \le \quad 32|t-s|^{\frac{3-q}{2q}} \times \left(\int_0^t (||\beta^\varepsilon - \beta^0||_\infty^u)^p du\right)^{\frac{1}{p}}. \tag{4.12}$$

Putting together (4.11), (4.12), we have

$$\left|m_2^\varepsilon(t,y) - m_2^\varepsilon(s,y)\right|^p \le C(K_f)(|t-s|+|x-y|^2)^{\frac{3-q}{2q}} \times \left(\int_0^t (||\beta^\varepsilon - \beta^0||_\infty^u)^p du\right)^{\frac{1}{p}}.$$

Choosing $q\in(\frac{3}{2},3)$, such that $\alpha = 3 - q/2q$ and noticing that $||\beta^\varepsilon-\beta^0||_\infty^u \le (1+u)^\alpha|\beta^\varepsilon-\beta^0|_\alpha^u$, we obtain that

$$|m_2^\varepsilon|_\alpha^t \le C(K_f)\left(\int_0^t ((1+u)^\alpha|\beta^\varepsilon-\beta^0|_\alpha^u)^p du\right)^{\frac{1}{p}}.$$

Thus, for $t\in[0,1]$, we have

$$(|\beta_t^\varepsilon - \beta_t^0|_\alpha^t)^p \le C(p,T,K_f)\left[\left(|m_1^\varepsilon(t)|_\alpha^t + |m_3^\varepsilon(t)|_\alpha^t\right)^p + \int_0^t (|\beta^\varepsilon-\beta^0|_\alpha^s)^p ds\right].$$

Applying Gronwall's Lemma to $\Psi(t) = (|\beta_t^\varepsilon - \beta_t^0|_\alpha^t)^p$, we have

$$(|\beta_t^\varepsilon - \beta_t^0|_\alpha^t)^p \le C(p,T,K_f)\left[\left(|m_1^\varepsilon(t)|_\alpha^t + |m_3^\varepsilon(t)|_\alpha^t\right)^p\right]e^{C(p,T,K_f)T}. \tag{4.13}$$

By (4.12) and (4.13), it is sufficient to prove that for any $\delta>0$,

$$\limsup_{\varepsilon\to 0} h^{-2}(\varepsilon)\log\mathbb{P}\left(\frac{|m_i^\varepsilon(t)|_\alpha^T}{a(\varepsilon)} > \delta\right) = -\infty \qquad\qquad i=1,3.$$

Step 1. For any $\varepsilon > 0$, $\eta > 0$ we have

$$\begin{aligned}\mathbb{P}\big(|m_3^\varepsilon(t)|_\alpha^T > a(\varepsilon)\delta\big) &\leq \mathbb{P}\big(|m_3^\varepsilon(t)|_\alpha^T > a(\varepsilon)\delta, |u^\varepsilon - u^0|_\infty^T < \eta\big)\\ &+ \mathbb{P}(|u^\varepsilon - u^0|_\infty^T \geq \eta) \qquad (4.14)\end{aligned}$$

By 4 and 6 in Lemma 1, $\big(\sum_{i=0}^\infty e^{-\mu_i^2(t-s)} w_i(x)w_i(y)\big).1_{[u\leq t]}$ satisfies (3.12)(see Lemma 3) for $\alpha_0 = \frac{1}{2}$. Applying Lemma 3, we have

$$F(t,x,u,z) = \big(\sum_{i=0}^\infty e^{-\mu_i^2(t-s)} w_i(x)w_i(z)\big)1_{[u\leq t]}, \alpha_0 = \frac{1}{2}, C_F = C, M = a(\varepsilon)\delta,$$

$\rho = \eta K_\sigma, Y^*(t,x) = \big(u^0(t,x) - u^\varepsilon(t,x)\big)1_{||u^\varepsilon - u^0||_\infty^T > \eta}$
we obtain that for all ε sufficiently small such that $a(\varepsilon)\delta \geq \rho C C(\alpha, \frac{1}{2})$

$$\mathbb{P}\big(|m_3^\varepsilon(t)|_\alpha^T > a(\varepsilon)\delta, ||u^\varepsilon - u^0||_\infty^T < \eta\big) \leq (\sqrt{2}T^2 + 1)\exp\big(-\frac{a^2(\varepsilon)\delta^2}{\eta^2 K_\sigma^2 C C^2(\alpha, \frac{1}{2})}\big). \qquad (4.15)$$

Since u^ε satisfies the LDP on $\mathcal{C}^\alpha([0,T]\times\mathcal{O})$

$$\begin{aligned}\limsup_{\varepsilon\to 0} \varepsilon \log \mathbb{P}(||u^\varepsilon - u^0||_\infty^T \geq \eta) &\leq \limsup_{\varepsilon\to 0} \varepsilon \log \mathbb{P}(||u^\varepsilon - u^0||_\alpha \geq \eta)\\ &\leq -\inf\{\mathcal{I}(f) \,:\, ||f - u^0||_\alpha \geq \eta\}.\end{aligned}$$

In this case, the good rate function $\mathcal{I} = \{\mathcal{I}(f) \,:\, ||f - u^0||_\alpha \geq \eta\}$ has compact level sets, the "$\inf\{\mathcal{I}(f) \,:\, ||f - u^0||_\alpha \geq \eta\}$" is obtained at some function f_0. Because $\mathcal{I}(f) = 0$ if and only if $f = u^0$, we conclude that

$$-\inf\{\mathcal{I}(f) \,:\, ||f - u^0||_\alpha \geq \eta\} < 0.$$

For $a(\varepsilon) \to \infty$, $\sqrt{\varepsilon}a(\varepsilon) \to 0$, we have

$$\limsup_{\varepsilon\to 0} a^{-2}(\varepsilon) \log \mathbb{P}\big(||u^\varepsilon - u^0||_\infty^T \geq \eta\big) = -\infty. \qquad (4.16)$$

Since $\eta > 0$ is arbitrary, putting together (4.14), (4.15) and (4.16), we obtain

$$\limsup_{\varepsilon\to 0} a^{-2}(\varepsilon) \log \mathbb{P}\left(\frac{||m_3^\varepsilon||_\alpha}{a(\varepsilon)} \geq \delta\right) = -\infty. \qquad (4.17)$$

Step 2. For the first term $m_1^\varepsilon(t)$, let

$$m_1^\varepsilon(t,x) = \int_0^t \int_{\mathcal{O}} \Delta G_{t-s}(x,y)\mathfrak{M}^\varepsilon(s,y)dsdy,$$

where

$$\begin{aligned}\mathfrak{M}^\varepsilon(s,y) = 4 \Bigg(&\left(\frac{(u^\varepsilon(s,y))^3 - (u^0(s,y))^3}{\sqrt{\varepsilon}}\right) - \left(\frac{u^\varepsilon(s,y) - u^0(s,y)}{\sqrt{\varepsilon}}\right)\\ &-\big(3(u^0(s,y))^2 - 1\big)\beta^\varepsilon(s,y)\Bigg)\end{aligned}$$

as stated in the proof of Theorem 5, we have

$$||\mathfrak{M}^\varepsilon||_\infty^T \leq C\frac{(||u^\varepsilon - u^0||_\infty^T)^2}{\sqrt{\varepsilon}}.$$

However, by the Hölder's continuity of Green function G, it is easy to prove that, for any $\alpha \in (0, \frac{1}{4})$

$$|m_2^\varepsilon|_\alpha^T \leq C(\alpha, T)||\mathfrak{M}^\varepsilon||_\infty^T.$$

From the proof of proposition 1, we obtain that

$$||u^\varepsilon - u^0||_\infty^T \leq C(T)||\widetilde{m}_2^\varepsilon||_\infty^T.$$

where

$$\widetilde{m}_2^{\varepsilon}(t,x)=\sqrt{\varepsilon\int_0^t\int_{\mathcal{O}}\Delta G_{t-s}(x,y)u^{\varepsilon}(s,y)W(dsdy)}.$$

Applying lemma 3, we have

$$F(t,x,u,z)=G_{t-u}(x,z)1_{[u\leq t]},\alpha_0=\frac{1}{2},C_F=C,\rho=\sqrt{\varepsilon}K(1+||u^T||_{\infty}^T+\eta)$$

$$Z^*(t,x)=\sqrt{\varepsilon}(1-u^{\varepsilon}(t,x))1_{[||u^{\varepsilon}||_{\infty}^T<||u^0||_{\infty}^T+\eta]},$$

for any $\eta>0$, we obtain that for all ε is sufficiently small such that $M\geq\sqrt{\varepsilon}(1+||u^T||_{\infty}^T+\eta)CC(\alpha,\frac{1}{2})$,

$$\mathbb{P}(||\widetilde{m}_2^{\varepsilon}||_{\infty}^T\geq M,||u^{\varepsilon}||_{\infty}^T<||u^0||_{\infty}^T+\eta)$$

$$\leq(\sqrt{2}T^2+1)\exp\bigg(-\frac{M^2}{\varepsilon K^2CC^2(\alpha,\frac{1}{2})(1+||u^0||_{\infty}^T+\eta)^2}\bigg).$$

For the same raison as (4.11), we obtain

$$\limsup_{\varepsilon\to0}a^{-2}(\varepsilon)\log\mathbb{P}(||u^{\varepsilon}||_{\infty}^T\geq||u^0||_{\infty}^T+\eta)$$

$$\leq\limsup_{\varepsilon\to0}a^{-2}(\varepsilon)\log\mathbb{P}(||u^{\varepsilon}-u^0||_{\infty}^T\geq\eta)=-\infty.$$

For any $\eta>0$, by Bernstein's inequality and the continuity of σ, we have

$$\limsup_{\varepsilon\to0}a^{-2}(\varepsilon)\log\mathbb{P}\bigg(\frac{|m_1^{\varepsilon}(t)|_{\alpha}^T}{a(\varepsilon)}\geq\delta\bigg)$$

$$\leq\limsup_{\varepsilon\to0}a^{-2}(\varepsilon)\log\mathbb{P}\bigg(\bigg(||\widetilde{m}_2^{\varepsilon}||_{\infty}^T\bigg)^2\geq\frac{\sqrt{\varepsilon}a(\varepsilon)\delta}{C(\alpha,T,K_f,C)}\bigg)$$

$$\leq\limsup_{\varepsilon\to0}a^{-2}(\varepsilon)\log\bigg[\mathbb{P}\bigg(\big(||\widetilde{m}_2^{\varepsilon}(t)||_{\infty}^T\big)^2\geq\frac{\sqrt{\varepsilon}a(\varepsilon)\delta}{C(\alpha,T,K_f,C)},$$
$$||u^{\varepsilon}||<||u^0||_{\infty}^T+\eta\bigg)+\mathbb{P}(||u^{\varepsilon}||\geq||u^0||_{\infty}^T+\eta)\bigg]$$

$$\leq\bigg(\limsup_{\varepsilon\to0}\frac{-\delta}{\sqrt{\varepsilon}a(\varepsilon)C(\alpha,T,K_f,C)K^2CC^2(\alpha,\frac{1}{2})(1+||u^0||_{\infty}^T+\eta)^2}\bigg)$$
$$\vee\bigg(\limsup_{\varepsilon\to0}h^{-2}(\varepsilon)\log\mathbb{P}(||X_{X_0}^{\varepsilon}||\geq||X_{X_0}^0||_{\infty}^T+\eta)\bigg)=-\infty.$$

5 CONCLUSION

In this paper, we have proved a CLT and a MDP for a perturbed stochastic Cahn-Hilliard equation in Hölder space by using the exponential estimates in the space of Hölder continuous functions and the Garsia-Rodemich-Rumsey's lemma. We can also examine the same situation in Besov-Orlicz space.

ACKNOWLEDGEMENT

The authors wish to thank the referees and editors for their valuable comments and suggestions which led to improvements in the document.

DECLARATION

The authors declare no conflict of interest.

REFERENCES

[1] Ben Arous, G., & Ledoux, M. (1994). Grandes déviations de Freidlin-Wentzell en norme hölderienne. *Séminaire de probabilités de Strasbourg*, 28, 293-299.
[2] Boulanba, L., & Mellouk, M. (2020). Large deviations for a stochastic Cahn–Hilliard equation in Hölder norm. *Infinite Dimensional Analysis, Quantum Probability and Related Topics*, 23(02), 2050010.
[3] Cahn, J. W., & Hilliard, J. E. (1971). Spinodal decomposition: A reprise. *Acta Metallurgica*, 19(2), 151-161.
[4] Cahn, J. W., & Hilliard, J. E. (1958). Free energy of a nonuniform system. I. Interfacial free energy. *The Journal of chemical physics*, 28(2), 258-267.
[5] Cardon-Weber, C. (2001). Cahn-Hilliard stochastic equation: existence of the solution and of its density. *Bernoulli*, 777-816.
[6] Chenal, F., & Millet, A. (1997). Uniform large deviations for parabolic SPDEs and applications. *Stochastic Processes and their Applications*, 72(2), 161-186.
[7] Freidlin, M. I. (1970). On small random perturbations of dynamical systems. *Russian Mathematical Surveys*, 25(1), 1-55.
[8] Li, R., & Wang, X. (2018). Central limit theorem and moderate deviations for a stochastic Cahn-Hilliard equation. *arXiv preprint arXiv:1810.05326*.
[9] Walsh, J. B. (1986). An introduction to stochastic partial differential equations. *Lecture notes in mathematics*, 265-439.
[10] Wang, R., & Zhang, T. (2015). Moderate deviations for stochastic reaction-diffusion equations with multiplicative noise. *Potential Analysis*, 42, 99-113.

PV-Battery hybrid system power management based on backstepping control

IJAMS Peer reviewed journal
International Journal of Applied Mathematics and Simulation

PV-Battery hybrid system power management based on backstepping control.

[1]Aimen Acil MAANANI, [2]Yacine MAANANI, 3[rd] Achour Betka [3], 4[th]AymenBenguessoum[4]

https://doi.org/10.69717/ijams.v1.i2.102

Abstract-With the increasing global energy consumption and the need for sustainable solutions, this article focuses on the energy management of a hybrid photovoltaic (PV)-battery system using the backstepping method. The research addresses the challenges of intermittent solar irradiation by implementing an incremental conductance maximum power point tracking (MPPT) algorithm for the PV panel and backstepping control for battery charging and discharging. The system's performance and control effectiveness were validated throughlaboratory experiments. The results demonstrate the system's robustness, stability, and ability to respond to fast changes, making it a promising solution for efficient energy management in hybrid PV-battery systems. The findings provide valuable insights for future research and advancements in this field.

Keywords: Energy management, Hybrid PV/battery system, Backstepping method, PV panels-Batteries-DC/DC boost converter, DC/DC bidirectional converter, Incremental conductance MPPT, Renewable energies, Energy storage-nonlinear control, experimental validation.

I. INTRODUCTION

Renewable energies are an alternative way to conventional fossil fuels, and they originate from natural phenomena caused by the sun and the earth. The six primary sources of renewable energy are solar, wind, hydro, geothermal, marine, and biomass. The potential of these sources depends on various factors like sunshine, wind exposure, topology, and land geometry [1]. To cover the load demand in arid zones, solar based devices are generally combined with storage elements to get Hybrid systems. The PV-battery hybrid system combines a photovoltaic (PV) panel with a battery storage element to increase the autonomy of the system,

In the literature, there are different types of energy systems (isolated energy systems, connected energy systems, single-source energy systems, and multi-source energy systems). In general, the term Hybrid Energy System (HES) refers to electric power generation systems that use multiple types ofsources in order to combine the advantages of each while taking into account their respective specifications. These hybrid sources combine very high specific energy and maximum power available for considerable durations. Today, the use of hybrid energy systems (HES) has advanced in several industrial sectors such as embedded systems (automobiles, airplanes, boats, etc.) as well as for powering isolated communities or even those connected to grids[11].

[1]LGEB Laboratory of Electrical Engineering of Biskra, Mohamed Khider University, Biskra, Algeria
Maanani.aimenacil@gmail.com
[2]LGEB Laboratory of Electrical Engineering of Biskra, Mohamed Khider University, Biskra, Algeria
yacine.maanani@gmail.com
[3]LGEB Laboratory of Electrical Engineering of Biskra, Mohamed Khider University, Biskra, Algeria
betkaachour@gmail.com
[4]LGEB Laboratory of Electrical Engineering of Biskra, Mohamed Khider University, Biskra, Algeria
aymenbeng2000@gmail.com

Communicated Editor: Nabil khelfallah

***Manuscript received** Dec 06,2023; **revised** May 19, 2024; **accepted** Nov 27, 2024; **published** Dec 28, 2024.*

II. PV-BATTERY HYBRID SYSTEM

Effective management strategies require an understanding of the behavior of a system in response to input data, and this understanding is achieved through a prior numerical simulation, based on an explicit modeling of the process, the first step is modeling the involved sources, which are the PV panel and the lead-acid battery, and then going in an analog way to a mathematical representation of the static converters, of the types of DC-DC boost and DC-DC buck-boost converters. The acquired models are essential for comprehending and enhancing the system's overall performance to harness its full potential and ensure stability in real-world scenarios.

In the framework of this study, a PV-battery hybrid system, which supplies a stationary load is presented in ’Fig .1" To permit an effective control and power management of the system, each source is equipped with a side DC-DC converter. An optimal operation of the PV panel is guaranteed via a quite adjusting of the related duty cycle. In the same point of view, the battery side converter is a Bidirectional DC-DC converter, which permits charging and discharging current of the battery.

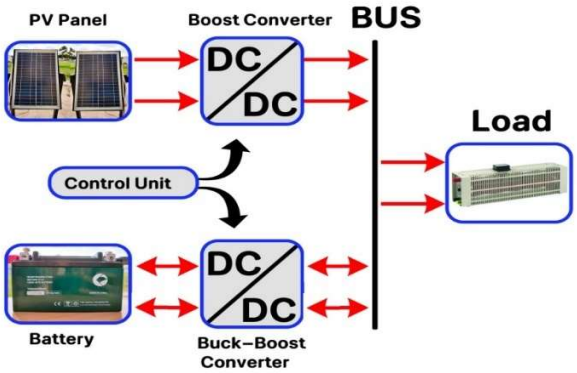

Figure 1.Synoptic scheme of the hybrid system

III. MODELINGOF SOURCES

A.PV Panel Model

Photovoltaic (PV) panels convert sunlight directly into electricity through the photovoltaic effect.
PV models range varies from simple single-diode models to complex multi-diode models. The selection of an appropriate model depends on the required accuracy and computational effort. The single-diode model, due to its balance between complexity and accuracy, is widely used in PV system design and simulation [2].
Photovoltaic panels are considered neither voltage nor current sources, but they can be estimated as voltage-controlled current generators, where the implicit four-parameter model (I_{pv}, R_s, V_{th}, and I_o) reflects the current-voltage characteristic with notable accuracy:

$$I_{pv} = I_{cc} - I_o \left[exp\left(\frac{V_{pv}+R_s.I_{pv}}{V_{th}}\right) - 1 \right] \quad (1)$$

This characteristic can be illustrated by the equivalent diagram (Fig.2) [14-15]; consisting of a variable current generator, mounted in parallel with a diode D characterizing the junction and a resistance Rs (series resistance) representing the losses by Joule effects.
The thermal voltage V_{th} and the diode saturation current Io are identified by:

$$I_o = (I_{cc} - I_{op}).exp[-\frac{V_{op}-R_s.I_{op}}{V_{th}}] \quad (2)$$

$$V_{th} = \frac{V_{op}+R_s.I_{op}-V_{oc}}{\log(1-\frac{I_{op}}{I_{cc}})} \quad (3)$$

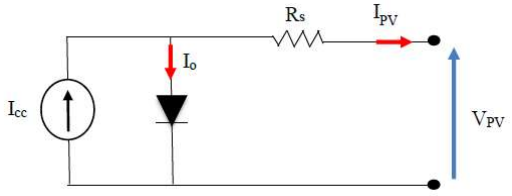

Figure 2. Equivalent diagram of the photovoltaic panel

IV. MODELING OF STATIC CONVERTERS

In the context of our study on 'Modelingof Static Converters,' we employ DC-DC boost converters and buck-boost converters in hybrid PV-battery systems. The average model simplifies analysis and facilitates control design, stability assessment, and energy management. The boost converter comprises a controlled switch, a flyback diode, and storage components (L, C), while Kirchhoff's laws aid in deriving average model equations for the buck-boost converter, enabling comprehensive system testing [13].

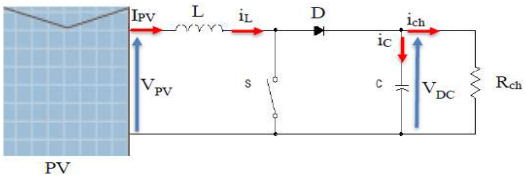

Figure 3. Descriptive diagram of the boost converter

A. *Modeling of PV Panel Boost Converter*

The average model for the PV panel boost converter is derived from the application of Kirchhoff's voltage and current laws (KVL and KCL) during the closed and open phases of the transistors [13]. This yields the following average model weighted bythe duty cycle α:

$$\begin{cases} \dot{x} = (A_1.x + B_1.Vpv).\alpha + (A_2.x + B_2.Vpv)(1-\alpha) \\ V_{dc} = [D_1.\alpha + D_2.(1-\alpha)].x \end{cases} \quad (4)$$

For this converter, the parameters are:

- Capacitance (C) = 2200 µF
- Inductance (L) = 15 mH
- Resistance (r) = 2.8 Ω

B. *Modeling of Battery Buck-Boost Converter (Bidirectional Converter)*

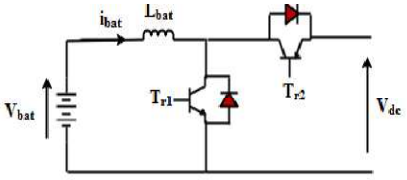

Figure 4. Converter associated with batteries.

Similarly, the average model for the battery buck-boost converter is obtained by applying Kirchhoff's voltage and current laws during the closed and open phases of the transistors, resulting in the following average model:

$$L_{bat}\frac{di_{bat}}{dt} = V_{bat} - (1-\alpha_{bat})V_{dc} \quad (5)$$

For this converter, the parameters are:

- Capacitance (C) = 2200 µF
- Inductance (L) = 12.21 mH
- Resistance (r) = 2.6 Ω

The model expressed in Equation (5) defines the battery's behavior during charging ($i_{bat} < 0$) and discharging ($i_{bat} > 0$), with switches Tr1 and Tr2 being complementary tuned, as presented in Equation (6):

$$\alpha_{Tr1} + \alpha_{Tr2} = 1 \quad (6)$$

V. CONTROL STRATEGIES FOR THE PV-BATTERY HYBRID SYSTEM

A. MPPT (Maximum Power Point Tracking) Algorithm

Maximum Power Point Tracking (MPPT) is a critical technology in photovoltaic (PV) systems. Its main purpose is to optimize power output by continuously tracking the Maximum Power Point (MPP), which varies with external factors like temperature and solar irradiation intensity. MPPT adjusts to these changing conditions, ensuring PV cells operate as close as possible to their MPP. This dynamic regulation maximizes power extraction, enhancing overall PV system efficiency. One widely used MPPT method is Incremental Conductance (IncCond)

B. The Incremental Conductance Method

The IncCond method, an advanced MPPT technique, computes the derivative of power with respect to voltage to pinpoint the MPP. By iteratively modifying the converter's duty cycle and adjusting the voltage, this method seeks the point where the derivative of power over voltage approaches zero, indicating the MPP. In "Fig 5", the flowchart of this technique is presented.

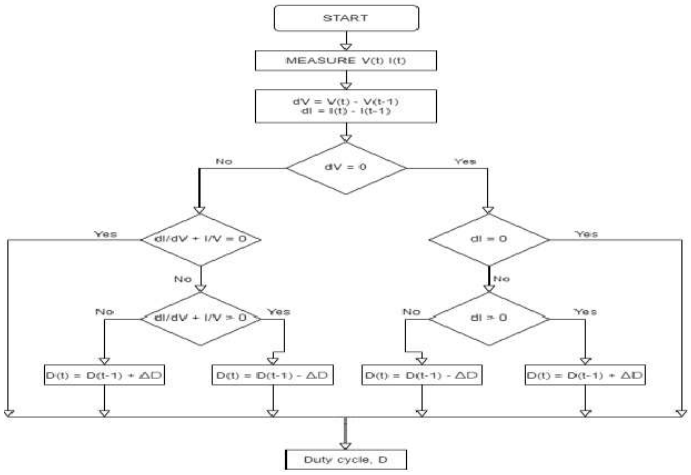

Figure 5. Flowchart of the IncCond MPPT Algorithm [12]

The algorithm hinges on the condition that the derivative of power (Ppv) with respect to voltage (Vpv) is zero at the maximum power point (MPP) and changes sign on either side of the MPP, represented by Equation (7).

$$\frac{dP_{pv}}{dV_{pv}} = 0 \qquad (7)$$

At the MPP, this equation can be explicitly expressed as a function of both PV voltage and current, as given by Equation (8).

$$V_{pv}\frac{dI_{pv}}{dV_{pv}} + I_{pv} = 0 (8)$$

The algorithm iteratively adjusts the converter's duty cycle, ensuring that dIpv/dVpv matches the absolute value of the instantaneous conductance Ipv/Vpv. This Incremental Conductance (IncCond) method excels in accuracy, rapid MPP detection, and steady-state oscillation elimination, enhancing energy efficiency.

IncCond is a practical choice for energy management in hybrid PV-Battery systems, selected based on specific system requirements and constraints. In this work, IncCond is utilized for PV side boost converter control, as depicted in the accompanying figure.

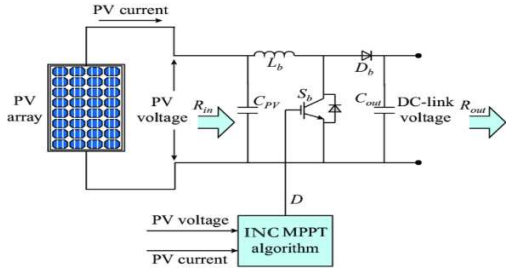

Figure 6. Synoptic Scheme of the Control of the PV Boost Converter [5]

VI. The Application of The Backstepping Method

A. In case of battery discharging:

The average model of the boost DC-DC converter is given as follows:

$$\begin{cases}\dot{x_1} = \frac{r}{L}x_1 - (1-u)\frac{x_2}{L} + \frac{E}{L} \\ \dot{x_2} = (1-u)\frac{x_1}{C} + \frac{I_{pvs}}{C} - \frac{x_2}{RC}\end{cases}(9)$$

Where the state vector is:$x = \begin{bmatrix} i_b \\ V_{dc} \end{bmatrix}$, and u is the converter duty cycle. In this model, I_{pvs} expresses the PV current on the DC bus side and is considered as a disturbance input. E denotes the battery voltage V_B.

1) Step One:

We first calculate the inductor current tracking error Z_1, given in (10). It is worth noting here that this choice is justified by the fact that the boost converter is an unstable non minimum phase system, and the deduction of the control law via the choice of the DC bus voltage tracking error as Z_1 fails. To overcome this situation, by choosing Z1 as (10), the dc bus voltage can be indirectly controlled[6].

$$Z_1 = x_1 - I_d(10)$$

Where the reference battery current I_d,is deduced through the power flow in steady state, as follows:

$$I_d = \frac{(\frac{V_{dc}^2}{R} - V_{PV}.I_{PV})}{E}(11)$$

And its derivative is:

$$\dot{Z_1} = \dot{x_1} - \dot{I_d} \ (12)$$

A first positive definite Lyapunov function is chosen as

$$V_1 = \frac{1}{2}Z_1^2(13)$$

By choosing the gradient of V_1 as semi-definite function, one gets:

$$\dot{Z_1} = -c_1 Z_1(14)$$

Where c_1 is a manipulated positive constant.

Plugging $\dot{x_1}$ from equation (9) in equation (14):

$$\dot{Z_1} = -\frac{r}{L}x_1 - (1-u)\frac{x_2}{L} + \frac{E}{L} - \dot{I_d} = -c_1 Z_1(15)$$

In this step, the stabilization part α_1 can be deduced as:

$$\alpha_1 = \frac{x_2}{L} = \frac{\left[c_1 Z_1 - \frac{r}{L}x_1 + \frac{E}{L} - \dot{I_d}\right]}{(1-u)}(16)$$

2) Step Two:

In an analog way, the second error Z_2 is expressed as follows, which means that the DC bus voltage is regulated through the stabilization part α_1: [8]

$$Z_2 = \frac{x_2}{L} - \alpha_1 \quad => \frac{x_2}{L} = Z_2 + \alpha_1(17)$$

We replace $\frac{x_2}{L}$in equation (15) with equation (17), one gets:

$$\dot{Z_1} = -(1-u)[Z_2 + \alpha_1] - \frac{r}{L}x_1 + \frac{E}{L} - \dot{I_d}(18)$$

Plugging α_1 from equation (16) in equation (18) To finally get:

$$\dot{Z_1} = -c_1 Z_1 - (1-u)Z_2(19)$$

The derivative α_1 can be explicitly given by:

$$\dot{\alpha_1} = \frac{\left[c_1 \dot{Z_1} - \frac{r}{L}\dot{x_1} + \frac{\dot{E}}{L} - \ddot{I_d}\right](1-u)}{(1-u)^2} + \frac{\dot{u}\left[c_1 Z_1 - \frac{r}{L}x_1 + \frac{E}{L} - \dot{I_d}\right]}{(1-u)^2}$$

(20)

$$\dot{\alpha_1} = \frac{-c_1^2 Z_1 - c_1(1-u)Z_2 + \frac{r^2}{L^2}x_1 + (1-u)\frac{rx_2}{L^2} - \frac{rE}{L^2} + \frac{\dot{E}}{L} - \ddot{I_d} + \dot{u}\alpha_1}{(1-u)}(21)$$

We replace both $\dot{\alpha_1}$ and $\frac{\dot{x_2}}{L}$ in the derivative of Z_2 one obtains:

$$\dot{Z_2} = \frac{\dot{x_2}}{L} - \dot{\alpha_1} (22)$$

$$\dot{Z_2} = (1-u)\frac{x_1}{LC} - \frac{x_2}{LRC} + \frac{\dot{i_{pvs}}}{LC} - \left[\frac{-c_1^2 Z_1 - c_1(1-u)Z_2 + \frac{r^2}{L^2}x_1 + (1-u)\frac{rx_2}{L^2} - \frac{rE}{L^2} + \frac{\dot{E}}{L} - \ddot{I_d} + \dot{u}\alpha_1}{(1-u)}\right] (23)$$

In this second step, a new positive definite Lyapunov function, extended to the second tracking error is proposed as:

$$V_2 = \frac{1}{2}Z_1^2 + \frac{1}{2}Z_2^2 (24)$$

$$\Rightarrow \dot{V_2} = Z_1\dot{Z_1} + Z_2\dot{Z_2} = Z_1[-C_1 Z_1 - Z_2(1-u)] + Z_2\dot{Z_2} (25)$$

The convergence of both Z_1, and Z_2 to zero, imposes that the gradient of V_2 takes the following form:

$$\dot{V_2} = -\dot{c_1}Z_1^2 - c_2 Z_2^2 (26)$$

According to this conclusion, the following equality is deduced:

$$\dot{Z_2} - Z_1(1-u) + C_2 Z_2 = 0 (27)$$

Plugging $\dot{Z_2}$ from equation (23) into equation (27):

$$(1-u)\frac{x_1}{LC} - \frac{x_2}{LRC} + \frac{\dot{i_{pvs}}}{LC} + \left[\frac{c_1^2 Z_1 + c_1(1-u)Z_2 - \frac{r^2}{L^2}x_1 - (1-u)\frac{rx_2}{L^2} + \frac{rE}{L^2} - \frac{\dot{E}}{L} + \ddot{I_d} - \dot{u}\alpha_1}{(1-u)}\right] - Z_1(1-u) + C_2 Z_2 = 0 (28)$$

We extract $\dot{u}$ from equation (28) to finally have the control law of our system:

$$\dot{u} = \frac{\left[\begin{matrix}[c1^2 - (1-u)^2]Z_1 + (c_1+c_2)(1-u)Z_2 + \ddot{I_d} + \left[\frac{(1-u)^2}{LC} - \frac{r^2}{L^2}\right]x_1 - (1-u)x_2\left[\frac{1}{RLC} + \frac{r}{L^2}\right] \\ + \frac{\dot{i_{pvs}}(1-u)}{LC} + \frac{rE}{L^2} - \frac{\dot{E}}{L}\end{matrix}\right]}{\alpha_1}$$

(29)

3) Zero Dynamics Study

The zero dynamics study focuses on the deduction of the steady state duty cycle, when both the tracking errors Z_1 and Z_2, as well as the control input gradient $\dot{u}$ tend to zero. A second order equation of the control law is obtained, having two possible roots, and as remarked, since the tolerable range of the duty cycle is between 0 and 1, only the following root u 2 is suitable[9]:

$$u_2 = 1 - \frac{1}{2}\left(-\frac{i_{pvs}}{x_1} - \left(\frac{1}{R} + \frac{r.C}{L}\right)\frac{x_2}{x_1} - \sqrt{\left(\frac{i_{pvs}}{x_1} - \left(\frac{1}{R} + \frac{r.C}{L}\right)\frac{x_2}{x_1}\right)^2 - \frac{4.(r.E - r^2 x_1).C}{L.x_1}}\right) (30)$$

B. In case of battery charging:

The average model of the boost DC-DC converter is given as follows:

$$\begin{cases}\dot{x_1} = \frac{-r}{L}x_1 - \frac{x_2}{L} + u\frac{E}{L} \\ \dot{x_2} = \frac{x_1}{C} + \frac{I_{pvs}}{C} - \frac{x_2}{RC}\end{cases} (31)$$

Where the state vector is: $x = \begin{bmatrix} i_b \\ V_{dc}\end{bmatrix}$, and u is the converter duty cycle. In this model, I_{pvs} expresses the PV current on the DC bus side, and is considered as a disturbance input. E denotes the battery voltage V_B.

1) Step One:

Firstly, the inductor current tracking error Z_1 is calculated, given in (32). It is worth noting here that this choice isfor the sake of continuity, because in the first scenario, Z_1 was given as the equation (10), therefore, Z_1 in this case is also given as (32).

$$Z_1 = x_1 - I_d (32)$$

And its derivative is presented in the following equation and is plugged by $\dot{x_1}$:

$$\dot{Z_1} = \dot{x_1} - \dot{I_d} = \frac{-r}{L}x_1 + \frac{u.E}{L} - \frac{x_2}{L} - \dot{I_d} (33)$$

Where the reference battery current I_d, is deduced through the power flow in steady state, as follows[7]:

$$I_d = \frac{(\frac{V_{dc}^2}{R} - V_{PV}.I_{PV})}{E} (34)$$

A first positive definite Lyapunov function is chosen as follows:

$$V_1 = \frac{1}{2} Z_1^2 (35)$$

By choosing the gradient of V_1 as semi-definite function, one gets:

$$\dot{Z_1} = -c_1 Z_1 (36)$$

Where c_1 is a manipulated positive constant.

Plugging $\dot{Z_1}$ from equation (32) in equation (36):

$$\dot{Z_1} = -\frac{r}{L} x_1 - \frac{x_2}{L} + \frac{u.E}{L} - \dot{I_d} = -c_1 Z_1 \quad (37)$$

In this step, the stabilization part α_1 can be deduced as:

$$\alpha_1 = \frac{x_2}{L} = c_1 Z_1 - \frac{r}{L} x_1 + \frac{u.E}{L} - \dot{I_d} \quad (38)$$

2) Step Two:

In an analog way, the second error Z_2 is expressed as follows, which means that the DC bus voltage is regulated through the stabilization part α_1[10]:

$$Z_2 = \frac{x_2}{L} - \alpha_1 \Rightarrow \frac{x_2}{L} = Z_2 + \alpha_1 (39)$$

We replace $\frac{x_2}{L}$ in equation (37) with equation (39), one gets:

$$\dot{Z_1} = -\frac{r}{L} x_1 - Z_2 - \alpha_1 + \frac{u.E}{L} - \dot{I_d} (40)$$

Plugging α_1 from equation (38) in equation (40) to finally get:

$$\dot{Z_1} = -c_1 Z_1 - Z_2 (41)$$

The derivative α_1 can be explicitly given by:

$$\dot{\alpha_1} = c_1 \dot{Z_1} - \frac{r}{L} \dot{x_1} + \frac{\dot{u}.E}{L} - \ddot{I_d} (42)$$

$$\dot{\alpha_1} = \frac{r^2}{L^2} x_1 - \frac{u.r.E}{L^2} + \frac{r}{L^2} x_2 + \frac{\dot{u}.E}{L} - \ddot{I_d} - c_1^2 Z_1 (43)$$

We replace both $\dot{\alpha_1}$ and $\frac{\dot{x_2}}{L}$ in the derivative of Z_2, one obtains:

$$\dot{Z_2} = \frac{\dot{x_2}}{L} - \dot{\alpha_1} (44)$$

$$\dot{Z_2} = \left[\frac{1}{C} - \frac{r^2}{L^2}\right] x_1 - \left[\frac{1}{RC} + \frac{r}{L^2}\right] x_2 + c_1^2 Z_1 + c_1 Z_2 + \frac{i_{pvs}}{C} + \frac{u.r.E}{L^2} - \frac{\dot{u}.E}{L} + \ddot{I_d} (45)$$

In this second step, a new positive definite Lyapunov function, extended to the second tracking error is proposed as:

$$V_2 = \frac{1}{2} Z_1^2 + \frac{1}{2} Z_2^2 (46)$$

$$\Rightarrow$$

$$\dot{V_2} = Z_1 \dot{Z_1} + Z_2 \dot{Z_2} = Z_1[-C_1 Z_1 - Z_2(1-u)] + Z_2 \dot{Z_2} (47)$$

The convergence of both Z_1, and Z_2 to zero, imposes that the gradient of V_2 takes the following form:

$$\dot{V_2} = -\dot{c_1} Z_1^2 - c_2 Z_2^2 (48)$$

According to this conclusion, the following equality is deduced:

$$\Rightarrow \dot{Z_2} - Z_1 + C_2 Z_2 = 0 (49)$$

Plugging $\dot{Z_2}$ from equation (45) into equation (50):

$$\left[\frac{1}{C} - \frac{r^2}{L^2}\right] x_1 - \left[\frac{1}{RC} + \frac{r}{L^2}\right] x_2 + c_1^2 Z_1 + c_1 Z_2 + \frac{i_{pvs}}{C} + \frac{u.r.E}{L^2} - \frac{\dot{u}.E}{L} + \ddot{I_d} - Z_1 + C_2 Z_2 = 0 (50)$$

We extract $\dot{u}$ from equation (50) to finally have the control law of our system:

$$\dot{u} = \frac{\left[\left[\frac{1}{C} - \frac{r^2}{L^2}\right] x_1 - \left[\frac{1}{RC} + \frac{r}{L^2}\right] x_2 + \frac{u.r.E}{L^2} + \frac{i_{pvs}}{C} + \ddot{I_d} + (c_1^2 - 1) Z_1 + (c_2 + c_2) Z_2\right]}{\frac{L}{E}}$$

(51)

3) Zero Dynamics study

The zero dynamics study focuses on the deduction of the steady state duty cycle, when both the tracking errors Z_1 and Z_2, as well as the control input gradient $\dot{u}$ tend to zero. Since the tolerable range of the duty cycle is between 0 and 1, an equation of the control law u is obtained:

$$u = \frac{-\left[\frac{1}{C}-\frac{r^2}{L^2}\right]x_1+\left[\frac{1}{RC}+\frac{r}{L^2}\right]x_2-\frac{i_{pvs}}{C}-\ddot{i}_d}{\frac{L^2}{r.E}} \quad (52)$$

The idea behind the deduction of this control law, is to avoid the saturation of the control law while using (51), caused mainly by the accumulation of errors, due to the imprecision of both voltage and current sensors.

C. logic commutation criteria

The choice of the bidirectional converter operation, whether to be a boost converter and discharge the battery or a buck converter and charge the battery depends on the sign of the reference battery current ($_{bref}$), which can be calculated using the next equation:

$$i_{bref} = \frac{\left[\frac{V_{dc}^2}{R}-P_{pv}\right]}{V_b} \quad (53)$$

As for the choice criteria itself, it's presented as follows:

$$\begin{cases} \text{if } i_{bref} > 0 \Rightarrow p_{ch} > P_{pv} \Rightarrow \textit{operate as boost} \\ \text{if } i_{bref} < 0 \Rightarrow p_{ch} < P_{pv} \Rightarrow \textit{operate as buck} \end{cases} \quad (54)$$

VII. Experimental Validation

To experimentally validate the control approaches, a small-scale hybrid system is assembled in the Renewable Energy Laboratory, where the implementation is performed using an Arduino Mega 2560 board. The explicit electronic scheme and the test bench is presented in **figure (7)**

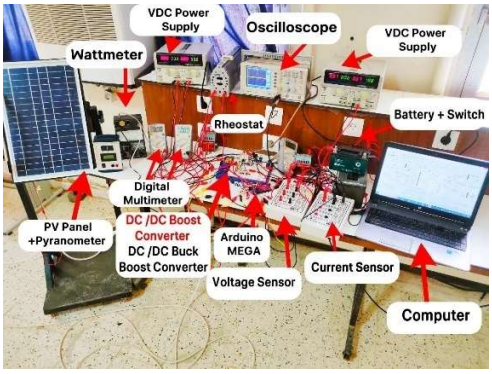

Figure 7: Picture of the Assembled Small-Scale Hybrid System in the RE Laboratory

The results of the backstepping-controlled boost converter are presented in this section, with a static load of R=20 Ω, and a reference voltage of V_{DCref}=25V

The obtained curves from testing the controller while discharging the battery are presented in the next figures.

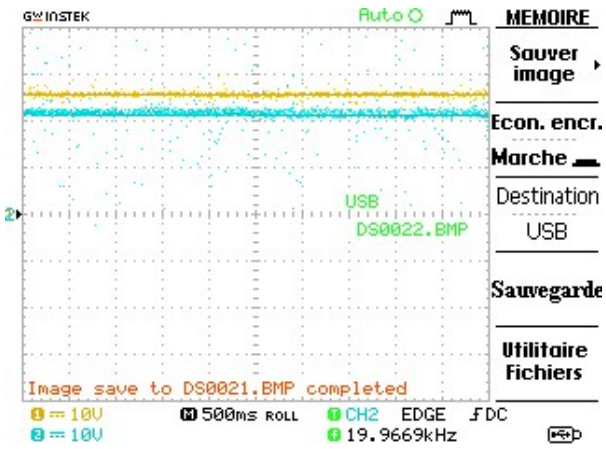

a) V_{DC} (blue) + V_{DCRef}(yellow)

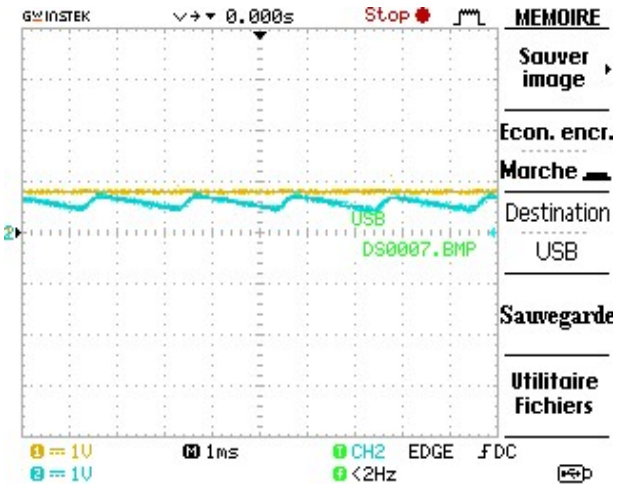

b) I_b(blue) + I_{bRef}(yellow)

Figure 8 : the obtained curves of the backstepping based controller :

V_{DC} ,V_{DCRef} , I_b, I_{bRef}.

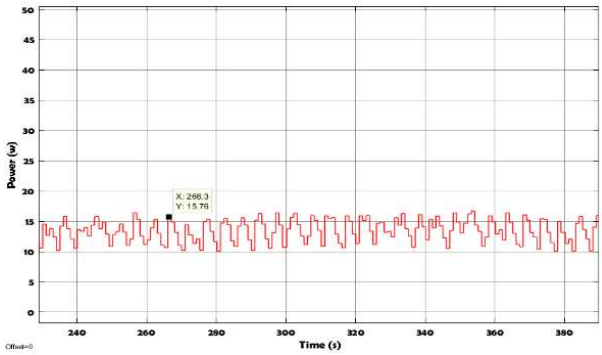

Figure 9 : the battery's power

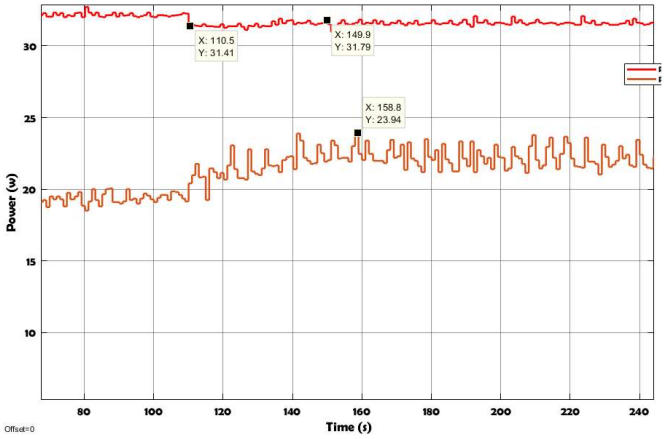

Figure 10: the load's power + the sum of the PV panel and the battery's power

The curves illustrate power management on the battery side using a backstepping-based controller via a boost DC-DC converter. The continuous bus voltage (VDC) stabilizes at VDC=21.5V, slightly below the reference value of 25V, showing a decrease of

approximately 3.5V. The battery current closely approaches the reference value (IbRef=0.64A), maintaining oscillations between Ibmax=0.64A and Ibmin=0.5A due to coil effects.

The combined power of the battery and PV panel fluctuates around Ptot=31W, matching the anticipated load power. However, the load's power hovers around Pch=23.5W, influenced by the reduced VDC. The PV panel's power oscillates around PPV=15W, while the battery's power compensates the load with a value around Pb=16W.

Overall, these curves demonstrate effective power management in the hybrid system by the controller

- Practical Obstacles

During the work on this article, several obstacles posed challenges and impeded the progress, resulting in limitations that affected the attainment of optimal outcomes. Some of these obstacles included:

-Faulty electrical and electronic components.

-Inadequate wiring leading to signal distortion and interference.

-The Arduino board's limited commutation frequency.

-The microcontroller's restricted processing capabilities.

To elaborate on the Arduino board's limitations, the PWM output frequency of the board is limited to f=490Hz, which is significantly lower than the required commutation frequency essential for achieving the desired system performance. This limited frequency range constrained our ability to accurately control and modulate the electrical signals, impacting the overall efficiency of the system.

VIII. CONCLUSON

Inthis research project, a PV-battery hybrid system was thoroughly investigated under the control of the nonlinear backstepping approach. Comprehensive insights into system components, models, and control laws were provided. Utilizing the Incremental Conductance MPPT algorithm with a DC-DC boost converter, power extraction from the solar panel was successfully optimized. Bus voltage regulation and battery control were effectively implemented using the backstepping method with a buck-boost converter, accommodating both discharging and charging modes. Simulations have demonstrated the effectiveness, responsiveness, robustness, and stability of the system and controls. It's acknowledged that experimental validation was limited to the discharging phase due to time constraints. Future work should encompass further experimental testing for a more comprehensive assessment.

REFERENCES

[1] MAAMIR, Madiha. *Techniques de supervision d'énergie d'un système d'entrainement Electrique hybride*. 2020. Thèse de doctorat. Université Mohamed Khider–Biskra. Search in Google Scholar, View

[2] DE SOTO, Widalys, KLEIN, Sanford A., et BECKMAN, William A. Improvement and validation of a model for photovoltaic array performance. *Solar energy*, 2006, vol. 80, no 1, p. 78-88. Search in Google Scholar, https://doi.org/10.1016/j.solener.2005.06.010

[3] ERICKSON, Robert W. et MAKSIMOVIC, Dragan. *Fundamentals of power electronics*. Springer Science & Business Media, 2007. Search in Google Scholar, View

[4] JYOTHI, Vellanki Mehar, MUNI, T. Vijay, *et al.* An optimal energy management system for pv/battery standalone system. *International Journal of Electrical and Computer Engineering*, 2016, vol. 6, no 6, p. 2538. Search in Google Scholar, View Article

[5] KUMAR, Vinit et SINGH, Mukesh. Derated mode of power generation in PV system using modified perturb and observe MPPT algorithm. *Journal of Modern Power Systems and Clean Energy*, 2020, vol. 9, no 5, p. 1183-1192. Search in Google Scholar, https://doi.org/10.35833/MPCE.2019.000258

[6] MOURAD, Loucif. *Synthèse de lois de commande non-linéaires pour le contrôle d'une machine asynchrone à double alimentation dédiée à un système aérogénérateur*. 2016. Thèse de doctorat. Ph. D. thesis, Université Aboubakr Belkaid–Tlemcen–Faculté de Technologie. Search in Google Scholar, View

[8] AMARA, Karima, MALEK, Ali, BAKIR, Toufik, *et al.* Adaptive neuro-fuzzy inference system based maximum power point tracking for stand-alone photovoltaic system. *International Journal of Modelling, Identification and Control*, 2019, vol. 33, no 4, p. 311-321. Search in Google Scholar, https://doi.org/10.1504/IJMIC.2019.107480

[9] RAHMAN, Sumaiya et RAHMAN, Hasimah Abdul. Use of photovoltaics in microgrid as energy source and control method using MATLAB/Simulink. *International Journal of Electrical and Computer Engineering*, 2016, vol. 6, no 2, p. 851. Search in Google Scholar, View Article

[10] ABD ALLAH, Boucetta et DJAMEL, Labed. Control of power and voltage of solar grid connected. *Bulletin of Electrical Engineering and Informatics*, 2016, vol. 5, no 1, p. 37-44. Search in Google Scholar, https://doi.org/10.11591/eei.v5i1.519